Mineralogical Magazine, June 2016, Vol. 80(4), pp. 585–637

The Stillwater Complex, Montana – Overview and the significance of volatiles

Alan E. Boudreau

Division of Earth and Ocean Sciences, Duke University, Box 90227, Durham, NC 27708, USA

[*Received 31 May 2015; Accepted 19 November 2015; Associate Editor: Brian O'Driscoll*]

ABSTRACT

The geology of the 2.7 Ga Stillwater Complex in South-Central Montana is reviewed with a focus on the role of volatiles in locally modifying both the crystallization sequence of the evolving parent magma and the initially precipitated solid assemblages to favour olivine ± chromite. A secondary origin for these two minerals is particularly probable for the olivine-bearing rocks of the Banded series and, at a minimum, also increasing their modal abundance in the Peridotite zone of the Ultramafic series. Direct evidence for volatiles includes the presence of high-temperature fluid inclusions in pegmatoids and hydrous melt inclusions (now crystallized) in chromite and olivine from both the Ultramafic and the Banded series rocks. Indirect evidence includes the boninitic character of the parent magma, the presence of volatile-bearing minerals including high-temperature carbonates, rock textures, and Cl / F variations in apatite. Mechanisms which favour the formation of olivine (± chromite) over pyroxene include volatile phase boundary shifts induced by added H_2O, incongruent melting of pyroxene by hydration of a partly-molten mush, and the near- to sub-solidus replacement of pyroxene by olivine and chromite by silica-undersaturated fluids. These mechanisms cast doubt that magmas with different liquid lines of descent were involved in the crystallization of the Stillwater Complex. A dry Stillwater magma would have been mineralogically and modally much less varied and lacking in high-grade platinum-group element and chromium deposits.

Keywords: Stillwater Complex, layered intrusions, J-M Reef, platinum-group element deposits.

Introduction

It now has been over half a century since the classic studies of Hess (1960), Jones *et al.* (1960), and Jackson (1961) on the Stillwater Complex. Since these studies, there have been a number of summary updates on the complex, most notably Page (1977), McCallum *et al.* (1980), Raedeke and McCallum (1984), Czamanske and Zientek (1985) and McCallum (1996).

In the last few decades, there have been several major advances in the interpretations of layered intrusions, some of which resulted from newer studies in the Stillwater Complex since these last reviews. These include the importance of crystal ageing, compaction and compaction-driven recrystallization as drivers of rock texture, the recognition of isotopic disequilibrium, the increasingly precise age determination, and the potential of volatiles to affect crystallization sequences or cause changes in the originally precipitated mineral assemblages. This paper represents a synthesis of this newer work, with a particular emphasis on the potential importance of volatiles in changing the crystallization sequence of the Stillwater magma or modifying the original magmatic assemblage. Although some coverage of basic geology of the Stillwater Complex is required, this review does not repeat material well-covered in earlier works.

This report does not use cumulus terminology in the descriptions of the rocks. As noted by McBirney (2008) cumulus terminology has interpretive implications and can have a pernicious effect on the understanding of the processes that formed the rocks. This is particularly true for the Stillwater Complex where there is abundant evidence of

E-mail: boudreau@duke.edu
DOI: 10.1180/minmag.2016.080.063

prolonged modification of rock textures and compositions over the long cooling history of the intrusion. Examples include the possibility that some Stillwater olivine and chromite is the result of incongruent melting owing to the fluxing effects of H_2O (Boudreau, 1999) or replacement (Meurer *et al.*, 1997). In the former instance the rocks more properly would be termed 'restites' (residual solid assemblages), and not cumulates. Thus, this report will instead use respectable but model-neutral rock names with modifiers as necessary (e.g. granular harzburgite or mela-norite).

Regional geology and geological history

The 2701 ± 8 Ma (Sm-Nd, DePaolo and Wasserburg, 1979; U-Pb, Premo *et al.*, 1990) Stillwater Complex is a layered ultramafic-mafic intrusion located along the northern front of the Beartooth Mountains in south-central Montana (Fig. 1). It has a maximum exposed stratigraphic thickness of 6.5 km and an exposed strike length of ~45 km. Beneath the central and western part of the complex, the footwall to the Stillwater Complex contains a variety of ~3270 Ma metasedimentary

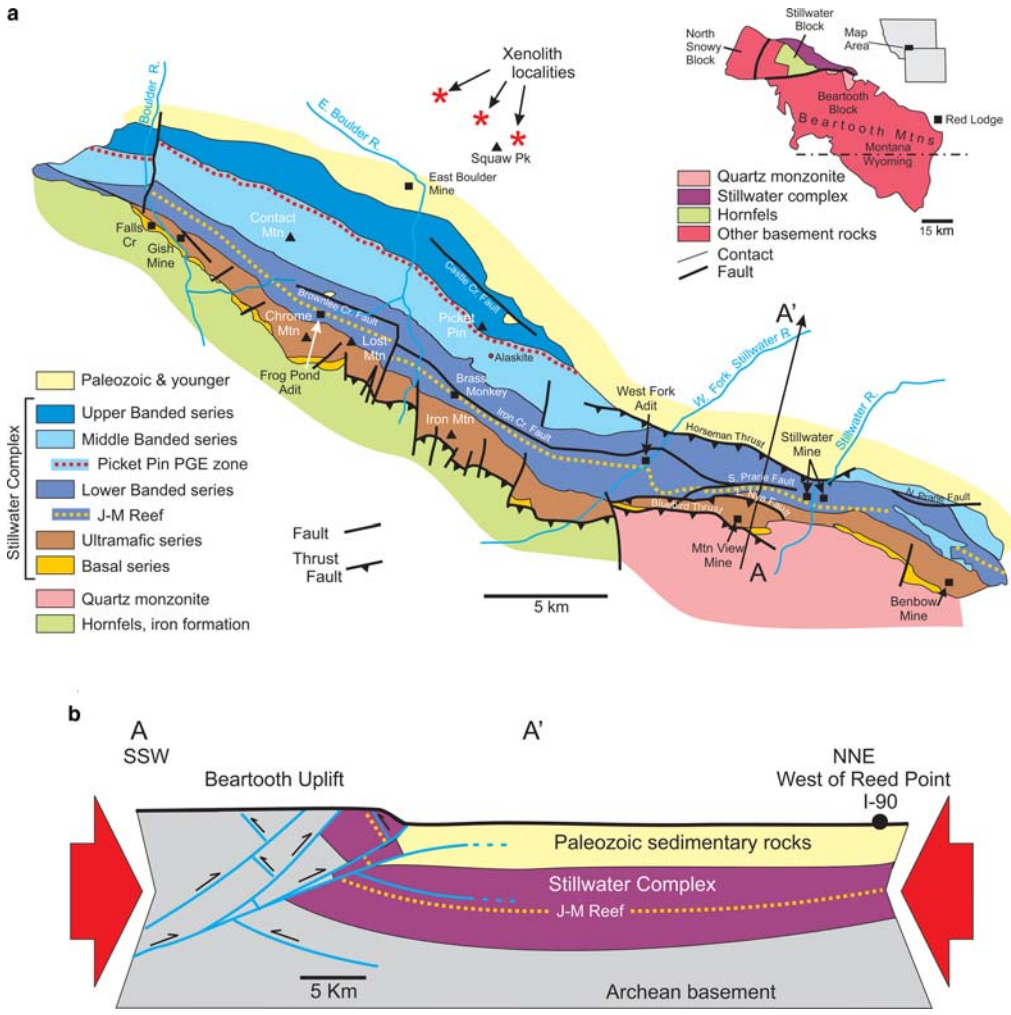

FIG. 1. Geology of the Stillwater Complex. (*a*) Geological map of the complex. The inset shows the relationship of the Stillwater Complex to the Archean blocks that make up the Beartooth Mountains. A–A′ = Partial line of section shown in bottom figure. Redrawn after Jackson, (1961) and McCallum (1996). (*b*) Simplified regional structure of the Stillwater Complex showing possible extension of the complex to the north at depth. Redrawn after Abbott *et al.* (2011).

https://doi.org/10.1180/minmag.2016.080.063 Published online by Cambridge University Press

rock types, principally metamorphosed volcaniclastic shale, greywacke and breccia, quartzite, and banded iron formation. Also present are sills, dykes and small bodies of massive sulfides immediately below the complex. Field relationships and radiometric age determination (Premo *et al.*, 1990) suggest that these footwall intrusive rocks are immediately pre- to contemporaneous with the magmas that formed the Stillwater Complex proper. The Stillwater Complex and the associated basement rocks define one of several Archean-age fault-bound blocks that occur across parts of Montana and Wyoming.

The country rocks farthest from the contact with the Stillwater Complex are composed in-part of a biotite schist interpreted by Labotka and Kath (2001) to have formed during an earlier low-pressure regional metamorphic event (525–550°C and 2 kbar). They and Helz (1995) concluded that the Stillwater was emplaced as a subvolcanic (or perhaps more specifically a sub-flood basalt province) sill at a depth of 6–7 km in regionally metamorphosed metasedimentary rocks. Mogk and Mueller (1990) further suggested that the Stillwater intruded within 50 Ma of this regional metamorphic event. The possibility of intrusion into hot country rock is consistent with the slow cooling implied by the relatively coarse-grained nature of the Stillwater rocks. For example, the granular orthopyroxene grain size of ~2 mm reported by Page and Moring (1990) is about four times as coarse as the ~0.5 mm average grain size reported for stratigraphically similar rock from the Lower and Critical zones of the Bushveld Complex (Boorman *et al.,* 2004). It is also consistent with the phaneritic nature of the marginal rocks as compared, for example, with the aphanitic marginal rocks of the Ferrar sills of the Dry Valleys, Antarctica (Marsh, 2004).

Intrusion of the Stillwater magmas further heated the country rocks to produce a wide metamorphic aureole. Because of faulting and the lack of laterally continuous units for correlation, the true thickness of the metamorphic aureole beneath the Stillwater Complex is somewhat uncertain. However, Labotka and Kath (2001) note that the pelitic rocks proximal to the complex have been thermally metamorphosed to hypersthene hornfels over a distance of 0.5–1 km from the contact and a more distal zone of cordierite-cummingtonite hornfels 0.5–1.5 km thick. Assemblages in the iron formation are consistent with peak metamorphic temperatures around 825°C and pressures between 3 and 4 kbar (Labotka, 1985). These pressures compare with the 1–2 kbar based on the experimental crystallization sequence in mixtures of presumed Basal and Ultramafic series magmas determined by Helz (1995). McCallum (1996) interpreted the pressure difference to reflect both the additional mass of the Stillwater intrusion and contact metamorphism that occurred after the injection of the pre-Stillwater age sills and dykes.

The Mouat quartz monzonite, exposed along the Stillwater River and to the east, was emplaced ~60 Ma after crystallization of the Stillwater and intrudes both the hornfels and (as a few small sills) the lower portion of the Stillwater Complex (Jones *et al.*, 1960). Later mafic dykes intruded the complex at 2.6, 2.4 and 1.6 Ga (Nunes and Tilton, 1971; Baadsgaard and Mueller, 1973). Regional metamorphism around 1.7 Ga locally produced greenschist assemblages wherever water infiltrated the complex (Nunes and Tilton, 1971; Nunes 1981; Page 1977), although for the most part the igneous mineralogy is preserved.

The upper portion of the intrusion was eroded prior to the mid-Cambrian and then subsequently covered by Paleozoic and Mesozoic sediments. Regional thrusting, faulting and uplift during the Late Cretaceous Laramide orogeny led to the current tilting (typically ~70° to the NNE but locally overturned in the vicinity of the Stillwater River) and exposure of the complex along the northern edge to the Beartooth plateau. Geophysical evidence suggests that the complex extends at depth for a distance of at least 25 km to the northeast (Kleinkopf, 1985), and a Stillwater Mining Company technical report (Abbott *et al.,* 2011) has it extending even farther (Fig. 1*b*). A buried northern extension is consistent with the presence of altered xenoliths of Stillwater affinities found in the Cenozoic volcanic rocks that erupted through the Paleozoic sedimentary cover 8–12 km to the north of the complex (Brozdowski, 1985).

Stratigraphy

Stratigraphic subdivisions of the Stillwater Complex

There have been literally dozens of proposed stratigraphic subdivisions of the Stillwater Complex. The more recent have been based on the stratigraphic mineral modal variations detailed by McCallum *et al.* (1980) and Raedeke and McCallum (1984) and which are followed here, with one important modification noted below concerning subdivisions of the Middle Banded series (Fig. 2).

https://doi.org/10.1180/minmag.2016.080.063 Published online by Cambridge University Press

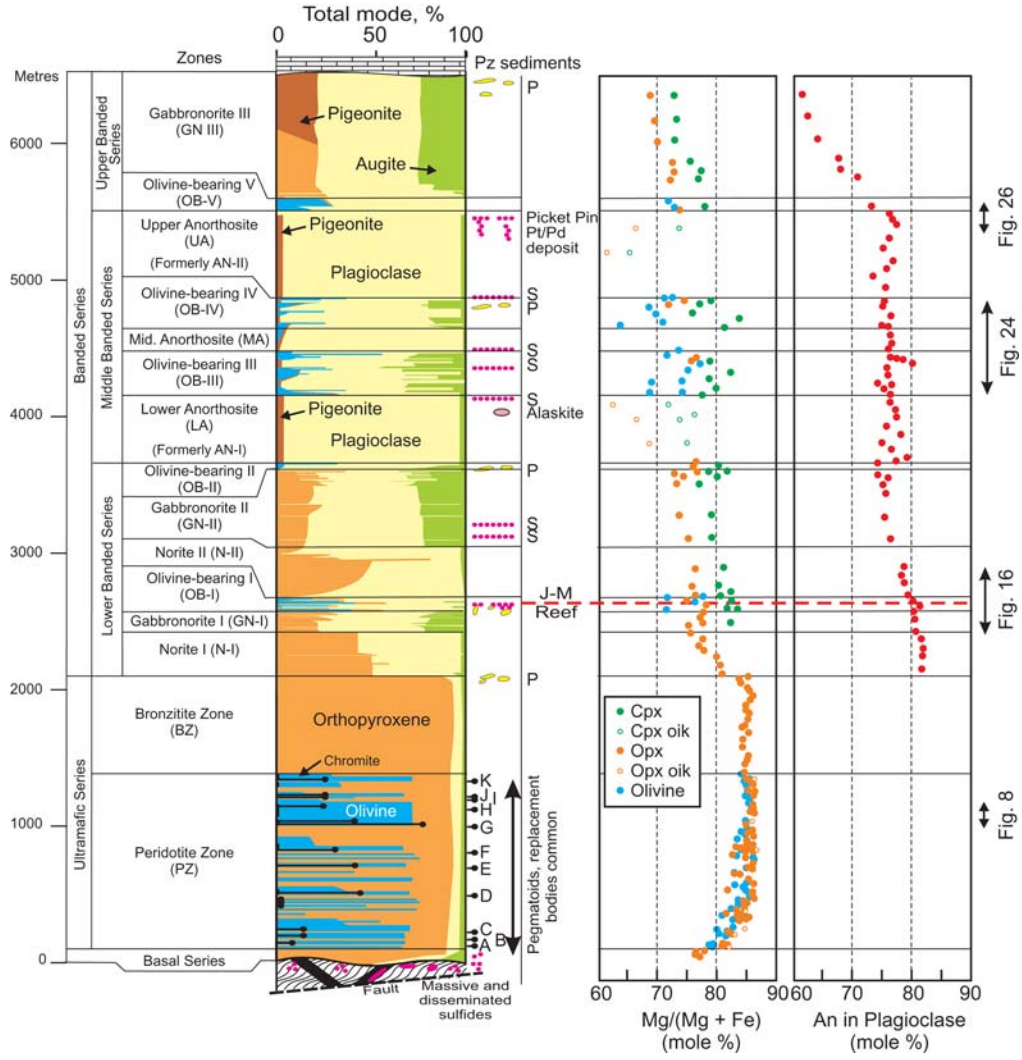

FIG. 2. Major mineral modes in the Stillwater Complex and mineral compositional trends as a function of stratigraphic height. Modal olivine in poikilitic and granular harzburgite from the Ultramafic series is in part schematic, based on average modes. Also shown are the locations of the A through to K chromitites (labelled 'A'–'K'), zones where pegmatoids and sulfides are common (labelled 'P' and 'S', respectively), the alaskite body described by Czamanske (1991), and the locations of the J-M reef and the Picket Pin PGE zone (labelled). Modal data and stratigraphic units after McCallum *et al.* (1980) and Raedeke and McCallum (1984), modified to define the three anorthosite units of the Middle Banded series as discussed in the text.

Beneath the Stillwater Complex proper but generally grouped with it is a complex assemblage of broadly contemporaneous gabbronorite and norite mafic sills and dykes, hosted in the basement metasedimentary rocks. Some of the sill/dyke rocks have been proposed to represent the parental Stillwater magma based on their geology, age and composition (Premo *et al*., 1990; Helz, 1985). Small bodies of massive sulfide occur with the igneous rocks in the metamorphic aureole, but the abundance of sulfide in general decreases markedly going into the Stillwater Complex.

https://doi.org/10.1180/minmag.2016.080.063 Published online by Cambridge University Press

Basal series

Where present and not cut out by later faulting, the base of the first laterally continuous norite defines the lowermost unit of the Stillwater Complex, the Basal series. The norite (with subordinate anorthosite, gabbro, and peridotite) grades upwards by an unsystematic decrease in plagioclase mode to an orthopyroxenite. The maximum thickness of the Basal series is ~400 m but more typically ranges from 60 to 240 m (Page, 1979; Zientek, 1983).

Ultramafic series

The base of the Ultramafic series is placed at the first significant appearance of olivine that defines the bottom of the first cyclic unit of the Ultramafic series, and the top at the base of the norite that defines the base of the Banded series. It is divided into a lower Peridotite zone and an overlying Bronzitite zone. The Ultramafic series overlies the Basal series, although in some areas the Ultramafic series is in fault contact with basement rock (e.g. Page 1977).

The Peridotite zone is comprised of a cyclic repetition of nominally peridotite/poikilitic harzburgite → granular harzburgite → orthopyroxenite that repeats 21 times at Mountain View (Raedeke and McCallum, 1984). Chromitite layers occur near the base of many cyclic units and are labeled A–K upwards from the bottom (Jones *et al.*, 1960). Mining of the thicker G and H chromitites occurred in the 1940s and again in the 1950s to early 1960s.

The Bronzitite zone at the top of the Ultramafic series is a generally uniform orthopyroxenite with interstitial plagioclase and augite, minor chromite and quartz and rare phlogopite, apatite and sulfides. It does have some modal layering near the bottom and top, and marked orthopyroxene size graduations from the typical 2–3 mm (Raedeke and McCallum, 1984) to >1 cm in size can occur locally throughout.

Banded series

The Banded series comprises all rocks above the Ultramafic series in which plagioclase is a major modal mineral. It has been subdivided into three units: the Lower, Middle and Upper Banded series. Based on the major rock type or the appearance of olivine as noted in Fig. 2, these three units are further subdivided into various zones and subzones. Olivine-bearing zone I (OB-I) of the Lower Banded series contains the J-M Reef, an economic concentration of platinum-group element (PGE) mineralization associated with sulfide-enriched rocks that is currently being mined by the Stillwater Mining Company.

The Middle Banded series is bounded by two thick (>500 m) anorthosite units, referred to by McCallum *et al.* (1980) as AN-I and AN-II. As described more fully below, these thick anorthosite units are modally and texturally distinct from the numerous thin anorthosites that occur throughout the Banded series. However, in the middle of the Middle Banded series is yet a third anorthosite with textural and compositional similarities to these two anorthosites. McCallum *et al.* (1980) originally kept the middle anorthosite as equivalent to the other two, but then discounted it owing to the occasional presence of olivine (I.S. McCallum, pers. comm.). The practical effect of this was that OB-III and OB-IV were juxtaposed without an intervening unit. Those authors wishing to refer to the similarities of the middle anorthosite with the others have informally called it AN-1.5 (e.g. Meurer *et al.* 1996*a*). Given the problematic nature of olivine in the Banded series in general and in the Middle Banded series in particular as detailed below, it is here suggested to return to the three anorthosite units for the Middle Banded series as proposed by Hess (1960). However, rather than renumber the anorthosites which would introduce confusion in the literature, the middle anorthosite is here referred to as the Middle Anorthosite zone and Anorthosite zones I and II of McCallum *et al.* (1980) are now the Lower and Upper Anorthosite zones of the Middle Banded series, respectively, as they have been called informally (Fig. 2).

Except for thin troctolite and norite units at the base, the Upper Banded series returns essentially to the crystallization of gabbronorite seen in the upper part of the Lower Banded series. An important mineralogical change that occurs in this unit is the appearance of abundant inverted pigeonite. Recrystallization during inversion caused initially isolated pigeonite grains to become crystallographically aligned, such that multiple pigeonite grains coalesced to form a poikilitic habit, although the granular nature of the original texture is evident from the multiple orientations of clinopyroxene exsolution lamallae. This has led to some confusion in the literature, as Segerstrom and Carlson (1982) mapped the inverted pigeonite unit as anorthosite (plagioclase as the only 'cumulus' mineral) whereas the modes and preserved original texture are consistent with the cotectic crystallization of plagioclase + pigeonite + clinopyroxene.

Occurring sporadically throughout the Stillwater Complex are pegmatoids and a variety of

https://doi.org/10.1180/minmag.2016.080.063 Published online by Cambridge University Press

discordant bodies. These are more common in some units than in others. An unusual low-K granophyre (alaskite) body occurs near the top of the Lower Anorthosite zone of the Middle Banded series south of Picket Pin Peak.

Mineral mode and composition trends

Comprehensive studies of the stratigraphic variations in mineral modes and compositional trends of the major minerals were carried out by McCallum *et al.* (1980) and Raedeke and McCallum (1984) and are shown in Fig. 2. More recent studies of the sulfide, halogen, and ore element trends in the complex were undertaken by Boudreau and McCallum (1989), Keays *et al.* (2012), Page and Zientek (1987) and Aird *et al.* (2016) and are shown in Fig. 3. Numerous other studies have detailed specific stratigraphic sections and their lateral variations; these are noted below in reference to the discussion of specific zones.

For the mafic minerals, olivine and the pyroxenes, the mineral trends define an initial trend of increasing Mg# with stratigraphic height from the Basal series into the lower third of the Ultramafic series. The Mg# in the upper two-thirds of the Ultramafic series shows only minor variations. Orthopyroxene with a poikilitic habit (in poikilitic harzburgite) has a slightly greater Mg# composition than orthopyroxene in nearby granular harzburgite; presumably, the Mg# is essentially buffered by the larger Mg# of the olivine-rich poikilitic harzburgite.

In contrast to the near-constant compositions seen in the upper part of the Ultramafic series, the

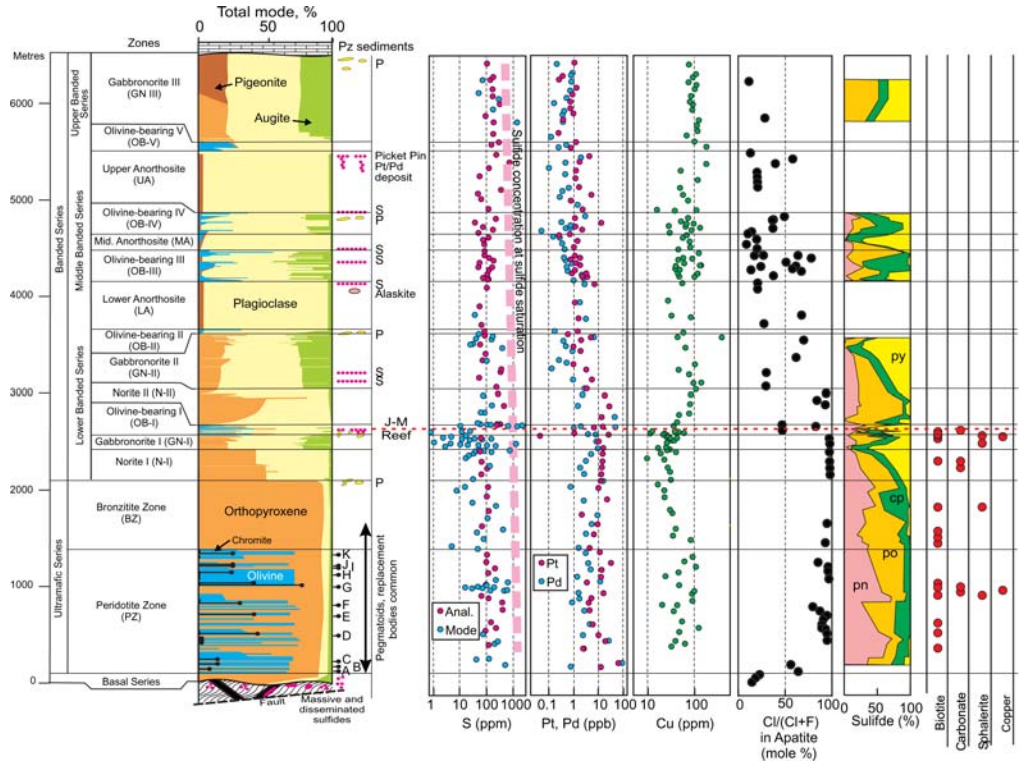

FIG. 3. Stratigraphic trends of the bulk-rock ore elements S, Pt, Pd, Cu, the molar Cl/(Cl + F) ratio in apatite, the relative proportions of the major sulfide minerals, and the stratigraphic occurrences of a selection of other trace minerals (biotite, high-temperature carbonate, sphalerite and native copper) in the Stillwater Complex. In the bulk S column, red circles labelled 'Anal.' are by whole-rock analysis (Keays *et al.*, 2012), the blue circles labelled 'Mode' are bulk S calculated from the sulfide mode by Aird *et al.* (2016) and the dashed pink line is the approximate sulfur concentration if the rocks were saturated in sulfide (Li and Ripley, 2009). Abbreviations: pn = pentlandite; po = pyrrhotite; cp = chalcopyrite; py = pyrite. After Boudreau and McCallum (1989), Keays *et al.* (2012) and Aird *et al.* (2016).

https://doi.org/10.1180/minmag.2016.080.063 Published online by Cambridge University Press

mafic minerals through the Lower Banded series show a systematic decrease in Mg# and plagioclase a decrease in An#. In the Middle Banded series, plagioclase has a near-constant average composition whereas the mafic phases are variable. The Upper Banded series resumes the fractionation trend interrupted by the Middle Banded series rocks: plagioclase shows a marked decrease in the An content whereas the mafic phases show a more modest decrease in the Mg# with stratigraphic height.

The compositional and modal trends of accessory apatite and the sulfide assemblage can be quite distinct from those of the major elements (Fig. 3). For apatite, the enrichment in the chlorapatite end-member in the Basal series into the lower part of the Peridotite zone roughly parallels the Mg# enrichment noted above. The near chlorapatite end-member compositions seen in the rest of the Ultramafic series up to the J-M Reef is comparable to a similar enrichment seen in the Bushveld Complex (Willmore *et al.*, 2000). Such Cl-rich apatite compositions are otherwise rare in layered intrusions. Hanley *et al.* (2008) report halite inclusions in olivine from the Peridotite zone. High-temperature carbonates and native Cu are also characteristic of the Cl-rich section (Aird and Boudreau, 2013). An abrupt change to more Cl-poor compositions occurs in Olivine-Bearing zone I, associated with the J-M Reef. Above the Reef, apatite is variable but overall the chlorapatite component decreases with stratigraphic height. In the Middle Banded series, the three thick anorthosite units have Cl-poor apatite as compared with the olivine-bearing units (Meurer and Boudreau, 1996*a*).

Sulfide minerals associated with the Peridotite zone and especially the chromitite zones (e.g. Page, 1971; Page *et al.,* 1985; Foose and Nicholson, 1990; Barnes *et al.*, 2015) and the J-M Reef (e.g. Barnes and Naldrett 1985; Godel and Barnes, 2008), have been generally well studied. Aird *et al.* (2016) characterized the trace sulfide assemblages in the barren rocks of the complex. In brief, the sulfide assemblage associated with the Cl-rich part of the Peridotite zone are unusually rich in pentlandite, whereas pyrite increases up towards OB-I and again towards OB-II. Apart from the few sulfide-enriched zones noted by McCallum *et al.* (1980) and noted on Fig. 3, overall bulk-rock S concentrations and sulfide modes are lower than expected from a S-saturated magma (Keays *et al.,* 2012; Aird *et al*., 2016). There is extensive petrographic evidence of high-temperature S loss seen, for example, by the partial replacement of sulfides by Ti-free iron oxide in otherwise fresh rocks (e.g. Barnes *et al.*, 2015, Aird *et al.*, 2016).

In contrast, the Pd and Pt concentrations in the rocks below the J-M Reef are unusually high, with bulk-rock concentrations that typically equal or exceed the assumed concentrations of the parent magma (Keays *et al.,* 2012). A similar trend is seen in the Bushveld complex (e.g. Maier and Barnes, 1999). If the magma was not yet sulfide saturated and no other phases host significant amounts of these elements then the concentrations should be determined by the trapped liquid abundance and should be no more than a few ppb at most (e.g. Barnes and Campbell, 1988). Keays *et al.* (2012) interpreted the high Pt and Pd concentrations to these elements behaving as compatible rather than excluded elements, but do not discuss which mineral is the host phase. In contrast, Kanitpanyacharoen and Boudreau (2012) and Aird *et al.* (2016) suggested that the rocks were sulfide-saturated, but later lost S and some ore metals during degassing of the crystal pile. They suggested that the ore metal distribution in both the Stillwater and Bushveld complexes could have developed by vapour refining of the crystal pile by chloride-carbonate-rich fluids during which sulfur and sulfide are recycled continuously, with sulfur moving from the interior of the crystal pile to the top during degassing.

Parent magma(s)

The intrusive rocks of the sill/dyke suite beneath the complex have been analysed by Helz (1985), who defined five compositional groups. She considered the group 2 and group 3 rocks to be the most likely candidates for Stillwater parent liquids, the others being fractionated, contaminated, or not liquid compositions. Premo *et al.* (1990) undertook U-Pb and Sm-Nd age determination of the sill/dyke suite and found the groups 1 and 4 to be slightly older than the Stillwater Complex whereas the groups 2, 3 and 6 are of similar age as the complex. More recently, however, Helz (1995) proposed that a mixture of magma types was required to produce the proper crystallization sequence.

These and a variety of other proposed parent magma compositions have been summarized by McCallum (1996, table 2 of that report). Briefly, most can be described as light rare-earth element (*REE*)-enriched, Ti-poor, siliceous high-magnesium basalts (SHMB), of which boninites would be the modern-day equivalent (e.g. Sun *et al.,* 1989)

https://doi.org/10.1180/minmag.2016.080.063 Published online by Cambridge University Press

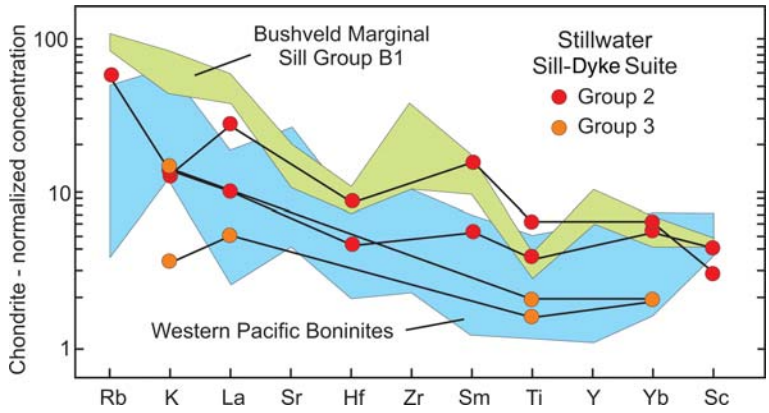

FIG. 4. Comparison of the Stillwater Group 2 and 3 sill/dyke suite rocks with other siliceous high-magnesium basalts (SHMB). After Boudreau *et al.* (1997).

(Fig. 4). As summarized by Crawford *et al.* (1989), boninites crystallize abundant pyroxene, have late plagioclase saturation, and can have olivine and chromite as phenocrysts. In addition, the formation of boninites by second stage hydration melting in the mantle has consequences for the halogen geochemistry of the Stillwater Complex, as noted below.

Hamlyn and Keays (1986) noted that the second-stage mantle melting origin of SHMB make them excellent source magmas for PGE deposits such as the J-M Reef. They proposed that some residual sulfide remains in the mantle during an initial or 'first-stage' partial melting event. Owing to the very high (sulfide liquid)/(silicate liquid) partition coefficients this residual sulfide retains much of the PGE and the first-stage liquids are consequently PGE-poor. Mid-ocean ridge basalt (MORB) is a possible example of such a PGE-poor first-stage melt, as this magma typically contains <1 ppb Pd (Hamlyn and Keays, 1986, and references therein). During a second melting event, however, the melt incorporates the residual PGE-rich sulfides to produce a relatively Mg-rich, Ti-poor magma that is also S poor but PGE rich. Again, the modern equivalent would be boninites, which contain typically ~15 ppb Pd and are sulfur-undersaturated at the time of eruption (e.g. Hamlyn *et al.,* 1985).

Boudreau and McCallum (1989) found that the Group 2 and 3 apatites had a higher chlorapatite component than did apatite from the other groups and, except for the Bushveld Complex, have high Cl concentrations compared with other intrusions as well. However, they are not as Cl rich as are seen in the rocks of the Ultramafic series and Lower Banded series below the J-M Reef. These group 2 and 3 apatite halogen concentrations were similar to apatite in the host hornfels.

Boudreau *et al*. (1997) suggested that the second stage mantle hydration-melting event postulated for boninite formation (e.g. Crawford *et al.,* 1989) would also add Cl and could explain the unusually high Cl concentrations of the Stillwater system. Boudreau also noted that volatiles are generally not considered in parent-magma experiments and model results but can strongly affect phase saturation. For example, addition of water will suppress the crystallization of plagioclase and enhance chromite and olivine crystallization (e.g. Kushiro *et al.*, 1968; Ford *et al.*, 1972; Kushiro, 1975) and is an alternative to the dry magma-mixing scheme proposed by Helz (1995) to produce the apparent crystallization sequence of Stillwater parent liquids as discussed below.

Isotopic and magnetic paleointensity variations

Shown in Fig. 5 are variations in radiogenic and stable isotope compositions and paleointensity variations, plotted against stratigraphic height. The latter have been used to infer that there has not been significant variation in the average strength of the Earth's magnetic field over the last 2.7 Ga (Selkin *et al.*, 2000, 2008).

A Sm-Nd isochron on mineral separates from a Gabbronorite zone I sample from the West Fork Adit portal gave an age of 2701 ± 8 Ma (DePaolo and Wasserburg, 1979). Nunes (1981) determined an age of 2713 ± 3 Ma on zircons from the Basal

https://doi.org/10.1180/minmag.2016.080.063 Published online by Cambridge University Press

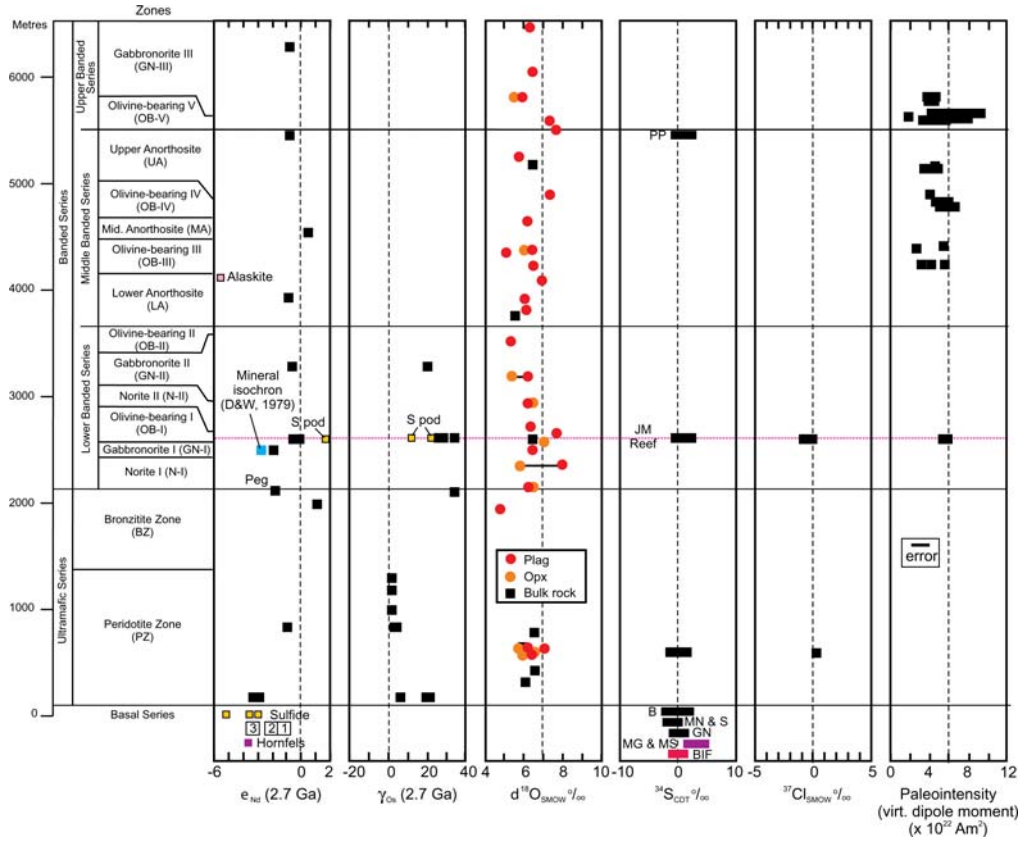

FIG. 5. Stratigraphic trends in the radiogenic isotope, stable isotope, and magnetic paleointentisty variations in the Stillwater Complex. γ_{Os} is the percent deviation from a chondritic reservoir with an initial Os isotopic composition at 2.7 Ga. Abbreviations of sulfur isotopes: BIF, banded iron formation; MG, meta-graywacke; MS, meta-shale; GN Gabbronorite; MN, mafic norite; S, massive sulfide stringers; B, Basal series; JM, J-M Reef; PP, Picket Pin PGE-sulfide zone. Paleointensity reported as virtual dipole moment, the equivalent geocentric dipole moment required to produce the observed paleointensity. Data from DePaolo and Wasserburg (1979), Lambert *et al.* (1994), Dunn (1986), Zientek and Ripley (1990), Boudreau *et al.* (1997) and Selkin *et al.* (2008). Errors for the paleointensity can be considerably more or less variable than the typical error shown; for the others the reported errors are equal to or less than the symbol size.

series and Premo *et al.* (1990) determined a U-Pb zircon age of 2705 ± 4 Ma for seven analyses from two samples from the Lower Banded series. Ongoing work by Corey Wall and James Scoates at the University of British Columbia is attempting to discern age variations within the complex. The data presented in abstracts to date suggests zircon and baddeleyite in the central portions of the complex are younger than those at the bottom and top of the complex (e.g. Wall *et al.*, 2009, 2012).

Isotopic variations at different stratigraphic levels in the complex have otherwise been used to infer parent-liquid affinities from initial isotopic ratios (see McCallum, 1996, for a review). However, recent work in the Bushveld complex and other intrusions has shown coexisting minerals are commonly out of isotopic equilibrium and with core-rim isotopic differences in individual minerals (e.g, Harmer *et al.*, 1995; Mathez and Waight, 2003; McBirney and Creaser, 2003; Chutas *et al.*, 2011). These studies demonstrate that inferences of the isotopic nature of the magma that precipitated the rocks using whole rock or even mineral separates can give erroneous results. In some cases, including the Stillwater Complex, it is clear the isotopic disequilibrium is the result of later alteration, particularly for Pb (e.g. McCallum *et al.*, 1999; Wall *et al.*, 2010; Friedman *et al.*, 2011) and

https://doi.org/10.1180/minmag.2016.080.063 Published online by Cambridge University Press

Sr (DePaolo and Wasserburg, 1979), which were affected by the mid-Proterozoic heating event.

However, in other cases it appears that the long periods of slow cooling over the ~100 ka estimated for large intrusions such as the Stillwater and Bushveld complexes to crystallize (e.g. Cawthorn and Walraven, 1998) can allow for cryptic infiltration of radiogenic components. For example, Bushveld pegmatoids can have different (enriched) isotopic signatures than the host rock (e.g. Prevec *et al.*, 2005). These studies suggest that late melts or fluids migrating through the crystal pile may be in local chemical equilibrium but out of isotopic equilibrium with the mineral assemblage, and it is only during a recrystallization event that this enriched signature is imparted to the crystals. As seen in Fig. 5, pegmatoidal rocks of the Lower Banded series, small bodies of massive sulfide associated with the J-M Reef, and an unusual alaskite associated with the Lower Anorthosite of the Middle Banded series (Czamanske *et al.,* 1991) can have markedly different isotopic signatures than other rocks of the Banded series. It would be especially instructive to learn the isotopic characteristics of the fluid inclusions described by Hanley *et al.* (2008), for example. Detailed studies that might look into the possibility of isotopic disequilibrium imparted during crystallization and solidification of the Stillwater Complex have yet to be done.

Sill/dyke unit

The sill/dyke unit has been conflated with the Norite zone of the Basal series (Page, 1979, Zientek, 1983), although it is beneath the Stillwater Complex proper. Textures are best seen on weathered surfaces; it can otherwise be difficult to tell intrusive rocks from the hornfels. The igneous rocks are typically no more than several metres in maximum dimension and can have finer-grained (chilled) margins. Norites and gabbronorites with a diabasic texture and that are typically poor in sulfides are most commonly associated with the hornfels, whereas a mafic norite in which sulfides make up from 2 to 40 vol.% of the rock occurs proximal to the Stillwater Complex (Page, 1979; Zientek, 1983). Olivine, common in the Peridotite zone, does not appear to be present in any of these rocks, even as resorbed cores in orthopyroxene (M. Zientek, USGS, pers. comm.). The only olivine-bearing samples were found in a drill hole from the Crescent Creek area (drill hole CC-2) and define the group 6 sill/dyke compositional group of Helz (1985).

Iron-nickel-copper sulfides, present as disseminated to small bodies of massive sulfide, are common from Mountain View east to the Benbow mine area. Sulfide is also concentrated in the lowermost portion of the Basal series but decreases markedly once one moves into the upper part of the Basal Bronzitite and the Peridotite zone. The bulk rock Cu + Ni content of the sulfide-bearing rocks average 0.5 wt.% with a Ni/Cu ratio of ~1.0. Zientek *et al.* (2008) note that average bulk-rock Pt + Pd + Rh = 20 ppb for all mineralized rock types that included the Basal series rocks and the maximum rarely exceeds 200 ppb, with Pd > Pt > Rh and with a poor correlation with sulfide mode.

Based on the low PGE tenor of the sulfide and similar S isotope composition as the banded iron formation, Zientek and Ripley (1990) suggested that S was derived from the iron formation and assimilated into a limited volume of magma at the base of the complex. It is noted, however, that the iron formation occurs nearest the complex only along the middle sections and is otherwise rare or not associated with the better-mineralized footwall regions. In contrast, Vaniman *et al.* (1980) noted that the contact-metamorphosed iron formation have sulfides (pyrite, pyrrhotite, chalcopyrite) associated with the olivine-bearing metamorphic assemblage and associated with fractures. They suggested that Cu and S in the iron formation were introduced from the Stillwater Complex.

Basal series

The irregular lower contact of the Basal series is unconformable with footwall stratigraphic units and it has been interpreted that the Stillwater magma intruded along a low-angle fault. Post-intrusion faulting has removed the Basal series in the central part of the complex (Fig. 1). The Basal series is divided into a lower Basal Norite zone and an upper Basal Bronzite (orthopyroxenite) zone. As for the sill/dyke igneous rocks, olivine is mostly absent, even as resorbed cores to orthopyroxene.

The Basal Norite zone is composed of norites with subordinate anorthosite, gabbro, and peridotite, all with and without sulfide mineralization. Orthopyroxene textures are typically subophitic. Although layered, the rock units are laterally discontinuous and difficult to correlate between drillholes. Large xenoliths of country rock can make locating the base of the complex from drill core difficult, as the Basal Norite can be texturally similar to the sill/dyke norite. The Basal Norite

https://doi.org/10.1180/minmag.2016.080.063 Published online by Cambridge University Press

zone grades into the Basal Bronzite zone with decreasing plagioclase mode (Page, 1979). The Basal Bronzite is composed of a granular orthopyroxenite that is texturally similar to pyroxenites of the Ultramafic series.

The lower part of the overlying Peridotite zone of the Ultramafic series is characterized by a systematic increase in the Mg# of olivine and orthopyroxene (Raedeke and McCallum, 1984), and although no studies of mineral composition trends in the Basal series have been undertaken, it is assumed that the Basal series would show a similar trend. These Mg# enrichment trends have similarities with those seen in other intrusions (e.g. Latypov, 2015). One possible cause is a progressive upwards decrease in the amount of trapped liquid, perhaps caused by more efficient compaction prior to final solidification of the rocks (Raedeke and McCallum, 1984).

However, the change from norite to orthopyroxenite in the Basal series occurs without any significant involvement of olivine. This would imply that the earlier magmas were more evolved or contaminated compared to later magmas, perhaps partly crystallizing and/or contaminated in a cooler feeder system until the plumbing system became fully established. If so, this has implications for using the sill/dyke rocks as proxies for the Stillwater parent magma. The observation that the apatite in this section becomes more Cl rich (Boudreau and McCallum, 1989) suggests yet a third possibility, that olivine was stabilized by the expansion of the olivine-phase field by vapour moving out to the crystallizing mush near the base of the complex. This possibility is explored more fully below.

Ultramafic series

The base of the Ultramafic series is defined by the first appearance of modally significant amounts of olivine, and the top at the level where plagioclase becomes a major modal mineral in the first norites of the Banded series. The thickness of the Ultramafic series ranges from 840 m at Chrome Mountain to ~2000 m at Mountain View (Raedeke, 1982; Raedeke and McCallum, 1984).

Peridotite zone

As noted above, the Peridotite zone is composed of a sequence of cyclic units; a complete cyclic unit averages just over 200 m in thickness and consists of the stratigraphic sequence of poikilitic harzburgite (± chromite) → granular harzburgite → orthopyroxenite. This 'ideal' sequence (Fig. 6*a*) is not always present and units may be missing from top or bottom. In detail there can be significant textural and modal variations within an individual cycle as well (Fig. 6*b*). For example, Page *et al.* (1972) subdivided the peridotite member in cyclic unit 2 from the Nye Basin into nine subunits. The possibility of secondary replacement further complicates interpretation.

Discordant dunites

In the lower parts of the Peridotite zone in the western parts of the complex discordant bodies of dunite are common. These are composed almost entirely of olivine with minor orthopyroxene oikocrysts and chromite. In form, they are broadly similar to some of the discordant troctolite-anorthosite bodies found in the Middle Banded series described below. As described by Raedeke and McCallum (1984) and McCallum (1996), these secondary bodies appear locally to replace original modal layering whereas elsewhere they cut layering. The latter may have abrupt terminations with overlying layers (Fig. 6*b*). Olivine and orthopyroxene compositions are similar to those of the host rock. However, the rocks are commonly serpentinized and have not been otherwise extensively studied. Associated with these bodies are pyroxene-rich pegmatoids that can have coarse-grained chromite concentrated along the contact with the host rocks. McCallum (1996) suggested that the dissolution of orthopyroxene during the replacement process released Cr that precipitated as chrome spinel.

The poikilitic/granular harzburgite transition

The contact between poikilitic harzburgite and the overlying granular harzburgite is marked by an abrupt increase in the amount of orthopyroxene and a change in the orthopyroxene texture from poikilitic to equigranular. While many of the contacts in the Ultramafic series are described as planar and conformable, the contact between the poikilitic and granular harzburgite is commonly described as irregular, and locally the poikilitic harzburgite may form 'fingers' intruding into the overlying granular harzburgite (Fig. 7). Layering in granular harzburgite can occur on a centimetre scale in the form of layers alternately rich in olivine or orthopyroxene.

https://doi.org/10.1180/minmag.2016.080.063 Published online by Cambridge University Press

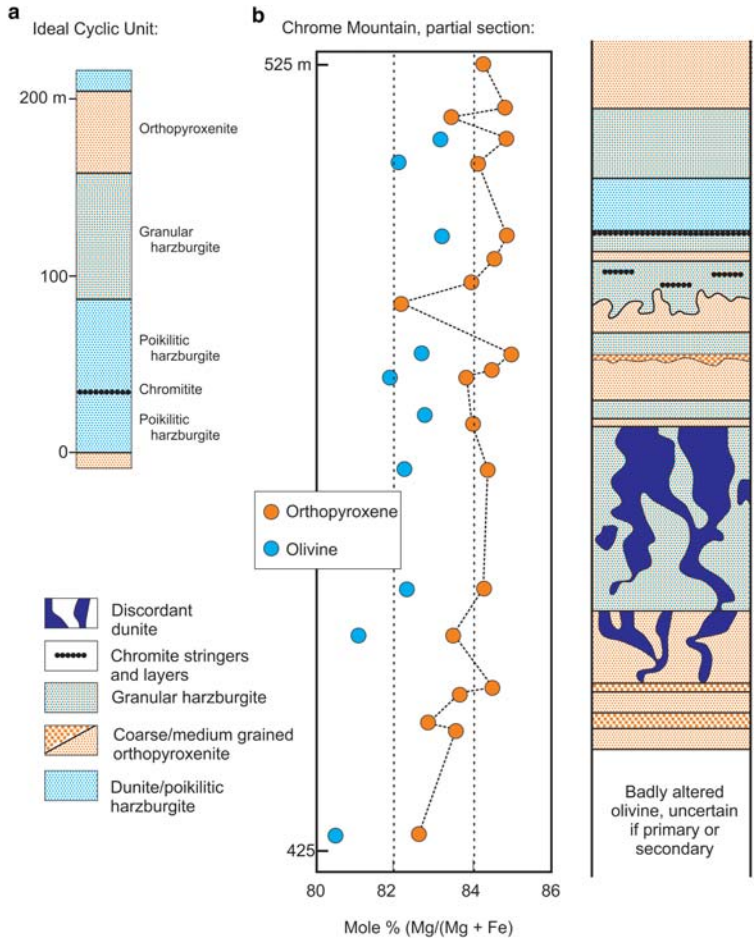

FIG. 6. Cyclic units of the Peridotite zone of the Stillwater Complex. (*a*) 'Ideal' Peridotite zone cyclic unit (After Jackson, 1963). (*b*) Detail of part of the Peridotite zone from Chrome Mountain, with olivine and orthopyroxene mineral composition trends. Redrawn after Raedeke and McCallum (1984); the middle of the section shown is 2/3 up into the Peridotite zone at Chrome Mountain.

Raedeke and McCallum (1984) suggested that this transition represents a turbulent mixing zone that became frozen into the final rock. However, the finger structures are typical of structures that developed during reactive focused flow in porous media (e.g. Kelemen *et al.,* 1995), and suggests that the irregular boundary represents a reaction front formed during solidification of the crystal-liquid mush. A simple model might envision interstitial liquid becoming enriched in volatile components degassed from cooled underlying interstitial liquids. This enrichment in volatiles could expand the olivine-phase field such that the olivine-orthopyroxene boundary changes from an equilibrium cotectic boundary to a peritectic reaction boundary. In this sense, the replacement is similar to that seen in the discordant dunite bodies.

Chromitites

Classic works on the chromitites of the Ultramafic series include that of Peoples and Howland (1941) and Jackson (1961). More recent work includes Page (1971), Foose and Nicholson (1990), and Talkington and Lipin (1986) on associated sulfide and PGE minerals; Loferski *et al*. (1990) on a detailed study of the lowermost cyclic unit; Lipin (1993) on the potential importance of pressure fluctuations; Campbell and Murck (1993) on the G and H units; Waters and Boudreau (1996) on a

https://doi.org/10.1180/minmag.2016.080.063 Published online by Cambridge University Press

FIG. 7. Photograph of fingers of poikilitic harzburgite replacing granular harzburgite on a boulder near the main portal of the Mountain View mine. Length of hammer head is ~17 cm.

re-interpretation of crystal size distribution (CSD) curves; Cooper (1997) on apparent unconformities; Horan *et al.* (2001) on Os isotopes; Spandler *et al.* (2005) on multiphase inclusions in the chromite; Pagé *et al.* (2011) on late textural maturation and recrystallization; Lenaz *et al.* (2012) on chromite variations seen in single-crystal x-ray diffraction analyses; and Barnes *et al.* (2015) on the PGE and chalcophile element distribution.

Layers of massive and disseminated chromite occur in the peridotite member of many but not all of the cyclic units. The main chromitite seams are traditionally referred to as A (lowermost) through K (uppermost). This labelling can be complicated by the fact that some zones can have multiple thick chromitites, such that the G and H at Mountain view actually have a G, G′, H and H′ chromitite. Furthermore, these units can be made up of numerous smaller interlayered chromitite/dunite-harzburgite units (Fig. 8).

Jackson (1961) noted the lognormal size distributions of chromite and olivine are similar to those seen in sedimentary rocks (Fig. 9*a*), but that otherwise the olivine and chromite are not 'hydraulically equivalent'. That is, although the chromite is denser, the greater size of the olivine implies a faster settling velocity. In contrast, Waters and Boudreau (1996) noted that crystal size distribution (CSD) curves for chromite are similar to those CSD curves that evolve during crystal ageing, during which larger grains grow at the expense of smaller grains owing to surface energy considerations (Fig. 9*b*).

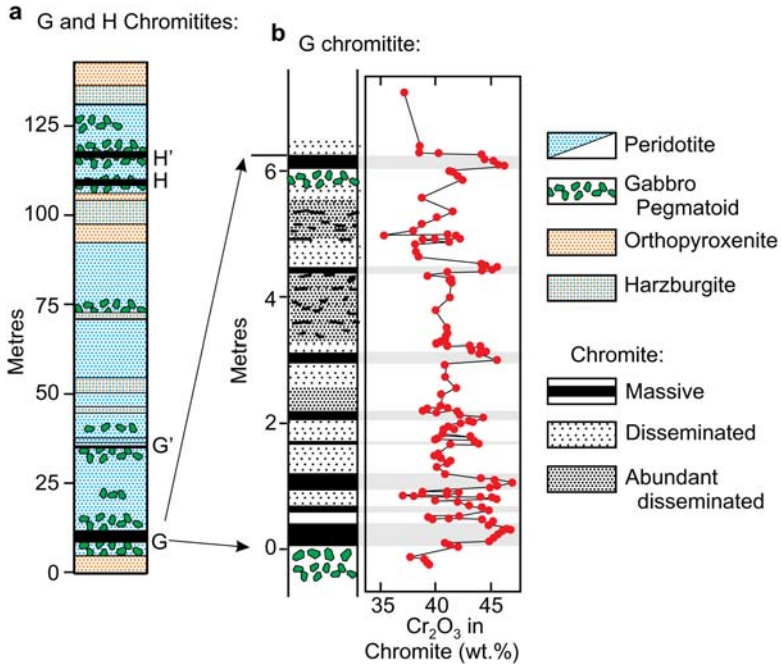

FIG. 8. Detail of chromitite units. (*a*) The G and H chromitite units as exposed at Mountain View. (*b*) Detail of the G chromitite, note higher Cr_2O_3 concentrations in chromite in the massive chromitite layers. Redrawn after Campbell and Murck (1993).

https://doi.org/10.1180/minmag.2016.080.063 Published online by Cambridge University Press

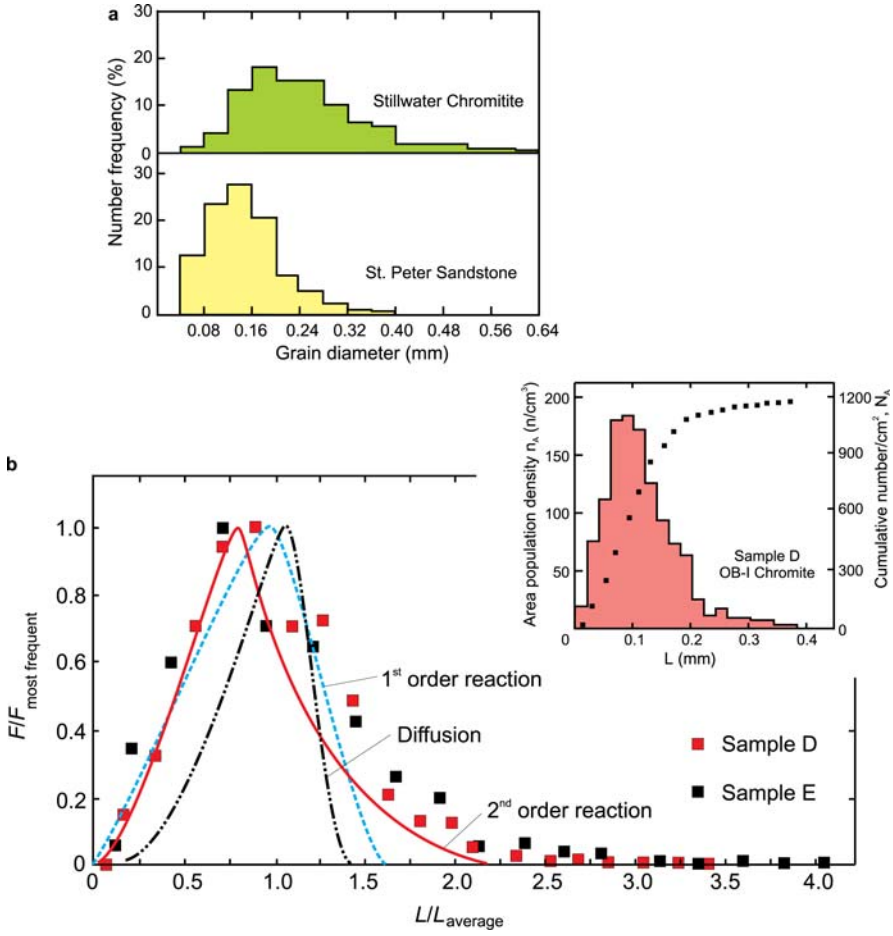

FIG. 9. Crystal size distribution (CSD) curves for Stillwater Chromite. (*a*) CSD comparison of Ultramafic series chromite with that of clastic sandstone grains. Redrawn after Jackson (1961). (*b*) Theoretical grain-size distribution curves for spherical grains as derived by Kahlweit (1975) for ageing controlled by diffusion, by first-order, or second-order crystal-growth kinetics (labelled curves). Also shown is the size distribution of chromite grains in two samples (D and E) from a thin chromitite layer from OB-I (Fig. 15*e*). The grain size, L, is normalized to the mean grain size, $L_{average}$ whereas the grain-size frequency, F, is normalized to the maximum value, $F_{most\ frequent}$. (Inset) Size-frequency histograms of the number of grains of a given size interval, n_A (shaded red), and cumulative frequency, N_A (black squares), for sample D.

Modal layering in chromite-bearing rocks ranges from poor to well layered, with the latter occurring on scales from ~metre-thick down to laterally extensive chromitite layers only a grain or two thick. Boudreau (1994, 1995) suggested that surface energy is a function of the surrounding minerals such that chromite has a lower free energy when surrounded by other chromite crystals rather than silicate minerals. This can lead to phase segregation over long cooling times to produce well-defined fine-scale modal layering. For example, modelling of crystal ageing in a two-crystal system in which the growth by crystal ageing of one phase (chromite) is faster than another (olivine) has shown that the system will evolve into olivine-only and olivine + chromite domains (Boudreau, 1994) (Fig. 10*a*). Figure 10*b* has been compiled from the data of Jackson (1961) on grain size variations in igneous layering composed of olivine and chromite from the Ultramafic series of the Stillwater Complex; chromite is shown black, olivine in white. While the initial modal distribution

https://doi.org/10.1180/minmag.2016.080.063 Published online by Cambridge University Press

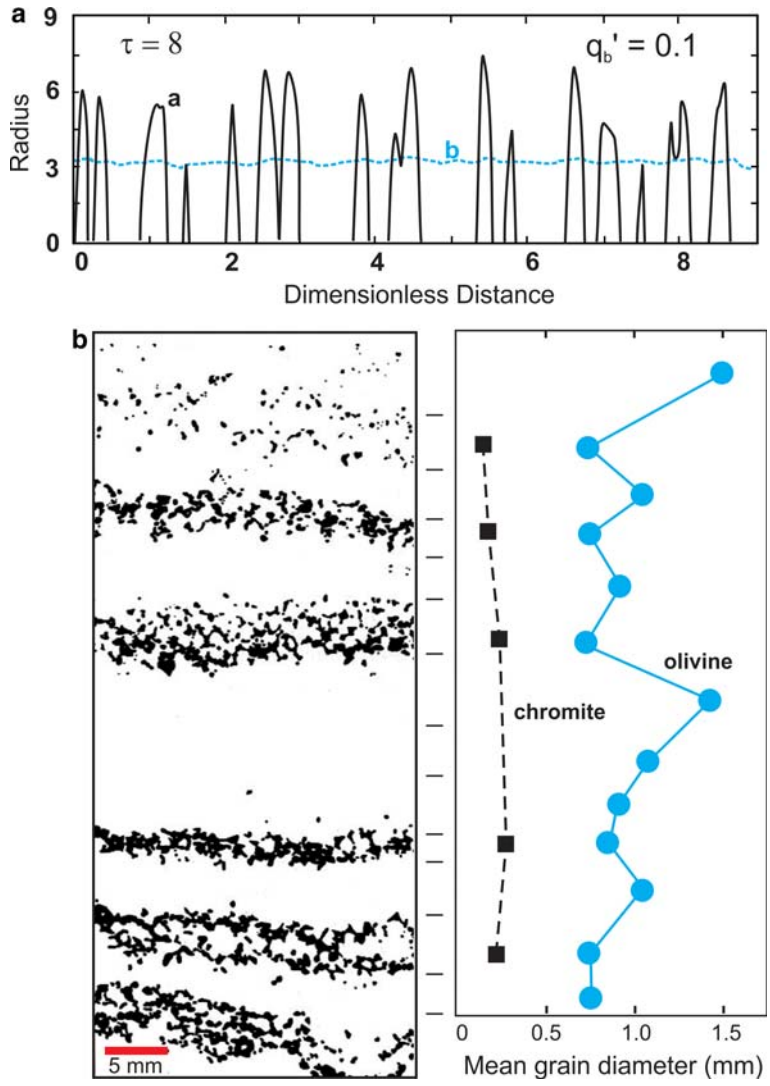

FIG. 10. Modelling chromitite layering as a consequence of pattern formation that can result from crystal ageing. (*a*) Result of numerical modelling in which an initial mixture of two grains, **a** and **b**, have different crystal ageing growth rates such that crystal **a** grows an order of magnitude faster that mineral **b**. Not shown is the original size distribution, which consisted of a uniform mixture of the two crystals but with minor size variations of both mineral **a** and **b**. The result shown is that regions of larger grains of **a** grow at the expense of nearby smaller **a** grains. The final result is a pattern of **a** + **b** – **b** – **a** + **b** – **b** …. Redrawn after Boudreau (1994). (*b*) Example of grain-size variations in olivine + chromite rock from the Peridotite zone (after Jackson, 1961). Chromite is shown black, olivine in white. Note the pattern is olivine – olivine + chromite – olivine and that olivine is largest in layers where chromite is absent.

of the minerals may have been induced by any number of nucleation or crystal-settling events, several features of this sample are consistent with at least additional development or enhancement of the layering during ageing of the cumulates.

(1) The layers are composed either entirely of olivine alone or of olivine + chromite. This is the predicted sequence if chromite is the phase that is the more active ageing phase. In contrast, the larger olivine grains would be less likely to locally

https://doi.org/10.1180/minmag.2016.080.063 Published online by Cambridge University Press

dissolve completely, because a larger average size implies that there is both more material per grain that must be transported and smaller concentration gradients in which to accomplish the segregation. (2) The thin chromite-rich layers are consistent with the numerical results that show that the more actively ageing crystal will typically develop relatively thin layers. There is also a tendency for the chromite layers both observed and in the model to form crude paired layers or 'doublets' (see also the discussion of inch-scale doublets of the Banded series below). (3) Layer contacts are relatively sharp. This points out an important feature of this mechanism: igneous layering that is either produced or enhanced by ageing is self-defining in that layers become more distinct with time. (4) The larger average grain size of either olivine or chromite occurs in those layers in which that mineral is volumetrically dominant. This is a predicted consequence of mineral ageing; ageing will be more rapid if grains are in contact with other grains of the same mineral as compared to the case in which they are separated by large distances or by another mineral phase.

Chromitite formation models

The formation of thick chromitite layers has been a longstanding petrological problem. If precipitated directly from a magma, the thick chromitite layers require an extensive period of crystallization of chromite alone, a mineral which otherwise would only crystallize in cotectic proportions of just a few percent. A number of models have been proposed to explain this, and are summarized in Fig. 11.

In brief, these models can be classified into one of five types. (1) magma-magma mixing in which an injection of primitive magma and mixing with fractionated magma drives the mixed magma into the chromite-only field (Fig. 11*a* dashed red mixing line) (e.g. Irvine, 1977; Campbell and Murck, 1993). (2) Contamination with a silica-rich composition (melted roof rock) moves the liquid into the chromite only field (Fig. 11*a* dashed blue mixing line) (e.g. Irvine, 1975; Spandler *et al.*, 2005). (3) Pressure changes on the magma chamber cause shifts in the chromite cotectic boundary such that an increase in the pressure on the magma moves the cotectic to crystallize chromite alone (Fig. 11*b*) (e.g. Loferski *et al.*, 1990; Lipin, 1993). (4) An increase in H_2O and/or other volatiles can also move the chromite cotectic such as to drive the magma to crystallize chromite alone (Fig. 11*c*) (e.g. Ford *et al.*, 1972). (5) Hydration melting of a chromite ± orthopyroxene ± olivine mush preferentially leaves behind chromite as a residual (restite) mineral (Fig. 11*d*) (e.g. Nicholson and Mathez, 1991; Armitage, 1992).

The first two models involve changes to the magma composition to drive it into the chromite-only phase field. The third involves changes in the chromite phase boundary as a result of a physical change on the magma chamber (pressure) without any significant change in magma composition, the fourth and fifth involve the addition of H_2O and the strong effect this has on shifting phase boundaries and the flux melting of the original magmatic assemblage.

The hydration models 4 and 5 have not been extensively called upon to explain the Stillwater chromitites outside of the smaller chromite seams that occur, for example, at the margin of the pegmatoids noted above and the minor chromite that occurs in Olivine-Bearing zone I (e.g. Boudreau, 1999). However, several lines of evidence are consistent with such a process operating in the main chromitite seams. These include: (1) the increase in Cl in apatite and the halite inclusions in olivine noted previously are consistent with a Cl-rich vapour moving upwards through the crystal pile. (2) Polyphase inclusions in chromite, interpreted to have crystallized from melt inclusions, are rich in volatiles (Spandler *et al.*, 2005), implying that the chromite grew from hydrated magmas (Fig. 12). Although Spandler *et al.* (2005) suggested the melt inclusions came from melting roof rock, contact metamorphism tends to produce an anhydrous assemblage, suggesting that the roof would have dehydrated prior to melting. (3) Discordant dunite may terminate at the tops of layers (Raedeke and McCallum, 1984, and Fig. 6), consistent with vapour having been injected directly into the chamber. (4) Injection of S-bearing vapour can lead to a local saturation of the magma in sulfide, which can be later lost (in part) to leave residual laurite as an insoluble phase. The result is elevated PGE, and particularly the less soluble IPGE (IPGE = Os, Ir, Ru) and Rh which strongly favours chromite but low bulk-rock S and the more soluble Pt and Pd owing to loss to continued degassing (e.g. Boudreau and McCallum, 1992*a*; Barnes *et al.*, 2015). (5) The increase in H_2O can change the olivine-orthopyroxene boundary from an equilibrium cotectic boundary to a peritectic relationship. This would suggest that the poikilitic harzburgite, the typical host to the chromite, crystallized from a magma with higher H_2O concentration than did the granular harzburgite. (6) Pagé *et al.* (2011) note that the chromite has

https://doi.org/10.1180/minmag.2016.080.063 Published online by Cambridge University Press

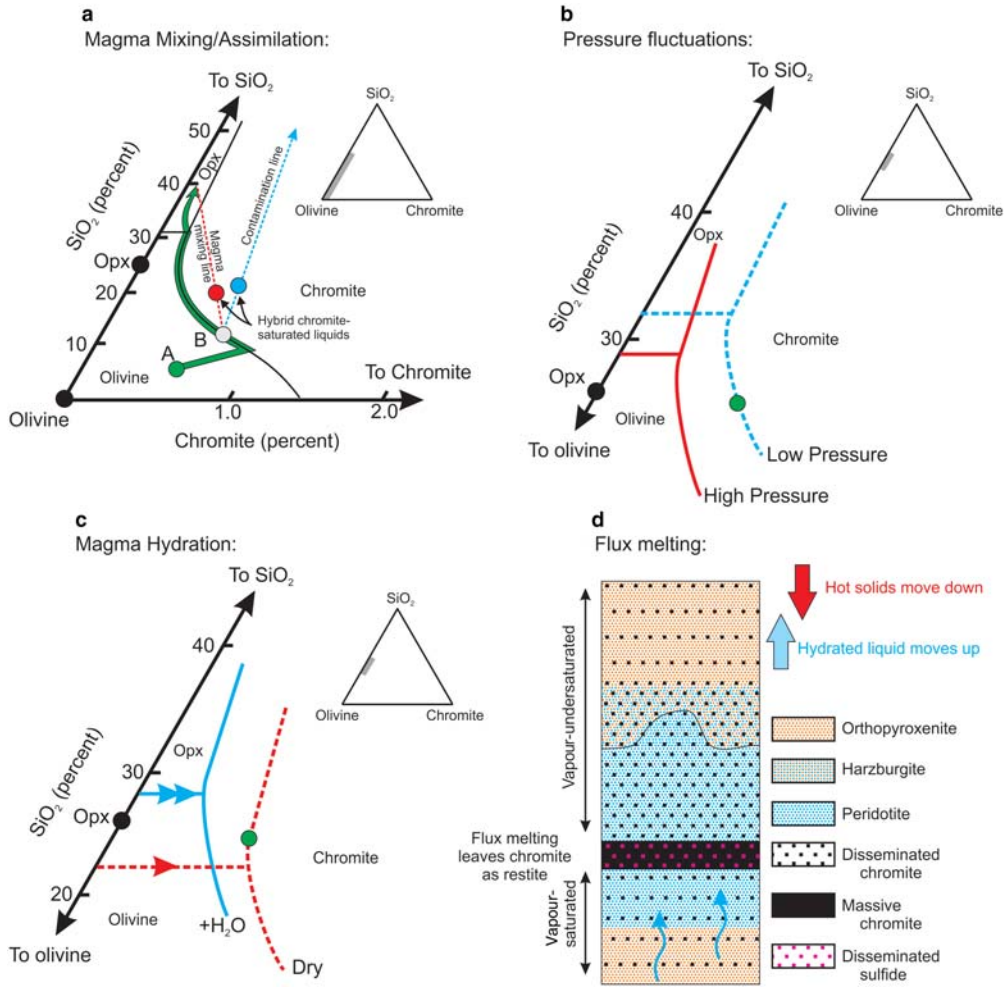

FIG. 11. Proposed models for formation of chromitites. (*a*) Detail of the chromite–olivine–SiO_2 systems showing a possible normal fractionation path for a liquid starting in the olivine phase field at point 'A'. After Irvine (1975, 1977). Also shown are mixing paths that pull an olivine + chromite-saturated liquid (point 'B') into the chromite field. The red dashed 'Magma mixing line' is the range of hybrid compositions produced by the mixing of liquid 'B' with more evolved, orthopyroxene-saturated liquid at the end of the green line. The 'Contamination' line is the hybrid compositions produced by mixing 'B' with a SiO_2-rich crustal assimilant (e.g. Spandler *et al.*, 2005). (*b*) Effect of changing pressure on the chromite phase field: Liquid on the olivine-chromite cotectic at low pressure (green circle on the blue dashed line), will become chromite saturated if pressure on the chamber increases. After the model suggested by Loferski *et al.* (1990) and Lipin (1993). (*c*) Effect of H_2O addition to magma to expand the olivine and chromite phase fields: Liquid on orthopyroxene-chromite cotectic in a relatively 'dry' magma (green circle on the red dashed line) becomes saturated in chromite alone with the shift of phase boundaries after the addition of H_2O (blue solid line). Note that expansion of the olivine field changes olivine-orthopyroxene from a cotectic in the dry system (red lines) to a peritectic in the wet (blue lines). Redrawn after Ford *et al.* (1972). (*d*) Flux melting model in which vapour exsolved from crystallizing interstitial liquid deeper in the crystal pile moves upwards until it encounters liquid that is not yet vapour saturated. Redissolution of vapour leads to sulfide saturation and partial melting leaving chromite ± olivine as a residual assemblage. Expanded after Armitage (1992).

https://doi.org/10.1180/minmag.2016.080.063 Published online by Cambridge University Press

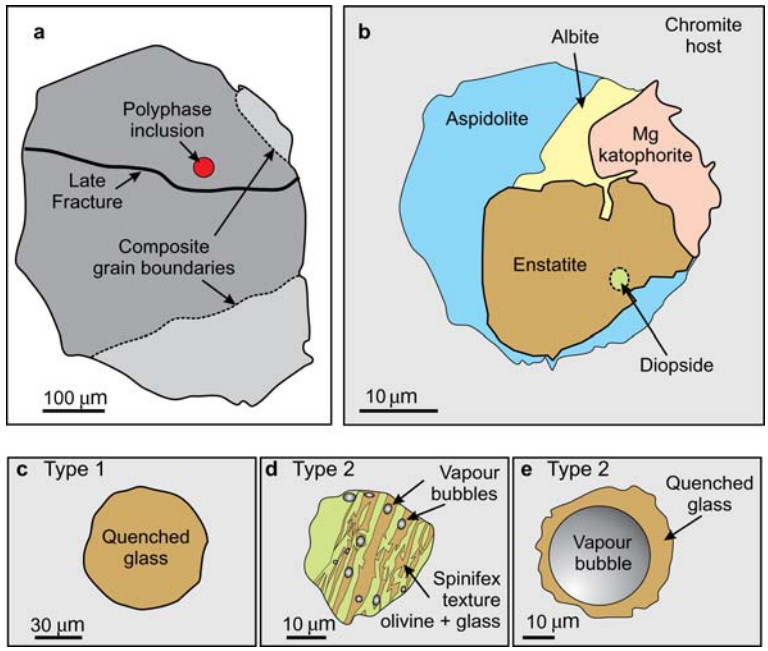

FIG. 12. Examples of polyphase inclusions in chromite from the G chromitite cyclic unit, Stillwater Complex, Montana. (*a*) Chromite grain with composite grain boundaries and polyphase inclusion (shown in red). (*b*) Detail of the inclusion shown in (*a*). Enstatite and aspidolite (Na-phlogopite) compose the majority of the inclusions, but can also include magnesio-katophorite (Na-Ca amphibole), albite, and diopside. (*c*–*e*) Three types of inclusions observed after reheating to 1450°C. (*c*) Type 1: quenched glass with no vapour bubbles. (*d*) Type 2: spinifex texture olivine + glass with some vapour bubbles. (*e*) Type 3: crystal free, vapour-rich. Redrawn after Spandler *et al*. (2005).

high-Ti concentrations, much higher than expected for a chromite crystallized from a boninite-like low Ti SHMB magma (Fig. 13). However, incongruent melting of orthopyroxene would liberate Ti as well as Cr, both of which would then be incorporated into the chromite. (7) The rocks that have both

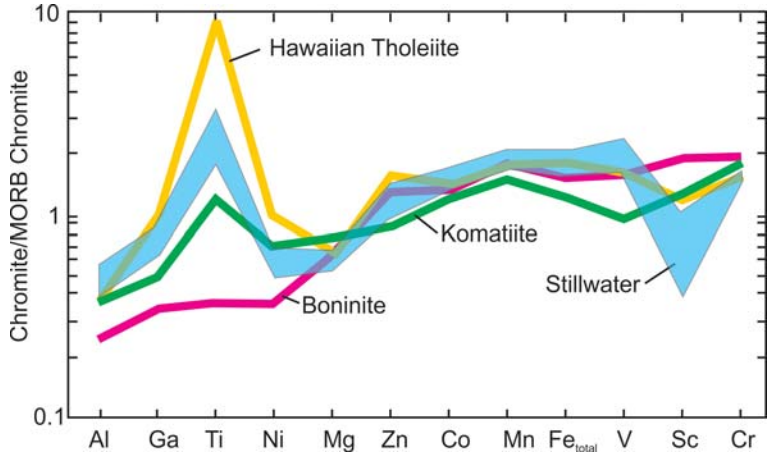

FIG. 13. Trace-element composition of chromite from the Stillwater Complex massive chromitites compared to chromite from komatiite, boninite and Hawaiian tholeiite, all of which have been normalized to the composition of MORB chromite. Redrawn after Pagé *et al.* (2011).

https://doi.org/10.1180/minmag.2016.080.063 Published online by Cambridge University Press

olivine and chromite can have chromite far in excess of cotectic proportions, consistent with enrichment by a partial melting model leaving chromite ± olivine as residual minerals.

The models presented are not necessarily independent of each other. For example, one could imagine that a conventional magma-mixing event pushes the hybrid magma into the chromite-only phase field. After accumulation on the floor, the assemblage is then further enriched in chromite by hydration melting and loss of the partial melt as vapour from the underlying mush migrates upwards into the hotter, vapour-undersaturated assemblage.

Bronzitite zone

The Bronzitite zone is described as relatively uniform except for a few thin layers containing olivine ± chromite that occur near the base and the top of the unit. However, grain size can change abruptly within the unit. The orthopyroxenites that make up the bulk of this zone are otherwise texturally and modally similar to those that occur in the Peridotite zone (Raedeke and McCallum, 1984).

Chondrite-normalized *REE* patterns in mineral separates from both the Peridotite zone but especially the Bronzitite zone can have a modest negative europium anomaly (Lambert and Simmons, 1988; Papike *et al.*, 1995) (Fig. 14). This has been used to support the suggestion that the thick anorthosites of the Middle Banded series were formed with plagioclase that crystallized during crystallization of the Ultramafic series but was either resorbed (Hess, 1960) or failed to accumulate on the floor of the magma chamber (Raedeke and McCallum, 1984: see also the extensive discussion in McCallum, 1996). The latter idea is further supported by the observation that, like the plagioclase of the Middle Banded series anorthosites which show no significant stratigraphic variation in average An concentration, the orthopyroxene of the Bronzitite zone also shows very little compositional variation (Fig. 2). This is consistent with both zones having formed from a magma in which the composition stayed nearly constant as new magma influx balanced crystallization. However, given the possibility of recrystallization and interstitial liquid migration driven by compaction, pyroxene could have developed a negative Eu anomaly from an evolved, plagioclase-saturated interstitial liquid. Unfortunately, whole-rock analyses of the orthopyroxenite are not available.

The orthopyroxenite does have some similarities in terms of a large volume of compositionally uniform orthopyroxene with the orthopyroxene-rich 'tongue' of the Basal Sill of the Jurassic-age Ferrar Large Igneous Province in the McMurdo Dry Valleys in Antarctica. The Ferrar tongue was emplaced as an orthopyroxene-phyric mush and locally is in excess of 350 m thick (Marsh, 2004). Although volumetrically it is probably a much smaller volume of orthopyroxenite than present in the original extant Stillwater Complex, it does suggest that large volumes of orthopyroxene could have been carried into the Stillwater magma chamber.

As summarized by Papike *et al.* (1995), the transition from the Bronzitite zone into the

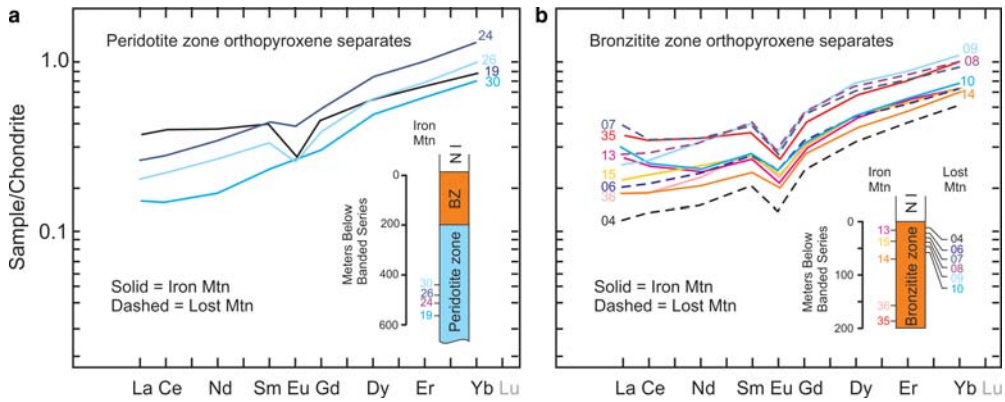

FIG. 14. Chondrite-normalized *REE* concentrations in orthopyroxene separates from (*a*) the Peridotite zone and (*b*) the Bronzitite zone. After Lambert and Simmons (1988).

https://doi.org/10.1180/minmag.2016.080.063 Published online by Cambridge University Press

overlying Banded series norite has the following characteristics: (l) norites immediately above the contact commonly contain pegmatitic and anorthositic segregations, and locally the layering is folded and disturbed (Thurber and McCallum, 1990); (2) selvages of chromite up to 3 mm thick are developed locally along the bronzitite-norite zone contact (Thurber and McCallum, 1990); (3) there is an increase in the amount of interstitial plagioclase and augite in the uppermost l0 m of the Bronzitite zone (Raedeke and McCallum, 1984); (4) orthopyroxene is compositionally homogeneous throughout the Bronzitite zone (Raedeke and McCallum, 1984); (5) there is a decrease in Mg/(Mg + Fe) (up to 4 mol.%), Cr_2O_3 and Al_2O_3, and an increase in TiO_2, from bronzitite to norite (Raedeke and McCallum, 1984; Lambert and Simmons, 1987; Papike *et al.*, 1995); (6) interstitial plagioclase in bronzitite has significantly higher (Ce/Sm), (Nd/Sm), and Eu/Eu* ratios relative to plagioclase in norite (Lambert and Simmons, 1988); (7) orthopyroxenes in both zones have similar absolute *REE* abundances, but the orthopyroxene in the Bronzitite zone has slightly higher (Ce/Yb) ratios and smaller Eu anomalies than does the orthopyroxene in the overlying norite. In the Mountain View area, orthopyroxene in a single norite sample also has distinctly higher Zr and Y abundances (Papike *et al.*, 1995).

The authors quoted in the above studies have proposed that the orthopyroxenite and the overlying norite formed from two separate magmas rather than a single magma following a liquid line of descent from orthopyroxene to orthopyroxene + plagioclase. An alternative interpretation might suggest that the changes in orthopyroxene composition (to lower Mg# in the norite unit) are caused by re-equilibration with an interstitial liquid in which the norite has a lower orthopyroxene/liquid mass ratio as suggested by the high Zr and Y concentrations noted above. Furthermore, compaction in a crystal mush in which there is a marked density contrast in the solid matrix across a boundary, such as occurs at the orthopyroxenite-norite transition that defines the base of the Banded series, can affect the compaction behavior. As modelled by Meurer and Boudreau (1996*c*), zones of high porosity can develop several meters below the actual boundary, and can explain the higher incompatible element concentrations and higher amounts of interstitial plagioclase and clinopyroxene just below the contact. Furthermore, as discussed more fully for the crystallization of the anorthosite units of the Middle Banded series, the interstitial liquid can evolve during crystallization and compaction. This evolved liquid signature can be imparted to the earlier phases during compaction-driven recrystallization or crystal ageing.

Lower Banded series and the J-M Reef

The Lower Banded series hosts the high-grade PGE zone, the Johns-Manville (J-M) Reef of Olivine-Bearing zone I (OB-I). Because of its economic importance, it has been the subject of a number of studies (e.g. Todd *et al*., 1982; Irvine *et al.*, 1983; Ryder and Spettel, 1985; Barnes and Naldrett, 1985, 1986; Lambert and Simmons, 1988; Page and Moring, 1990, Braun *et al.*, 1994 Boudreau, 1988, 1999; Godel and Barnes, 2008; Zientek *et al.*, 1990 and many more).

At the base of the Banded series, Norite zone I (N-I) consists of a modally and texturally uniform norite with cotectic proportions of plagioclase and orthopyroxene (Fig. 15*a*). While much of N-I is massive and modally uniform, pegmatoid and modal layering are common just above the contact with the Ultramafic series, and a distinctive anorthosite layer occurs in the middle of the unit. N-I is overlain by gabbronorite of Gabbronorite zone I (GN-I). The lower part of GN-I continues the cotectic proportions of plagioclase, orthopyroxene and clinopyroxene, whereas in the upper part of GN-I modal variations become more pronounced to produce modal layering ranging from melanogabbronorite to anorthosite. Qualitatively, the modal layering appears to be essentially a segregation of pyroxene from plagioclase, with overall proportions being approximately cotectic.

Olivine-bearing zone I is highly variable along strike in terms of thickness and mineralogy and even its stratigraphic location can be variable. With this caveat, the section at the Frog pond area south of Contact Mountain can be considered the 'type section' to which lateral variations can be compared (McCallum *et al.,* 1980; Todd *et al.,* 1982). Here, OB-I is relatively pyroxene-rich in the lower half (the 'Gabbronorite subzone' of Todd *et al*., 1982) and anorthositic in the upper half (divided into three subzones by Todd *et al*., 1982, but here is simply called the Anorthosite subzone) (Fig. 16). The rocks in the Gabbronorite subzone are mainly gabbronorite with minor interlayered anorthosite, norite and medium- to coarse-grained troctolite and subordinate dunite, typically with pegmatoidal texture (Figs 15*d* and 17). Rare chromitite seams

https://doi.org/10.1180/minmag.2016.080.063 Published online by Cambridge University Press

FIG. 15. Photographs of features of the Lower Banded series up to OB-I. (*a*) Massive norite from N-I (*b*) Discordant pegmatoid from GN-I. (*c*) Soft-sediment layer deformation in GN-I. (*d*) Mixed dunite-anorthosite typical of the olivine-bearing rocks in the lower part of OB-I. (*e*) Chromite seam in OB-I. (Compare with chromite seam from the Rum Complex, figure 23 of Emeleus and Troll, 2014). (*f*) Lateral pothole-like change from gabbronorite to poikilitic anorthosite; photo has been rotated from vertical to show original subhorizontal orientation. Figures *a–e* are from the Frog Pond areas, Figure (*f*) is from the Minneapolis Adit.

occur locally (Fig 15*e*). Although locally variable, PGE-enriched sulfides of the J-M Reef are most commonly concentrated within the lower part of OB-I, and are particularly associated with the contact between the Gabbronorite and Anorthosite subzones. PGE-sulfide mineralization can occur in rocks ranging from norite and gabbronorite to troctolite-dunite. The Anorthosite subzone of OB-I is composed predominantly of anorthosite, anorthositic troctolite (both with minor oikocrysts of augite and orthopyroxene), and norite. Layers need not be laterally continuous, and abrupt lateral pothole-like terminations can occur, most commonly with the olivine-bearing lithologies against gabbronorite but also with anorthosites against gabbronorite (Fig. 15*f*).

This 'type section' can be compared with the section as it occurs between the Stillwater River and

https://doi.org/10.1180/minmag.2016.080.063 Published online by Cambridge University Press

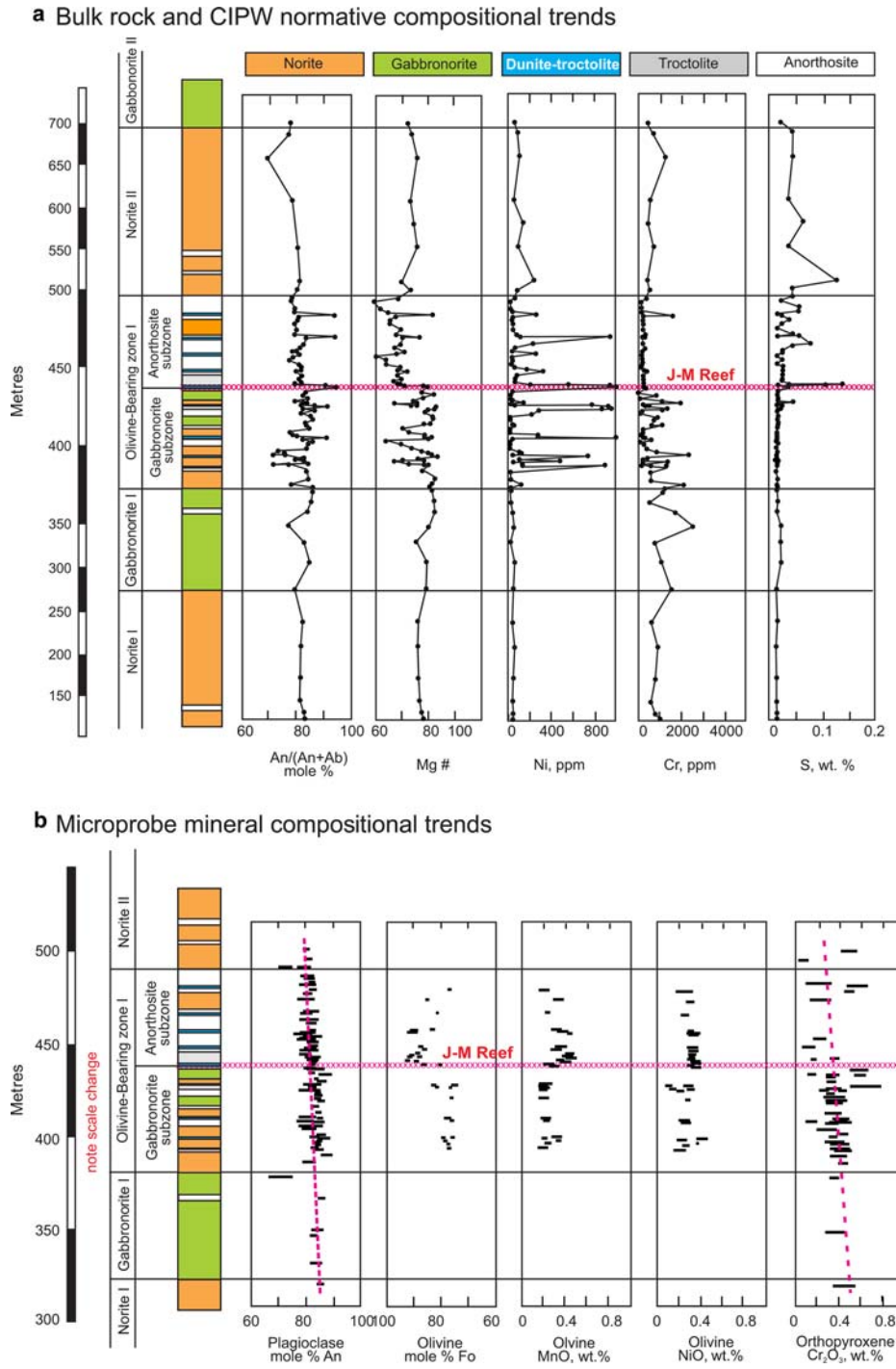

FIG. 16. Mineral and bulk-rock compositional trends from the upper part of N-I to the base of GN-II. (*a*) Bulk rock and CIPW normative mineral trends. (*b*) Electron microprobe mineral compositional trends. Redrawn after Todd *et al.* (1982).

https://doi.org/10.1180/minmag.2016.080.063 Published online by Cambridge University Press

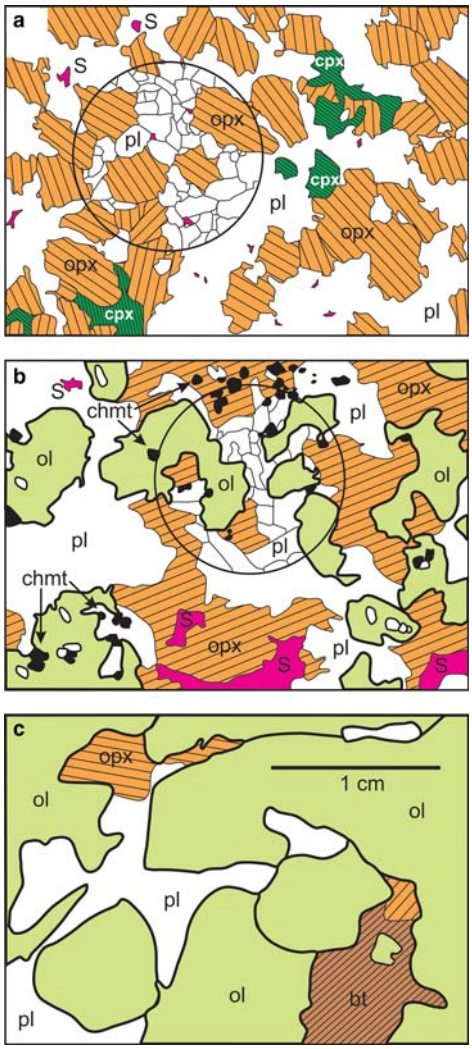

FIG. 17. Examples of rock textures of the J-M Reef. Red, marked 'S' = sulfide; opx = orthopyroxene; cpx = clinopyroxene; ol = olivine; pl = plagioclase; bt = biotite; chmt = chromite. Scale bar is the same for all three figures. (*a*) Mineralized norite. (*b*) Mineralized chromite-troctolite. (*c*) Pegmatoidal dunite. For (*a*) and (*b*) the circled area shows a detail of plagioclase texture.

the East Fork of the Stillwater River. Here, OB-I cuts down into the underlying section, locally reaching the lower parts of N-I (Turner *et al.*, 1985). Within this apparent unconformable region, the thickness of OB-I itself decreases, such that at the deepest penetration into the underlying cumulates, there is a very narrow transition from N-I to N-II. The olivine-rich layers of the Gabbronorite subzone again can show abrupt lateral pothole-like changes to melanocratic gabbronorite layers (Turner *et al.*, 1985). The overlying Anorthosite subzone also thins, giving the regional appearance that the Gabbronorite and Anorthosite subzones both form an apparent angular unconformity at their contact. The surface of the unconformity itself is broadly defined by PGE-sulfide mineralization of the J-M Reef, although mineralization is considerably less abundant and locally absent in the region of the unconformity (Dahy *et al.,* 1995). Boudreau (1995) interpreted the unconformity, thinning of the olivine-bearing and overlying anorthosite units, and the poor mineralization to be due to slumping and local loss of a reactive volatile-rich mush. This area has otherwise not been studied extensively.

Structurally above OB-I, the rocks return to the mineral sequence observed in N-I and GN-I to form the N-II and GN-II zones. The rocks retain their plagioclase-rich nature into the lower parts of Norite zone II, the contact defined where orthopyroxene changes from an oikocrystic habit to a subhedral-euhedral mineral. Modal abundance of orthopyroxene increases from the base of N-II to more typical cotectic proportions similar to those seen in N-I. However, mineral compositions in N-II and GN-II are more evolved than those in the lower units (McCallum *et al.*, 1980; Todd *et al.*, 1982, Barnes and Naldrett, 1986). Indeed, mineral compositional trends from N-I, through OB-I and into N-II and GN-II show very little evidence for any kind of distinctly different magma compositions being injected into the Stillwater chamber to form OB-I (Fig. 16). For plagioclase, the only major mineral found in all units, there is overall a continuous trend upwards to lower An compositions with little evidence of compositional offsets. While olivine shows an offset at the boundary between the Troctolite and Anorthosite subzones of OB-I, the change is to more Fe-rich compositions in leuco-troctolite of the structurally higher Anorthosite subzone and probably represents a compositional shift from variable olivine/trapped liquid abundance.

Norite zone II and the lower parts of Gabbronorite zone II are typically massive, commonly laminated, and not modally layered. The rocks again become modally layered in the upper part of GN-II as the thick anorthosites of the Middle Banded series are approached, forming a number of macrorhythmic units (Criscenti, 1984). Olivine-bearing zone II (OB-II) defines the top of the Lower Banded series and contains the distinctive 'pillow troctolite' of Hess (1960). The origins of OB-II are discussed

https://doi.org/10.1180/minmag.2016.080.063 Published online by Cambridge University Press

with similar rocks occurring in the Middle Banded series. This unit is overlain by the first thick anorthosite unit of the Middle Banded series.

Pegmatoids

Pegmatoids in the Lower Banded series are common along the contact of the Ultramafic series with the Banded series but rare elsewhere in N-I. They again become common in the upper parts of GN-I and in the Gabbronorite subzone of OB-I. The reappearance of pegmatoids in GN-I coincides with locally significant layer deformation (Fig. 15*b* and *c*). The pegmatoids are composed of the same minerals (plagioclase, orthopyroxene, and clinopyroxene) as the host rocks and in approximately the same proportions, but with grains that may be in excess of several tens of centimetres in length and the pyroxene variably replaced with hornblende. As described by Braun *et al.* (1994), pegmatoid whole-rock compositions are enriched in lithophile incompatible major and trace elements relative to the host rocks. Whereas average N-I and GN-I have a whole-rock molar 100 Mg/(Mg + Fe) ratio of 81 ± 1.5 and a normative An content of 85 ± 1.5, almost all pegmatoid samples have lower values with 100 Mg/(Mg + Fe) ratios as low as 71 and normative An as low as 58. Ratios of soluble/insoluble lithophile trace elements such as Ba/Zr are variable. These pegmatoids locally have cores of massive sulfide up to ~0.5 m in diameter. The example shown in Fig. 18 occurs adjacent to a pothole-like feature in the gabbronorite subzone of OB-I.

Hanley *et al.* (2008) describe a variety of fluid inclusions in the pegmatoids below the J-M Reef that they interprets as ranging from magmatic-hydrothermal to lower temperature metamorphic fluids. Those interpreted to be high-temperature primary inclusions range from hydrosaline to carbonic fluids and can have up to 16 precipitated solid phases. Strontium concentrations range from 100–1000 ppm, but the isotopic characteristics of the inclusions are lacking. They note that ~10% of the brine inclusions have significant concentrations of Pt, ranging from 0.4 to 4 ppm. Cu/Pt ratios in the brine range from 27 to 342, which compares with the Cu/Pt ratio of ~400 for the J-M Reef. The pegmatoids are also enriched in *REE*. The Cl-rich nature of the fluid inclusions is also consistent with the interpretation that the unusually Cl-rich apatite below the J-M Reef equilibrated with a Cl-rich vapour (Boudreau *et al.*, 1986; Boudreau and McCallum, 1989).

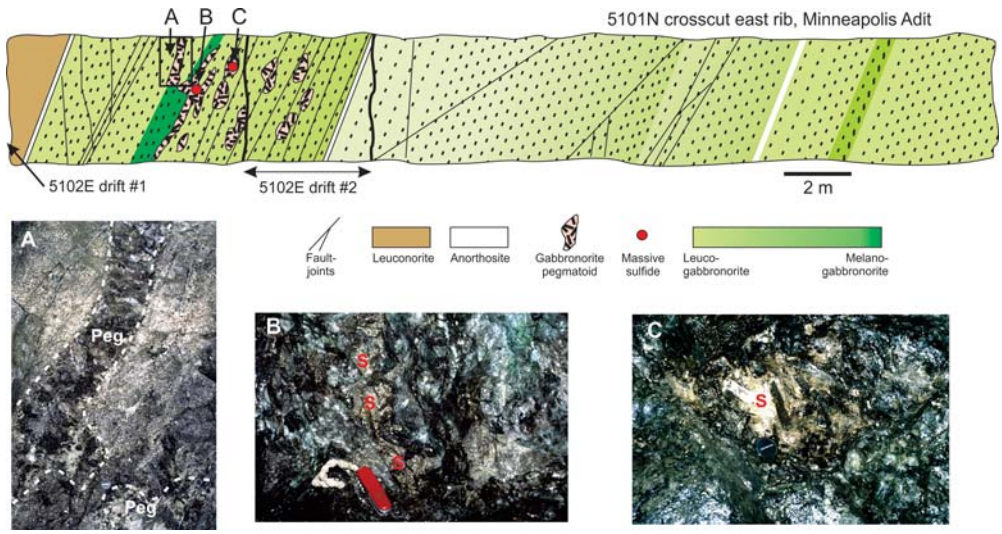

FIG. 18. Massive sulfide-hosting pegmatoids from the J-M reef of OB-I, Minneapolis adit. The top drawing is of a crosscut in the Minneapolis adit, looking east. The rocks are dipping ~70° to the north and stratigraphic 'up' is to the left. Gabbronorite pegmatoids occur at the same stratigraphic level as the J-M reef. Occurring within the pegmatoids are massive sulfide pods up to 0.5 m in diameter. The zone of pegmatoidal rocks is hosted by gabbronorite, but immediately to the west the host rocks are mineralized olivine-bearing rocks at the same stratigraphic level.

https://doi.org/10.1180/minmag.2016.080.063 Published online by Cambridge University Press

Olivine-Bearing zone I (OB-I) and the J-M Reef

The J-M Reef is the only zone of mineralization in the Stillwater Complex currently being mined. The PGE occur primarily in solid solution within disseminated base-metal sulfides (typically up to 5% volume, and locally in small bodies of massive sulfides in cores of discordant pegmatoids) and in a variety of discrete trace PGE-rich mineral phases (e.g. Bow *et al.*, 1982; Barnes and Naldrett, 1985; Godel and Barnes, 2008; Turner *et al*. 1985; Zientek *et al*. 1985, 2002; Corson *et al.,* 2002). The J-M Reef has the largest average Pt + Pd grade of all known PGE deposits (~18 ppm with an average Pd/Pt ratio of 3; Zientek *et al.,* 2002). Stillwater Mining Company geologists have noted that the PGE tenor in the sulfide is higher in the Stillwater mine than in the Boulder River mine.

The Reef is generally defined by sulfide-bearing mineralized rocks and although regionally stratabound, mineralization is heterogeneous on smaller scales. Although described typically as a zone of mineralization 2–5 m thick below the contact of the Gabbronorite-Anorthosite subzones of OB-I, mineralization can be discontinuous such that effective mining requires drilling at ~15 m centres to avoid excessive mining of barren rock.

Ballrooms

'Ballrooms' is an informal Stillwater Mine term that refers to local thickening of disseminated sulfide mineralization that extends up to 10 m into lithologies below the main stratigraphic level of the J-M Reef. Ballrooms include mineralization referred to by Raedeke and Vian (1986) as Footwall zone, Basal zone, and Main zone mineralization. Ballroom mineralization can occur abruptly along strike and commonly crosses modal layering in the host rock. Sulfide textures are generally similar to those found in the main J-M Reef although coarse sulfides with irregular radial 'veinlets' up to 5 cm long are a common feature of gabbronorite- and norite-hosted ballroom mineralization (Childs *et al.*, 2002).

Childs *et al.* (2002) and Harper (2004) have described three general types of ballrooms (Fig. 19): (1) The most common type is a thickening of the mineralized zone extending from roughly the lower contact of the Anorthosite subzone of OB-I into the lower units of OB-I, and in the areas of the regional unconformity into GN-I and N-I. Mineralization crosses existing modal layering, but there otherwise appears to be no major- or trace-element difference between mineralized ballroom rock and adjacent barren rocks except for the presence of PGE-sulfides (Harper 2004). The distribution of ballroom mineralization in this instance has some similarities with the disseminated sulfide mineralization seen in the Picket Pin sulfide zone at the top of the Middle Banded series (Boudreau and McCallum, 1985; see below). (2) The second type involves a thickening of mineralization within a thickened olivine-bearing package of rock. This second type is broadly analogous to the potholes of the Bushveld Merensky Reef. (3) The least common type occurs as apparently isolated pockets of mineralization in footwall lithologies ~10 m below the main level of the J-M Reef. Mineralization can occur with isolated bodies of olivine-bearing rock that can be either stratabound or discordant to local layering.

Models for the Formation of the J-M Reef

Models for the petrogenesis for OB-I and the J-M Reef range from strictly magmatic models (e.g. Irvine *et al.*, 1983; Campbell *et al.*, 1983; Barnes and Naldrett 1986; Wooden *et al.*, 1991, Lambert and Simmons, 1988; Lambert *et al.*, 1994; Godel and Barnes, 2004; Godel *et al.,* 2006, 2008) to those that involve volatile fluids percolating up from below (Boudreau, 1988; Boudreau and McCallum, 1989; Boudreau 1999). Although details among the various 'orthomagmatic' models vary, these studies have attributed crystallization changes to two distinct parent magma types. Below OB-I, the rocks are interpreted to have crystallized from a 'U' magma of 'ultramafic' parentage and record the apparent crystallization order olivine ± chromite → orthopyroxene → orthopyroxene + plagioclase → orthopyroxene + plagioclase + augite. This progression is interrupted in OB-I where the rocks now include troctolites, anorthosites and dunites. This change is proposed to have resulted from a mixing event that blended the evolved 'ultramafic' liquid with an anorthositic 'A' liquid that had plagioclase as the first mineral to crystallize. In these models, the observed stratigraphic modal changes document variations in primary crystallization resulting from these magma mixing events, and volatiles are assumed to have played only a secondary role in modifying original textures (Barnes and Campbell, 1988).

In contrast to these orthomagmatic models are those that have interpreted the mineral changes in OB-I as the result of incongruent melting of pre-existing, partly-molten rock induced by fluid

https://doi.org/10.1180/minmag.2016.080.063 Published online by Cambridge University Press

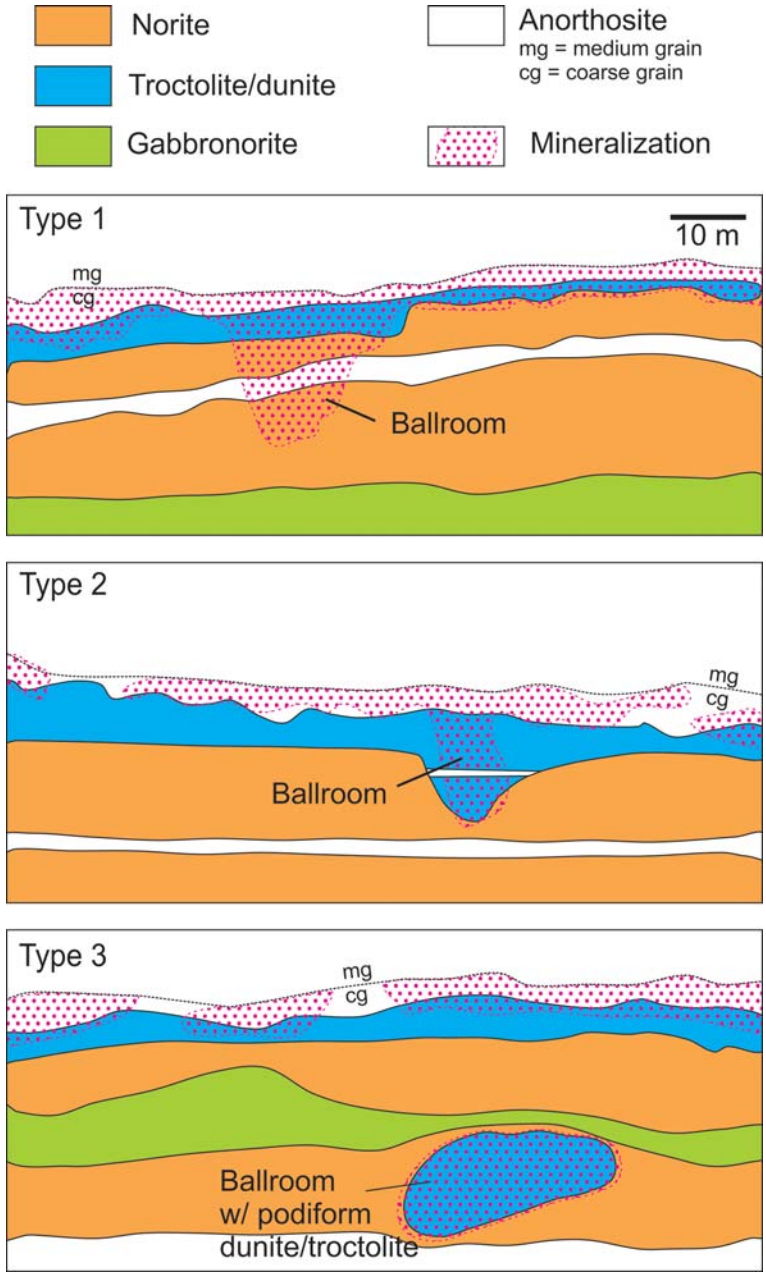

FIG. 19. Schematic cross-section examples of ballroom mineralization in the JM Reef of OB-I. Redrawn from Harper (2004).

fluxing (Boudreau, 1988, 1999). These 'hydromagmatic' models are analogous to the hydration melting models proposed for arc magmatism where it is envisioned that volatiles coming off a subducting slab induce partial melting in the overlying hotter mantle wedge. In the case of the

https://doi.org/10.1180/minmag.2016.080.063 Published online by Cambridge University Press

Stillwater Complex, vapour rising from the cooler, crystallizing rocks below the J-M Reef rise upwards into hotter rocks where they induce partial melting.

The hydromagmatic model makes three claims. (1) The mineralization was introduced by the upward migrating Cl-rich vapour that re-dissolves into vapour-undersaturated liquids near the top of the crystal pile. (2) The olivine and minor chromite in the Gabbronorite subzone are the result of incongruent melting as a result of this hydration event. (3) The anorthosite and troctolite of the Anorthosite subzone represent mixing of hydrated partial melt generated in the crystal pile with the drier magma above the floor of the chamber.

Lines of support of vapour as the mineralizing agent (point 1 above) include the following. (1) The pegmatoidal nature of the rocks and relative abundance of hydrous minerals associated with mineralization is consistent with a buildup of volatiles. (2) Pegmatoids are common below the J-M Reef, consistent with increasing volatile concentrations and late channelling of fluids exsolved from these and underlying rocks (Braun *et al*., 1994). In contrast, pegmatoids are not found in the Anorthosite subzone of OB-I and in the immediate overlying units of N-II. This is consistent with the interpretation that the overlying rocks had not yet crystallized at the time these fluids were migrating upwards, and that the Gabbronorite subzone–Anorthosite subzone transition in OB-I marks the approximate floor of the chamber during this fluid introduction event. (3) There is an abrupt change in halogen concentration in apatite at the level of the J-M Reef (Fig. 20). The drop to lower Cl concentrations in apatite in the overlying Anorthosite subzone is consistent with these rocks not having seen significant vapour. (4) The metal ratios in fluid inclusions in the pegmatoids below the J-M Reef are broadly similar to the metal ratios seen in the J-M Reef (Hanley *et al.,* 2008). (5) Sulfide abundances are higher than expected from 'cotectic' abundances, consistent with the addition of S by vapour. (6) There is petrographic and geochemical evidence of loss of the more soluble components S, Cu and the PGE (Rh, Pt, and Pd) from the rocks below the Reef (e.g. Aird *et al.*, 2016).

Evidence for olivine and chromite in the Gabbronorite subzone having formed by incongruent melting during this hydration event (point 2 above) includes the following (Boudreau, 1988, 1999). (1) The common presence of hydrous melt inclusions (now crystallized to polymineralic

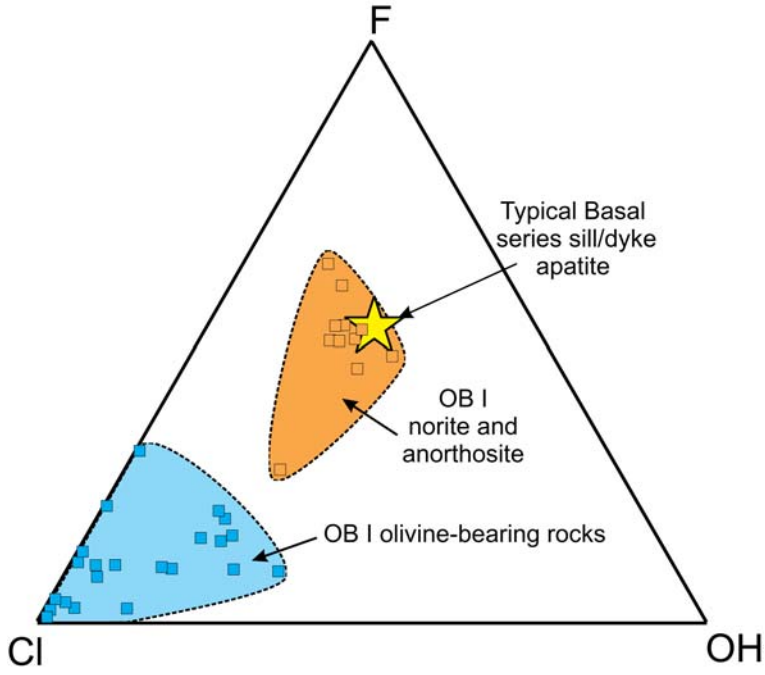

FIG. 20. Ternary F–Cl–OH compositional variation in apatite from OB-I. Redrawn after Boudreau and McCallum (1989).

https://doi.org/10.1180/minmag.2016.080.063 Published online by Cambridge University Press

assemblages) in olivine and chromite are similar to the inclusions seen in the Peridotite zone chromite (Fig. 12) and are consistent with the growth of these minerals from a hydrated liquid. (2) The relative abundance of hydrous minerals and the Cl-rich nature of the apatite in the mineralized, olivine-bearing rocks are again consistent with a local hydration event. (3) The observation that mineral compositional trends from GN-I up into N-II, particularly for plagioclase, do not show offsets expected from injection of more primitive magma. (4) The rounded and reversely zoned plagioclase found in the olivine-bearing rocks is consistent with the partial remelting of plagioclase. (5) The locally isolated nature of olivine-bearing rocks and textural similarities of the 'amoeboidal' olivine of the coarser-grained rocks of OB-I with replacement troctolite of OB-II and the Middle Banded series discussed below. (6) The pothole-like structures are analogous to seafloor pockmarks that can form where rapid fluid escape from the underlying sediments blows out sediment from the seafloor (e.g. Boudreau, 1992). In the Stillwater, the vapour migrating up through the pothole induces incongruent melting rather than the physical removal of pre-existing crystals. (7) More broadly, the change from massive to increasingly modally layered rocks in the Lower Banded series as the reef is approached from below is consistent with volatile increase and mineral segregation in the mush that can arise from the process of constitutional zone refining as describe by McBirney (1987). This increase in volatile concentrations can perturb the crystallization to favour mafic over felsic minerals and can give rise to modal layering.

The effect of H_2O on liquidus phase assemblages is illustrated in Fig. 21. Shown in Fig. 21*a* is the ternary system forsterite–anorthite–SiO_2, which is the base of the four-component system anorthite–forsterite–silica–H_2O (generalized after Kushiro *et al.,* 1968; Kushiro, 1975). The initial (dry cotectic) norite assemblage of anorthite + enstatite (green circle) is in equilibrium with the dry liquid shown by the red circle and the bulk solid + liquid shown by the blue circle. In Fig. 21*b*, these three compositions are plotted on the base of the anorthite–B–H_2O system, where point 'B' represents the anorthite-liquid extension shown in Fig. 21*a*. Addition of an H_2O-rich vapour to the initially vapour-undersaturated bulk composition (blue circle) leads to migration of the bulk composition towards the H_2O apex as illustrated by the blue line in Fig. 21*b*. As long as liquid, anorthite and enstatite are all present, a tieline from the bulk solid (green line) and the evolving liquid (red line) are constrained to pass through bulk solid, as is shown. The result is the preferential melting of anorthite and the production of an enstatite-rich restite (residual solid assemblage). As more H_2O is added the orthopyroxene begins to melt incongruently to produce an olivine-bearing assemblage. Although not shown, as described by Boudreau (1999), at higher degrees of partial melting Cr liberated from pyroxene can also allow chromite precipitation. In either event, what remains is a residual assemblage (restite) relatively enriched in the mafic minerals and depleted in plagioclase.

As the hydrated silicate liquid produced by hydration melting moves away from the region of hydration (by interstitial liquid advection or compaction), the hydrated partial melt can mix in with drier magma above the crystal pile. The mixing of these two liquids produces a hydrated liquid that is saturated in plagioclase alone, as is illustrated in Fig. 21*c*. (More formally, as the interstitial liquid is buffered by the presence of plagioclase and pyroxene, the result is that the liquid will be constrained to the cotectic by dissolution of pyroxene and precipitation of plagioclase, but the result will still be the preferential enrichment in plagioclase). The result is the production of anorthosites and leuconorites above melanorite and mela-gabbronorite (at low degrees of flux melting) or anorthosites and leucotroctolites above olivine-rich rocks. Sulfide would be concentrated at the top of the vapour-saturated region (Fig. 21*d*), which could move up over time until the footwall rocks became degassed.

The variations in *REE* in plagioclase separates from the Lower Banded zone (Fig. 22) are an example of the conflicting orthomagmatic and hydromagmatic interpretations. Lambert and Simmons (1988) interpreted the higher *REE* concentrations of plagioclase from anorthosites as characteristic of an *REE*-rich 'A' magma type as compared with the 'U' magma that crystallizes plagioclase in norites and gabbronorites. In contrast, the enrichment in the *REE* seen in the pegmatoids and the relatively high *REE* concentrations in fluid inclusions reported by Hanley *et al.* (2008) would suggest that a plagioclase-saturated magma produced by mixing a hydration melt with the resident magma would be similarly *REE* rich.

Inch scale 'doublets'

Above OB-I in the Stillwater River Valley is an occurrence of the striking inch-scale 'doublet' layering. The fine-scale layering is characterized

https://doi.org/10.1180/minmag.2016.080.063 Published online by Cambridge University Press

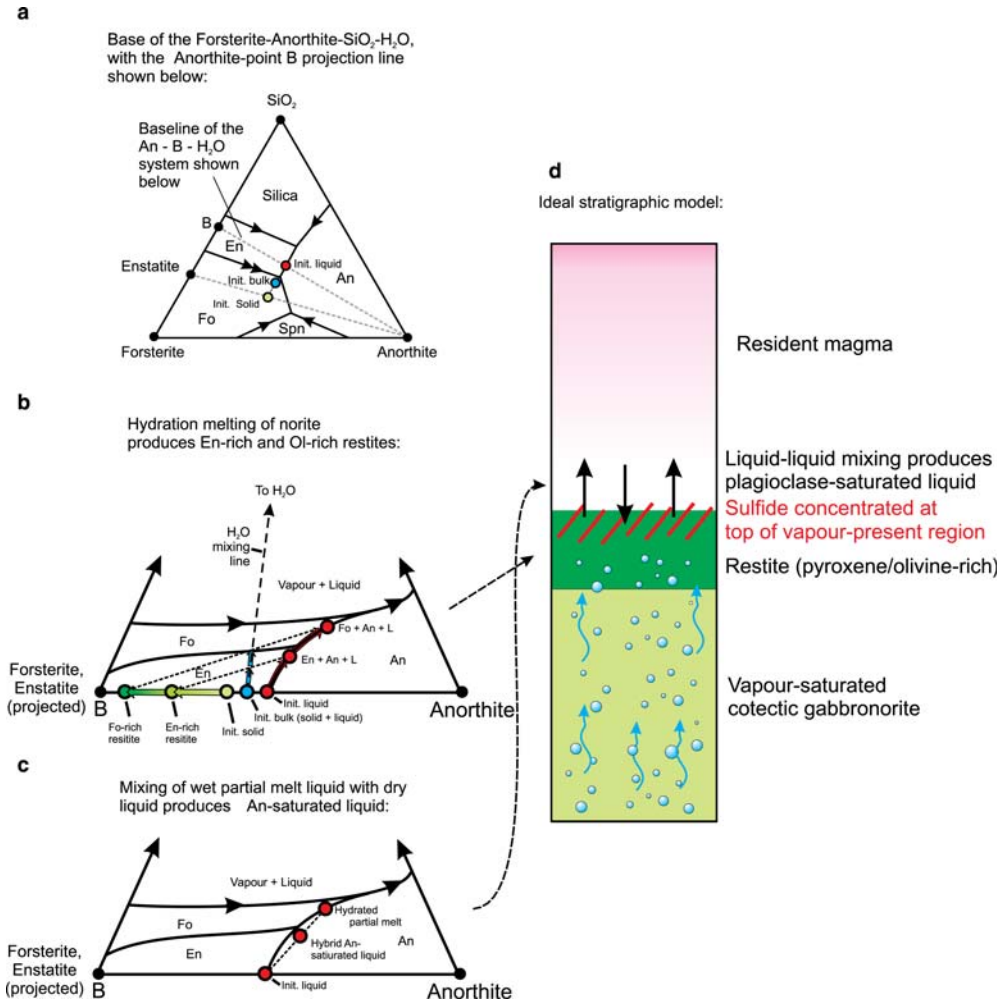

FIG. 21. Hydration melting model for the generation of melano-gabbronorite and troctolite/dunite and anorthosites of the OB-I. (*a*) The forsterite–anorthite–SiO_2 system, which forms the base of the forsterite–anorthite–SiO_2–H_2O (exaggerated after Kushiro *et al.,* 1968 and Kushiro, 1975, to show details). The line from anorthite to point 'B' forms the base of the anorthite–B–H_2O projection section shown in (*b*) and (*c*). Also shown are the initial 'dry' liquid, composition (red), initial dry cotectic norite solid (light green) and initial liquid + solid bulk composition (blue). (*b*) The system anorthite–B–H_2O, where B is the intercept of the anorthite–initial (dry cotectic) anorthite + enstatite-saturated liquid tieline projected to the forsterite–SiO_2 sideline as shown in (*a*). A small addition of H_2O to the initially dry bulk composition leads to hydration melting and the production of an enstatite-rich restite (residual solid assemblage), and troctolite/dunite with increasing H_2O added. (*c*) Same system as for (*b*), but illustrating the mixing of the wet partial melt generated in the crystal pile with the original dry resident cotectic liquid to produce an anorthite-saturated hybrid liquid. (*d*) Stratigraphic expression of the process. See text for detailed discussion.

by pairs of pyroxene-rich layers that repeat rhythmically for several tens of metres. (Fig. 23*a*). Models for its formation range from suggestions of a rhythmic back and forth sloshing of magma in the chamber (Hess, 1960), periodic precipitation of pyroxene (McBirney and Noyes, 1979), and mineral segregation driven by a spatially ordered crystal ageing (Ostwald ripening) (Boudreau, 1987, 1995, 2011; Boudreau and McBirney, 1997). The numerical model of pattern formation that can

https://doi.org/10.1180/minmag.2016.080.063 Published online by Cambridge University Press

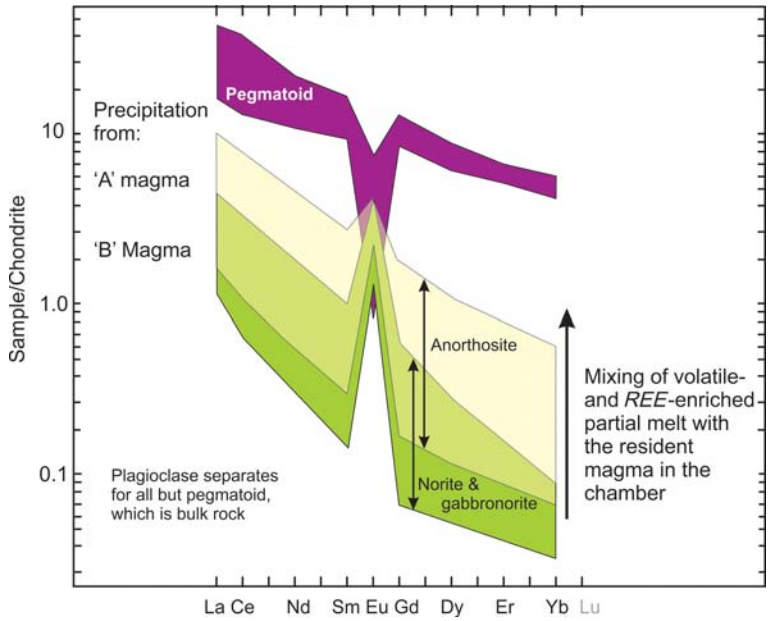

FIG. 22. Chondrite-normalized *REE* patterns in plagioclase separates from N-I, GN-I and OB-I (data from Lambert and Simmons, 1988) and bulk rock *REE* from GN-I pegmatoid (data from Hanley *et al.*, 2008). In the model of Lambert and Simmons, *REE* variations are the results of mixing of two different magma types, the 'A' and 'U' magmas; the former giving rise to the anorthosite of the Lower Banded series and the latter to norites and gabbronorites. In contrast, the model of Boudreau (1999) would interpret the 'A' magma as the result of mixing of an enriched incongruent hydration melt, similar to the enrichment seen in the pegmatoid, with the original 'U' magma in the chamber.

occur as a result of crystal ageing by Boudreau (1995) is able to reproduce the doublet pattern and relative layer spacing (Fig. 23*b*). As for the case of fine-scale layering in chromitites discussed above, modest gradients in grain size, temperature, and composition expected in a crystallization front can result in layered segregation during crystal ageing. As for the chromitite seams, this unusual example of fine-scale layering illustrates that sharp modal layering boundaries in general need not have been originally present in the initial magmatic assemblage but instead can develop slowly over a prolonged period of textural maturation. In this regard, modal layering has similarities with metamorphic banding in that both can develop spontaneously and evolve with the rock texture and become more sharply defined with time (Boudreau, 2011).

Middle and Upper Banded series

The Middle Banded series hosts the qualitatively distinctive thick anorthosites of the Stillwater Complex. Ignoring the oikocrystic minerals in the anorthosite units, the Middle Banded series as a whole shows very little stratigraphic variation in the composition of the major modal minerals, especially plagioclase (Fig. 2). Otherwise, it has an apparently different crystallization sequence compared with the rest of the complex, with much less orthopyroxene that texturally crystallized after clinopyroxene rather than before (McCallum *et al.,* 1980). Although this has been interpreted to have been the result of the addition of a magma with a different liquid line of descent into the complex, the unusual occurrences of olivine in Middle Banded series and the immediately surrounding rocks again suggests that alternative explanations should be considered, as discussed below.

The Upper Banded series is the least studied unit of the Stillwater Complex with little in the way of published studies. The layered troctolite that forms the base of Olivine-Bearing zone V (OB-V) would appear to reproduce the crystallization sequence of OB-III with wispy-layered troctolite above a thick anorthosite. However, unlike the Middle Banded series' mix of troctolite, olivine-gabbro and gabbro, the rocks above OB-V instead return to a norite-

https://doi.org/10.1180/minmag.2016.080.063 Published online by Cambridge University Press

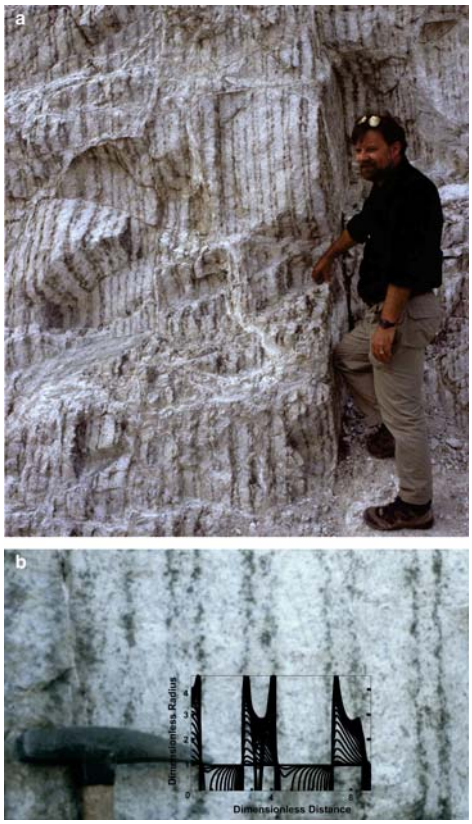

FIG. 23. Photographs of fine-scale layering in the Lower Banded series. (*a*) Inch-scale 'doublets' as exposed on the Mountain View mine road above the Stillwater mine in the Stillwater Complex: rocks have been tilted to near vertical, original stratigraphic 'up' is the right. Fat bastard (the author) shown for scale (photo: Tony Philpotts). (*b*) Detail of the doublets. Superimposed is the doublet pattern produced by numerical simulation of layer development during crystal ageing at different model times. Reproduced from Boudreau (1995, figure 8) with kind permission from Springer Science + Business Media.

gabbronorite sequence similar to that of the Lower Banded series. The Upper Banded series also returns to a trend of a more fractionated assemblage with stratigraphic height, such that towards the exposed top of the complex inverted pigeonite replaces orthopyroxene.

Quantitative characterization of rock texture and compaction of the crystal mush

The rocks of the Middle Banded series show a range of rock textures ranging from massive without any obvious mineral lamination or lineation to those which have well-developed lamination but without a significant lineation (Fig. 24). Meurer and Boudreau (1998*a*,*b*) quantified mineral lineation in sections cut both normal and in the plane of layering using a measured alignment factor (AF) that varies from 0.0 (random) to 1.0 (perfectly aligned). They also characterized individual mineral grains by their length/width aspect ratio.

An example of petrofabric analysis is shown in Fig. 24 from the Middle Banded series (Meurer and Boudreau, 1998*b*). The example shown here is typical of most of the rocks of the Banded series, in that the rocks will have a poor- to well-developed foliation but generally do not have any significant mineral lineation. Gee *et al.* (2004) arrived at essentially the same conclusions using a more refined quantification of mineral texture. Furthermore, the better-foliated rocks tend to have lower bulk-rock incompatible-element concentrations. These textural and compositional features are consistent with a pure shear expected during compaction. In contrast, crystals settling from a flowing liquid or simple shear within the mush would both impart a lineation to the crystals, which occurs only locally. Meurer and Boudreau (1998*b*) also observed that the foliation is best seen in rocks where there is an increase in the Cl/(Cl + F) ratio of apatite, the presence of discordant troctolites, and extensive hornblende veins that imply compaction was enhanced by the presence of larger than normal volatile concentrations.

The Anorthosite zones

The anorthosites of the Middle Banded series have been unusually well studied, both for their intrinsic interest and comparison with other terrestrial anorthosites, their PGE ore potential, and as proxies for lunar anorthosites (e.g. Readeke and McCallum, 1980; Salpas *et al.*, 1983, 1984, 1987; Haskin and Salpas, 1985; Salpas and Moss 1989; Pass and Salpas 1990, 1991; Czmanske and Loferski, 1996). The thickness of the Lower Anorthosite zone (AN-I of McCallum *et al.*, 1980) is variable from a maximum of 400 m in the eastern part of Contact Mountain to less than 200 m west of the Boulder River. The Upper Anorthosite zone (AN-II of McCallum *et al.*, 1980) varies from 600 m thick in the Contact Mountain area to less than 200 m thick at Picket Pin. Owing to the homogeneity of these units and poor exposures it is not clear if this variable thickness is entirely

https://doi.org/10.1180/minmag.2016.080.063 Published online by Cambridge University Press

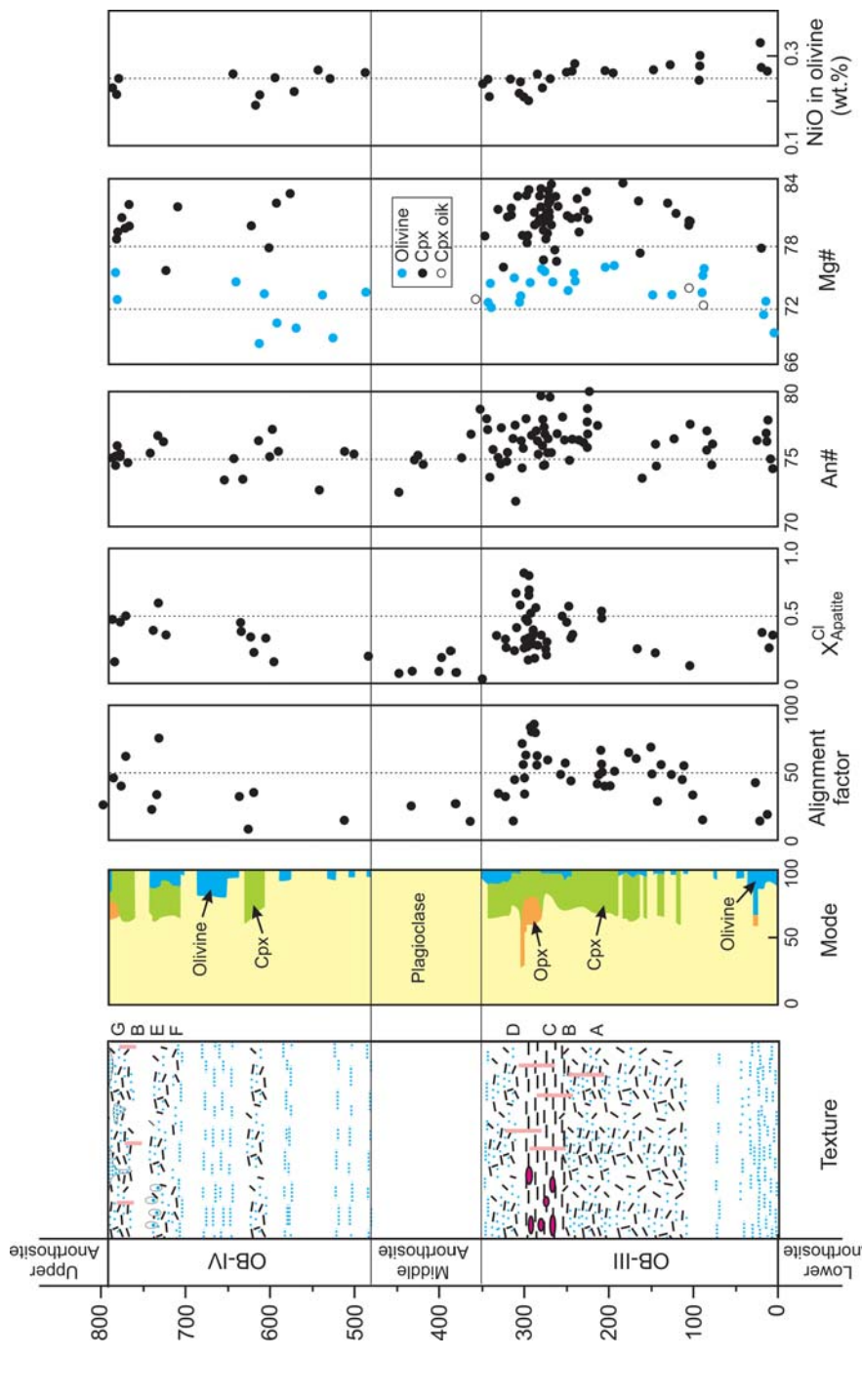

FIG. 24. Textures and compositional features of the rocks between the Lower and Upper Anorthosite zones of the Middle Banded series. The texture column shows a cartoon of olivine (dots), the qualitative development of foliation in gabbroic rocks (short lines), and various discordant features. Letters adjacent to the texture column: A = polycrystalline plagioclase clots, B = hornblende-bearing dykes and veins, C = pegmatoids, D = granophyric dykes and segregations, E = fine-scale layering, F = Hess' eggs, and G = discordant bodies. Redrawn after Meurer and Boudreau (1998*a*,*b*).

https://doi.org/10.1180/minmag.2016.080.063 Published online by Cambridge University Press

fault-related. The Middle Anorthosite zone is the thinnest, at ~100–120 m thick. The following description focuses on the Upper Anorthosite zone, although the other two are similar.

Most of the Upper Anorthosite zone is composed of a Coarse-Grained Anorthosite member that is characterized by relatively coarse plagioclase and from 0 to 25 vol.% (average 11 vol.%) of oikocrystic augite and inverted pigeonite, along with interstitial to oikocrystic quartz (1–5 vol.%) and magnetite, sulfides (pyrrhotite, pentlandite, chalcopyrite ± pyrite), and apatite (Fig. 25). A prominent zone of disseminated low-grade Pt-Pd sulfides, the Picket Pin Pt-Pd zone, occurs near the top of the unit, at and below a marked change in grain size that occurs ~10 m below the upper contacts of the Upper Anorthosite zone (Boudreau and McCallum, 1992*b*). Above this level, the anorthosite typically is medium grained, and interstitial minerals (mainly pyroxene and minor sulfides) make up <5 vol.% of the rock and commonly they are completely absent. This thin capping unit is termed the Medium-Grained Anorthosite member. Unlike the underlying Coarse-Grained Anorthosite member, this unit

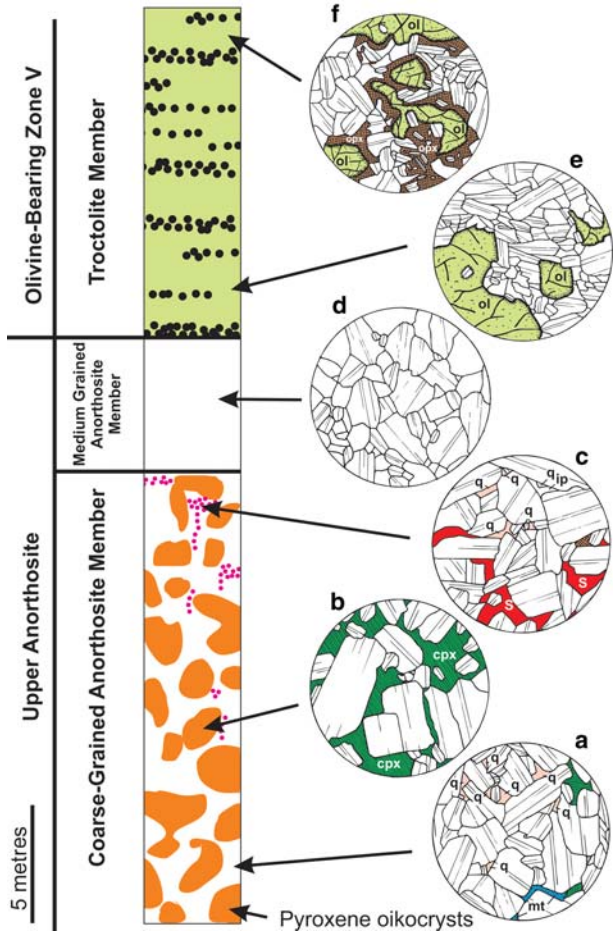

FIG. 25. Detail of the Picket Pin sulfide zone textures at the top of the Upper Anorthosite zone. All petrographic sketches are 1 cm in diameter. (*a*) Plagioclase (showing orientation of albite twins) with minor interstitial augite (green-ruled). (*b*) Plagioclase enclosed within oikocrysts of augite (green-ruled); also minor quartz (q) and ilmenite (blue-stippled). (*c*) Interstitial PGE-bearing sulfide (red), quartz (q), and minor pyroxene (brown-cross ruled). (*d*) Monomineralic anorthosite with well-developed triple junctions of the Medium-Grained Anorthosite member. (*e*) Troctolite with olivine (pale green) and plagioclase. Olivine may enclose grains of plagioclase. (*f*) Olivine rimmed with low-Ca pyroxene (brown-cross ruled). The amount of pyroxene increases up-section within the Troctolite member.

https://doi.org/10.1180/minmag.2016.080.063 Published online by Cambridge University Press

shows local modal layering defined by minor variations in pyroxene mode and the plagioclase grain size is more typical of the rest of the Banded series. This thin capping anorthosite unit has been interpreted as having formed by a compaction-driven infiltration metasomatic mechanism as plagioclase-saturated liquids from the Upper Anorthosite zone percolated up through the overlying olivine + plagioclase assemblage of the troctolite, replacing olivine with plagioclase (Boudreau and McCallum, 1992). The following discussion focuses on the Coarse-Grained Anorthosite member that makes up the bulk of the anorthosite.

Within the Coarse-Grained Anorthosite member, plagioclase shows a range in grain sizes, typically between 1 and 10 mm that are two to three times larger than plagioclase crystals elsewhere in the intrusion (Scheidle, 1983; Czamanske and Scheidle, 1985; Boudreau and McCallum, 1986). Preferred orientation of plagioclase as measured in the Middle Anorthosite zone is weak, see Fig. 26 (Meurer and Boudreau, 1998*a*). Plagioclase grains enclosed within pyroxene and adjacent to quartz are commonly subhedral and tabular while those in pyroxene-poor areas are anhedral with annealed textures. Average compositions of plagioclase in the Upper Anorthosite zone (An76) show no systematic variation in major- and trace-element compositions with stratigraphic height (McCallum *et al.*, 1980; Salpas *et al.,* 1983; Czamanske and Loferski, 1996). This large-scale homogeneity contrasts sharply with the heterogeneous nature of individual plagioclase grains (Fig. 27). A single thin section may show grains with normal, reversed, patchy, convoluted and asymmetric zoning patterns (Czamanske and Scheidle, 1985), suggesting that the plagioclase had a complex growth history that is atypical for plagioclase elsewhere in the complex. Indeed, analysis of plagioclase in a single thin section can show about the same compositional variability as does the entire anorthosite unit. For example, in a sample from the Upper Anorthosite zone, Czamanske and Scheidle (1985) found that almost all compositions range between An69 and An83 and it is just as common for rims to be reversely zoned as normally zoned. They also note that most of the zoning appears to be a primary feature (including zoning patterns that suggest some grains were broken prior to deposition) although compaction, dissolution and reaction with migrating interstitial silicate liquid and volatile fluid have also modified plagioclase compositions.

The Coarse Grained Anorthosite member contains oikocrystic pyroxene-rich and pyroxene-poor domains on a scale of decimetres to metres (Fig. 28). Haskin and Salpas (1992) and Czamanske and Loferski (1996) have shown that the entire stratigraphic range mineral modes in the

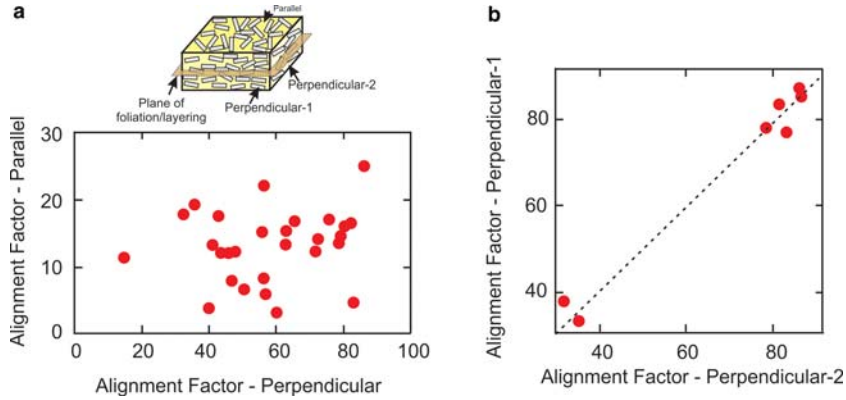

FIG. 26. Examples of petrofabric analysis of Middle Banded series rocks. (*a*) Comparison of mineral alignment of prismatic crystals in planes that are parallel and perpendicular to the plane of foliation/layering. The inset shows the faces for which petrofabric data are referenced. Shearing caused by current flow or simple shear of the crystal mush should produce a positive correlation between these two parameters, whereas fabric controlled by compaction (pure shear) should show no correlation, as is observed. (*b*) Variation in the fabric for orthogonal faces that are perpendicular to the plane of foliation/layering, with a 1:1 correlation line shown for reference. The uniformly developed alignment in both planes illustrates the lack of a lineation and is consistent with compaction. Redrawn after Meurer and Boudreau (1998*b*).

https://doi.org/10.1180/minmag.2016.080.063 Published online by Cambridge University Press

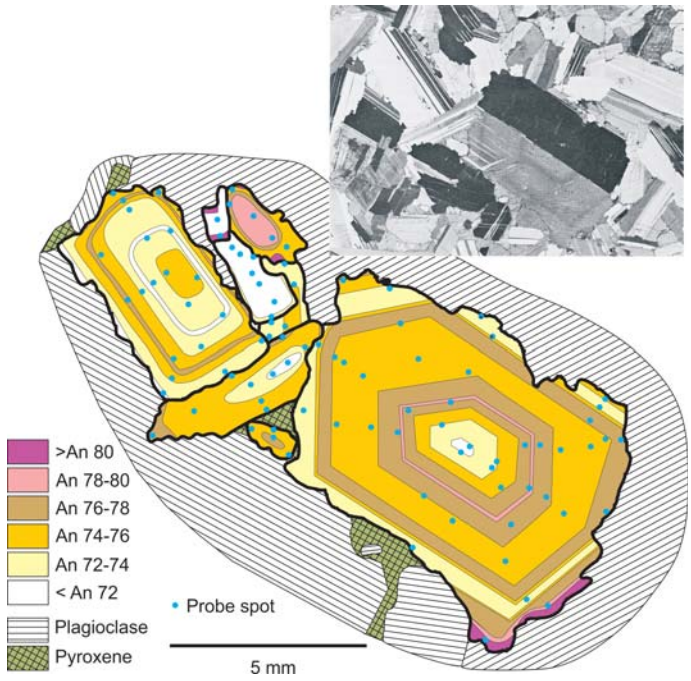

FIG. 27. Example of compositional zoning in plagioclase from the Upper Anorthosite zone of the Middle Banded series. Redrawn after Czamanske and Scheidle (1985).

Upper Anorthosite zone can be seen in a single outcrop, and that bulk-rock compositional trends can be correlated with pyroxene mode. Oikocrysts of pyroxene are normally zoned over a range of Mg# of ~8 mol.% (Gitlin *et al*. 1985; Fig. 29). Pyroxenes are richer in Fe than those of the overlying troctolite units, containing abundant inverted pigeonite. Locally present are cm-sized oikocrysts of Fe-Ti oxide (now exsolved to magnetite-ilmenite). The modal abundances of quartz and apatite tend to vary inversely with pyroxene abundance. The compositional zoning and heterogeneous distribution of the oikocrysts suggest that widely spaced nucleation (on the decimetre scale) and growth of pyroxene progressively displaced the compositionally evolving residual interstitial liquid. Evidence for this includes the high Sc (pyroxene-compatible), low

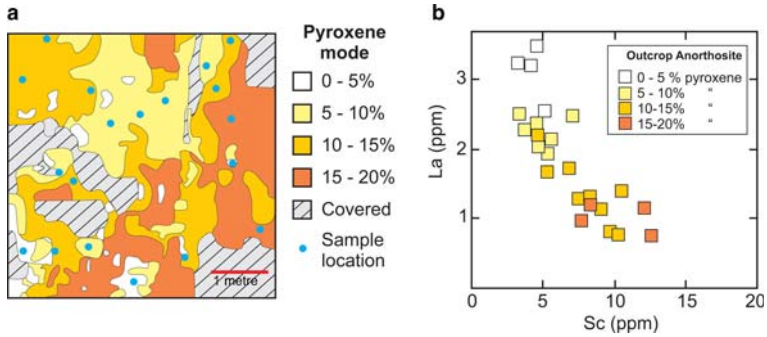

FIG. 28. Example of modal and bulk-rock compositional variation in the Upper Anorthosite zone of the Middle Banded series. (*a*) Map of the modal variation in pyroxene in an outcrop of the Upper Anorthosite zone, Contact Mountain area. (*b*) Plot of bulk-rock La *vs*. Sc in samples from the outcrop. Both redrawn after Salpas *et al.* (1983).

https://doi.org/10.1180/minmag.2016.080.063 Published online by Cambridge University Press

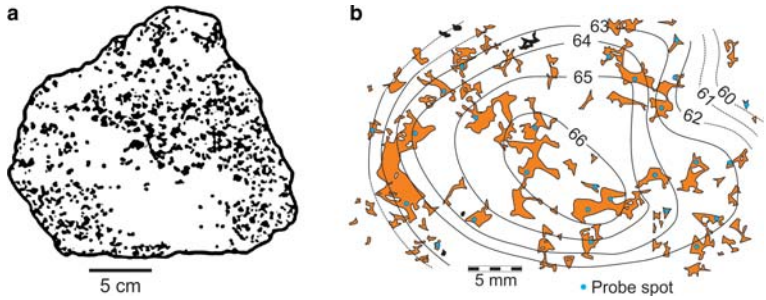

FIG. 29. Detail of modal and compositional variation in a boulder from the Upper Anorthosite zone of the Middle Banded series. (*a*) Pyroxene distribution in a boulder from the outcrop of Fig. 27. (*b*) Map of Mg# variation in a single pyroxene oikocryst from the same boulder, as determined by electron microprobe analysis. Both redrawn after Gitlin *et al.* (1985).

La concentrations seen in the pyroxene-rich rocks (Fig. 28*b*). The crystallization of late-forming minerals, such as quartz, apatite, and Fe-Ti oxide, was limited to residual interstitial pockets of evolved liquid where pyroxene is less abundant.

Based on phase equilibria and modal abundances of pyroxenes, Raedeke and McCallum (1980) suggested that the anorthosites retained up to 30% trapped liquid. However, the textural and modal evidence that pyroxene and other minerals crystallized from a trapped liquid contrasts with incompatible trace-element abundances, which indicate that the rocks contained no more than a few percent of a residual trapped liquid component (Salpas *et al.*, 1983). This suggests that the rocks either are heteradcumulates in the classic sense or have lost a late, evolved interstitial liquid. Evidence for the migration of evolved interstitial liquid in the Upper Anorthosite zone is seen in high bulk-rock *REE* concentrations (La = ~10 × chondrite) in some rocks that have flat to slightly negative Eu anomalies. These high *REE* concentrations occur in anorthosites for which the plagioclase separates from the same rocks have strong positive Eu anomalies and compose 85% + of the rock mode (Boudreau, 1986; Loferski *et al*., 1994) (Fig. 30). Other evidence for the late loss of an evolved component is seen in the presence of a discordant alaskite body near the contact of the Lower Anorthosite zone with the overlying OB-III unit. Although Czamanske *et al.* (1991) suggested the alaskite precipitated from a high-temperature

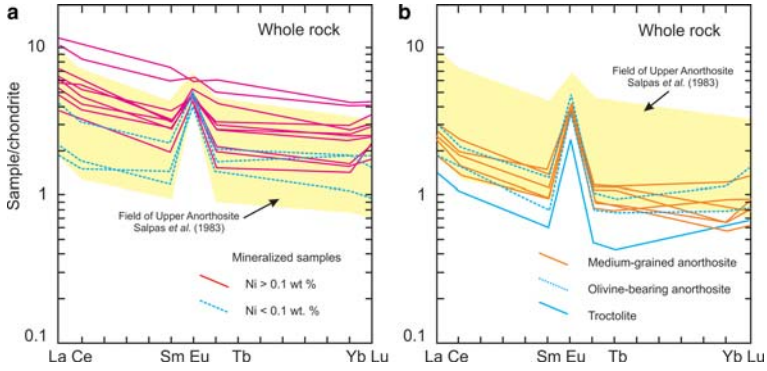

FIG. 30. Chondrite-normalized whole-rock *REE* abundances from the Upper Anorthosite zone and OB-V. (*a*) Whole-rock *REE* in mineralized anorthosite from the Picket Pin PGE zone, comparing poorly-mineralized (Ni < 0.1 wt.%) and well-mineralized (Ni > 0.1 wt%) samples. The shaded pale yellow area is the range for the Upper Anorthosite zone samples reported by Salpas *et al.* (1983). (*b*) Whole-rock *REE* in unmineralized anorthosite from the Medium-Grained anorthosite member of the Upper Anorthosite zone and olivine-bearing anorthosite and troctolite from the overlying OB-V. Redrawn after Boudreau (1986).

https://doi.org/10.1180/minmag.2016.080.063 Published online by Cambridge University Press

chloride solution, their stratigraphic location suggests they could have been liquids filter-pressed out from the underlying anorthosite.

Loferski and Arculus (1993) have described multiphase inclusions consisting of clinopyroxene + ilmenite + apatite that occur within plagioclase from the Middle Banded series of the intrusion. The textures and constant modal mineralogy of the inclusions indicate that they were incorporated in the plagioclase as liquid droplets that later crystallized rather than as solid aggregates. Their unusual assemblage, including a distinctive manganiferous ilmenite and the presence of baddeleyite (ZrO_2), indicates formation from an unusual liquid. They proposed that small globules of an immiscible silicate liquid, enriched in Mg, Fe, Ca, Ti, P, *REE*, Zr and Mn, exsolved from the main liquid that gave rise to the anorthosites and subsequently trapped and crystallized as inclusions in plagioclase. They were uncertain if the immiscibility occurred in compositional boundaries around crystallizing plagioclase grains or pervasively throughout the magma.

The Picket Pin PGE-Sulfide zone of the Upper Anorthosite zone

Sulfides modestly enriched in the platinum-group elements occur in the coarse-grained anorthosite immediately below the medium-grained anorthosite member of the Upper Anorthosite zone and have been described by Boudreau and McCallum (1985, 1986). The sulfide zone is stratabound in the sense that it is traceable at the same stratigraphic interval over 22 km of exposed strike length. However, in detail, the zone is characterized by erratically developed podiform and lenticular accumulations of 1–5 vol.% disseminated sulfides (mainly chalcopyrite, pyrrhotite and minor pentlandite). Discordant trails of spotty disseminated sulfides and larger transgressive sulfide-rich 'pipes' occur to depths of ~150 m into the Upper Anorthosite zone (Fig. 31). These discordant zones of mineralization typically underlie the better-mineralized sections near the top of the anorthosite.

Sulfide mineralization is most commonly associated with the pyroxene-poor, incompatible element-rich parts of the Upper Anorthosite zone. Accessory minerals include quartz and apatite, but mineralization is not associated with the Fe-Ti oxides noted above. Locally the sulfide forms the core of small (10–20 cm) patches of pegmatoidal anorthosite, where the sulfide is extensively weathered but what remains is predominantly pyritic. These pegmatoidal accumulations occur on the ridge crest just west of the East Boulder River where large blocks of the overlying troctolite layers appear to have 'foundered' into the upper part of the anorthosite. Sulfur isotopes of the Picket

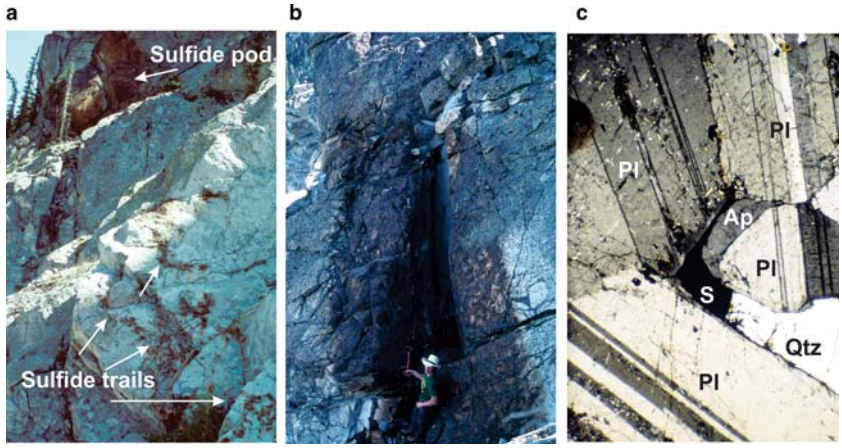

FIG. 31. Photographs of features of the Picket Pin PGE zone of the Upper Anorthosite zone. (*a*) Example of trails of disseminated sulfides in the upper part of the Upper Anorthosite zone leading up-section to the sulfide pod at the top of the photo. Note hammer for scale to the right of the 'Sulfide trails' label. (*b*) Discordant pipe with several percent disseminated sulfide ~100 m below the top of the Upper Anorthosite zone, Lewis Gulch area. (*c*) Photomicrograph of sulfide (S) associated with quartz (Qtz) and apatite (Ap) interstitial to plagioclase (Pl) from the pipe shown in (*b*).

https://doi.org/10.1180/minmag.2016.080.063 Published online by Cambridge University Press

Pin zone are similar to other disseminated sulfides of the complex (excluding the slightly anomalous values seen in the Basal series), with $\delta^{34}S$ averaging 1.2 per mil (Zientek and Ripley, 1990). Some sulfide occurs in the Medium-Grained Anorthosite member at the top of the zone, but these sulfides are PGE-barren. Sulfide is also rare in the overlying barren troctolite of OB-V.

The transgressive zones of sulfide leading up to the main sulfide concentrations, the association of the sulfides with the late-crystallizing minerals quartz and apatite, and the incompatible-element-rich nature of the sulfide pipes and pods led Boudreau and McCallum (1986) to the interpretation that the ore component was introduced by the percolation of mineralizing solutions during solidification of the Upper Anorthosite. The discordant pipes and sulfide trails were interpreted as fossil channelways or the plutonic equivalent of fumarolic zones, through which both late-evolved liquid and the mineralizing fluids migrated upwards.

Boudreau and McCallum (1986) noted that the sulfide grains commonly have haloes of greeenschist-grade alteration affecting the surrounding silicates. While Boudreau and McCallum did not rule out minor ore element redistribution during alteration, they did not think this alteration was the primary source of mineralization. They note that relatively unaltered silicates occur locally with sulfide, alteration occurs to some degree in most rocks of the complex, the sulfide occurs with a distinctive igneous assemblage that includes interstitial quartz and apatite, and mineralization is stratigraphically controlled.

In contrast, Corkery (2002, 2003) noted that patches and stringers of clinozoisite-epidote-quartz lead up section to the PGE-enriched sulfide intervals. Assay values of these clinozoisite patches away from obvious sulfide mineralization are up to 600 ppb combined PGE, whereas the surrounding rocks are barren. The alteration mineralogy is zoned about the sulfide: epidote-magnetite-albite ± quartz occurs away from the sulfides and clinozoisite-quartz-albite occurs in contact with the sulfides. Corkery (2002, 2003) suggested that a hypersaline hydrothermal fluid at an approximate temperature of 500–550°C transported the PGE to enrich a pre-existing sulfide; he does not otherwise explain the podiform distribution of sulfide in the Upper Anorthosite zone. An interpretation including both points of view is that mineralization began as a high-temperature event (a mineralizing fluid in equilibrium with the igneous silicate assemblage) but that fluid continued to move through the anorthosite as temperature fell over time to produce the later, but still relatively high-temperature alteration. The observed PGE enrichments below the sulfide pods noted by Corkery (2002, 2003) may be the result of a chromatographic effect as sulfur moves upwards and leaves some of the PGE behind (e.g. Meurer *et al.* 1998). Radiometric age determination could confirm if the alteration is related to cooling of the intrusion or the ~1.7 Ga regional metamorphic event.

Anorthosite crystallization model

McCallum (1996) presented a detailed formation model for the Middle Banded series anorthosites. In summary, the large size and complex zoning of the plagioclase suggests a long period that plagioclase was suspended in the magma, and the lack of internal stratification/layering (except near the upper contacts) and the lack of stratigraphic compositional trends in the plagioclase suggests the units formed initially as thick plagioclase + liquid mushes. The observation that the average plagioclase compositions are similar to those of the Lower Banded series and the negative Eu anomalies seen in orthopyroxene of the Ultramafic series would support the interpretation that the plagioclase was the complement of the mafic minerals that crystallized and formed all or part of the Ultramafic series (McCallum *et al.*, 1980). Whether the initial assemblage formed by such a process or injected into the Stillwater chamber as a plagioclase-phyric magma (Czamanske and Bohen, 1990), the net result was the formation of three thick zones of plagioclase + liquid mush (Fig. 32*a*). The bulk rock at this point has relatively low *REE* bulk-rock abundances with a marked positive Eu anomaly.

Cooling of the mush led to the eventual saturation of the interstitial liquid in pyroxene (pigeonite + augite). Because of the very slow cooling of these thick mushes, pyroxene growth proceeded from widely separated nucleation centres (Fig. 32*b*). As the pyroxene grew, it occluded porosity and displaced the interstitial liquid. In contrast, plagioclase had many existing grains on which growth from the interstitial liquid could continue. The net effect is that the interstitial liquid becomes increasingly compositionally evolved (Fig. 32*c*).

Towards the end of crystallization the interstitial liquid became saturated in the minerals quartz, Fe-Ti oxide, and apatite, and may have reached sulfide saturation. The most evolved interstitial liquid has

https://doi.org/10.1180/minmag.2016.080.063 Published online by Cambridge University Press

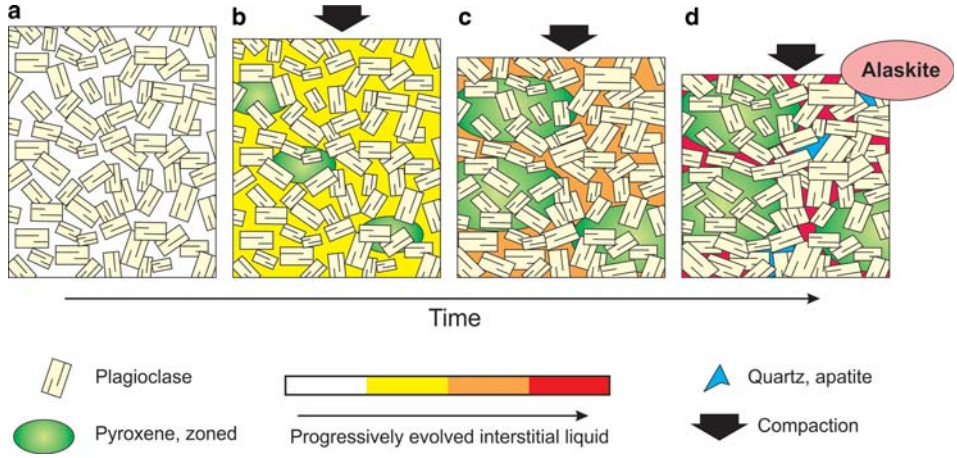

FIG. 32. Cartoon showing the textural and compositional evolution of the Middle Banded series anorthosites. See text for discussion.

high *REE* abundances with a strong negative Eu anomaly. Late migration of the strongly evolved interstitial liquid (driven by modest compaction of the mush or liquid advection within the mush) locally displaces less-evolved liquid and dominates the bulk-rock *REE* abundance to produce a flat to slightly negative Eu anomaly. These last regions to crystallize also become the channelways by which mineralizing fluids migrate upwards to produce the Picket Pin PGE zone (Fig 32*d*). High f_{S_2} in the mineralized rocks led to the preferential precipitation of sulfide rather than Fe-Ti oxide.

Discordant troctolite-anorthosite bodies of OB-II and the Middle Banded series

In Olivine-Bearing zone II (OB-II, below the Lower Anorthosite zone) and in at least three stratigraphic localities in the Middle Banded series discordant bodies of troctolite and anorthosite are common (Fig. 33). These are similar in size to the discordant dunite bodies of the Peridotite zone. The troctolite-anorthosite assemblages defines OB-II, where isolated pods of troctolite are hosted in a discordant anorthosite (the 'pillow troctolite' of Hess, 1960), both of which crosscut well-foliated gabbronorite. The troctolite can have cores of gabbronorite, the foliation of which can be rotated relative to that of the surrounding gabbronorite. The discordant bodies in the Middle Banded series are elongate perpendicular to the layering of the host cumulates with local concordant apophyses (Fig. 34).

Below the Upper Anorthosite zone is an unusual olivine gabbro in which single olivine crystals up to several cm in size have distinctive haloes of pure plagioclase in otherwise medium-textured gabbro (Fig. 33*e*). Hess (1960) noted the egg-like appearance of these features and they have since become known as 'Hess's eggs'. Locally, these eggs become more numerous and can merge with the discordant bodies (Fig. 33*f*), leading to the interpretation that they represent an incipient version of the gabbro to troctolite-anorthosite transformation.

In general, the plagioclase in the discordant bodies is blocky and about twice the size of that in the hosts gabbroic rock, where the plagioclase is more tabular/prismatic. The olivine forms large, lobate 'amoeboidal' grains with rounded plagioclase inclusions. Ophitic and subophitic pyroxene, if present, is minor. All bodies lack any discernible foliation (in contrast to the well-foliated gabbro host) and have sharp margins with no evidence of disrupted host-mineral foliations, implying they formed after the main compaction-driven texture of the host rock had formed.

Average olivine in the host rocks is slightly more magnesian than that of the discordant bodies by ~1–2 Mg# but NiO contents are similar, and plagioclase compositions are indistinguishable. Whole-rock major- and trace-element compositions of the discordant bodies are generally indistinguishable from layered troctolite with similar modal abundance. However, bulk compositions of anorthositic cores from the discordant bodies are

https://doi.org/10.1180/minmag.2016.080.063 Published online by Cambridge University Press

FIG. 33. Photographs of examples of discordant troctolites from OB II and the Middle Banded series. (*a*) Discordant 'pillow troctolite' (terminology of Hess, 1960) of OB II. Stratigraphic 'up' is towards the top of the photo. (*b*) Detail of transition from the host gabbronorite to the troctolite pillows. (*c*) Discordant troctolite bodies in a boulder from OB-III. A plagioclase + quartz + hornblende vein also cuts the boulder, which are otherwise rare in the complex. (*d*) Discordant troctolite in OB-IV just below the Upper Anorthosite zone. Stratigraphic 'up' is towards the top of the photo. (*e*) Example of the 'egg' texture described by Hess (1960), with a transition to discordant troctolite in OB IV. (*f*) Detail of 'egg' texture; black olivine defines the 'yoke' in the centre-bottom of the surrounding plagioclase-rich 'egg white'. Note lens cap and hammer for scales.

enriched in K, Na, Ba, Sr and P (Meurer *et al.*, 1997).

Salpas and Pass (1990) note that the *REE* pattern of gabbronorite surrounding the pillow troctolite of OB-II overlaps that of the mineralogically and texturally similar underlying gabbronorite. In contrast, the anorthosites of the pillow troctolite are slightly enriched in the light *REE* but have much lower heavy *REE* concentrations (Fig. 35*a*). The troctolite *REE* concentrations are mostly intermediate between the gabbronorite and anorthosites, but extend into the anorthosite field. Salpas and Pass suggested a model that involves olivine growth at the top of the Lower Banded series followed by influx of an anorthosite magma or mush that entrains the pods of troctolite and gabbronorite and plates onto the bottom of the Lower Anorthosite zone. In contrast, Meurer *et al.* (1997) suggested that the discordant bodies formed when cooler volatile fluids or fluid-rich silicate

https://doi.org/10.1180/minmag.2016.080.063 Published online by Cambridge University Press

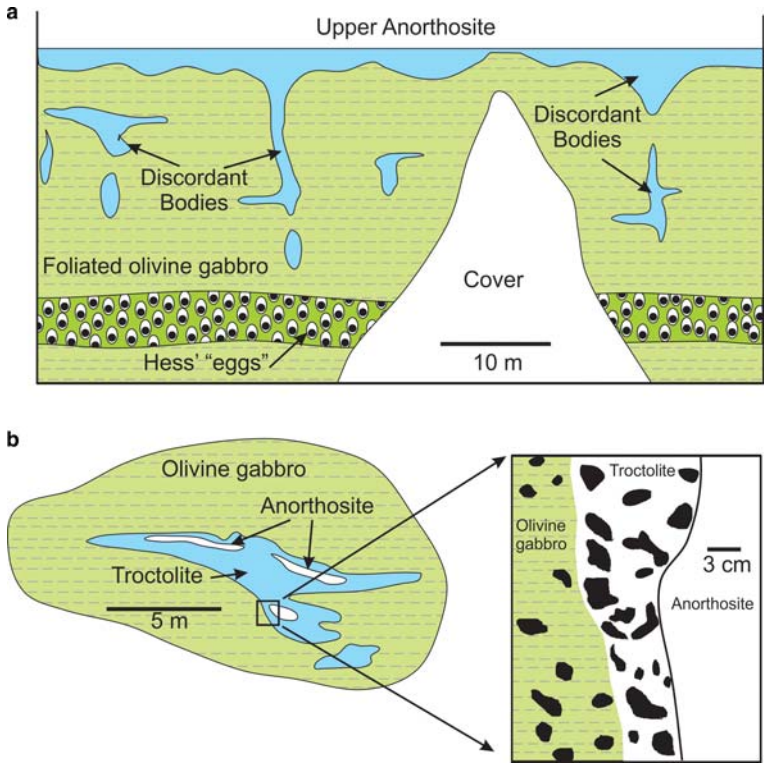

FIG. 34. Discordant troctolites of the Middle Banded series. (*a*) Schematic relations of discordant bodies in the uppermost portions of OB-IV. (*b*) Example of a zoned discordant body with anorthosite cores and detail of the characteristic irregular 'amoeboidal' olivine (black) going from well-foliated olivine-gabbro host rock to anorthosite. Redrawn after Meurer *et al.* (1997).

liquids moved upwards into hotter rocks and became undersaturated in silica and pyroxene components as the fluid became heated (Fig. 35*b*). Reaction of the fluid produced olivine after pyroxene by preferential loss of silica at low fluid/rock mass ratios and the loss of all mafic components, leaving just plagioclase, at higher fluid/rock mass ratios. Continued liquid/fluid fluxing increased the permeability along the flow path and focused the flow, modifying the original bulk compositions and leaving zoned plagioclase-rich troctolite and anorthosite replacement bodies. Once the fluid reached equilibrium with the host rock, it moved through the system without further reaction.

The continuing problem of olivine in the Banded series

The discussion above has presented evidence that that the olivine of OB-I, the host zone of the J-M Reef, formed by volatile fluxing (Boudreau, 1988, 1999). It is also clear that the discordant olivine-bearing rock of OB-II is of a replacement origin (e.g. McCallum *et al.* 1977). Indeed, it is questionable that OB-II should be considered a separate stratigraphic zone at all given that olivine-bearing rocks are only developed sporadically along strike. There is also the common occurrence of discordant bodies in the Middle Banded zone and their compositional similarities of plagioclase and olivine with the olivine-bearing host rocks. This leads one to ask if the troctolite units above the thick anorthosites, the anomalous olivine-gabbro units, and the lack of orthopyroxene as a primary mineral in the Middle Banded series are the result of interaction with silicate liquids or volatile fluids escaping from the underlying anorthosites that modified the normal Stillwater crystallization sequence.

Conversion of gabbronorite to a troctolite and anorthosite can occur by near-solidus to subsolidus

https://doi.org/10.1180/minmag.2016.080.063 Published online by Cambridge University Press

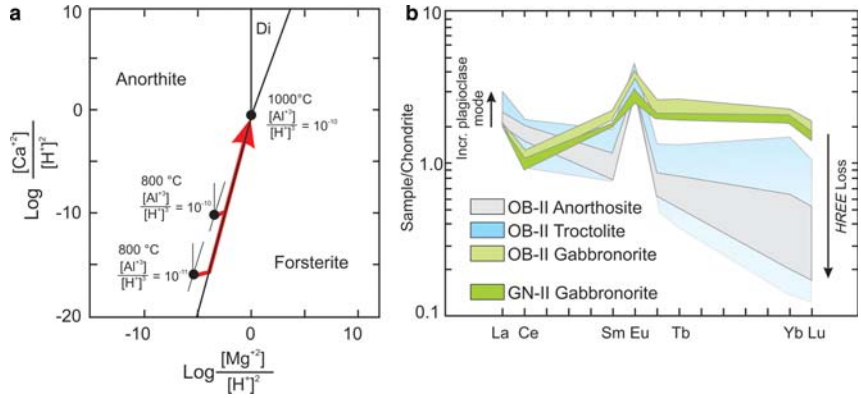

FIG. 35. Hydrothermal replacement model for the formation of the discordant troctolites of the Banded series. (*a*) Activity diagram showing the stability field of anorthite, diopside and forsterite as a function of the activity ratios $[Ca^{+2}]/[H^+]^2$ and $[Mg^{+2}]/[H^+]^2$. Filled circles are the intersection of the triple-saturated intersection at 1000 and 800°C for values for different activity ratios $[Al^{+3}]/[H^+]^2$, as noted. Fluids in equilibrium with a cooler three-phase assemblage become nominally saturated in plagioclase alone when heated. The red line shows the reaction paths as these cooler fluids react with the higher-temperature assemblage. Redrawn after Meurer *et al.* (1997). (*b*) Effect of replacement on the bulk-rock *REE* patterns. Progressive replacement of gabbronorite → troctolite → anorthosite leads to preferential loss of the heavy *REE*, whereas the increase in modal plagioclase leads to a modest increase in the light *REE*. *REE* fields redrawn from data of Salpas and Pass (1990).

replacement, as suggested above for the discordant troctolite-anorthosite bodies of the Middle Banded series. Alternatively, addition of H_2O may occur while the rocks are still partly molten. For example, a simple *R-MELTS* calculation (Gualda and Ghiorso, 2015) shows that the addition of as little as 0.6 wt.% H_2O can convert a partially molten gabbronorite (dry composition listed in Table 1) into an olivine gabbro at 1150°C (Fig. 36). This model 'olivine gabbro' would have the late crystallization of orthopyroxene after clinopyroxene typical of the Middle Banded series. These results cast doubt that the gabbroic rocks of the Middle Banded series require the influx of a magma with a different liquid line of descent.

It is proposed that vapour released during the solidification of the thick anorthosites migrated into the overlying magma/mush and altered what would have been a typical norite or gabbronorite if not for this hydration event. More specifically it is suggested that this alteration occurred by a process of incongruent melting induced by hydration and by the supersolidus loss of silica during vapour migration through a (partly molten) norite/gabbronorite protolith.

Evidence for this is as follows. (1) Cl/(Cl + F) ratios of apatite from anorthosites average ~0.15 whereas for the rest of OB-III and OB-IV it is at least twice this (Meurer and Boudreau 1998*b*). The lower Cl concentrations of the anorthosite apatite is consistent with Cl loss to degassing from the anorthosites and added to the olivine-bearing units. (2) As noted, the composition of olivine from both discordant bodies and the host are similar, both in terms of Mg# and NiO concentrations. (3) The

TABLE 1. Bulk rock (dry) composition of gabbronorite and leuconorite used in the *MELTS* model results of Fig. 36.

	GN-89-159*
SiO_2	51.41
TiO_2	0.17
Al_2O_3	14.48
Fe_2O_3**	0.10
FeO	5.92
MnO	0.14
MgO	13.63
CaO	13.10
Na_2O	1.01
K_2O	0.03
Total	99.99

*Duke University gabbronorite in-house standard from Gabbronorite zone I.
**A small amount of ferric iron was added for computational stability in *MELTS*.

https://doi.org/10.1180/minmag.2016.080.063 Published online by Cambridge University Press

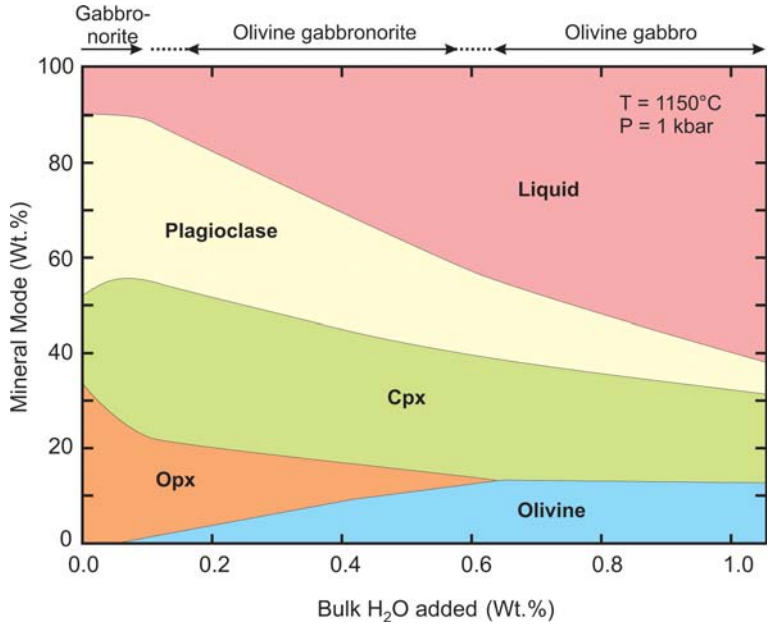

FIG. 36. A *MELTS* Excel (Gualda and Ghiorso, 2015) calculation on the modal changes of a gabbronorite + liquid with addition of H_2O at 1150°C and 1 kbar pressure. The initial dry bulk composition is that of a Lower Banded series gabbronorite as listed in Table 1. The phase assemblages are calculated as a function of water added to this initial composition. Cpx – clinopyroxene; Opx – orthopyroxene.

overall sequence as seen at the top of the Upper Anorthosite zone and into the Upper Banded series of fine-grained anorthosite-troctolite-norite mimics the zoning seen in the discordant troctolite-anorthosite bodies. (4) The wispy-layered troctolite units that directly overly the thicker Lower and Upper Anorthosite zones are thin relative to the underlying anorthosite unit: the ratio of troctolite thickness/underlying anorthosites thickness is 0.17 for the Lower Anorthosite zone and 0.14 for the Upper Anorthosite zone. This would be expected if vapour emanating from the anorthosite controlled the formation of the overlying rocks; a thicker anorthosite would produce a thicker troctolite. (5) Similar to what is observed in OB-I, the compositions of the major phases show little in the way of evidence for a more primitive magma entering the chamber. (6) Although olivine in the troctolite units is more equant than the amoeboidal olivine in the replacement bodies, as seen in Fig. 25 they do have irregular shapes and plagioclase inclusions as does the replacement olivine. Furthermore, similar to the plagioclase chadacrysts in olivine in OB-I, the OB-V plagioclase inclusions are reverse-zoned by an average of 4.4 mol.% An (unpublished data) and are consistent with silica and sodium loss from the rocks. If they did form by silica loss to vapour from a gabbronorite or norite protolith, it probably happened at a higher temperature than that at which the discordant troctolites formed, which allowed the olivine to develop a more equant but still poikilitic habit.

If the thick anorthosite units formed either as injections of a plagioclase-rich mush or from plagioclase accumulating at a density-neutral buoyancy point in the magma column, then these thick mushes would be qualitatively very different from a normal crystal mush. That is, the normal growth of the crystal pile involves minerals being either added to, or growing from, the top of the pile. Compaction reduces porosity quickly such that, away from the cold margins of the intrusion, the interstitial liquid is readily lost: high porosity crystal + liquid mush is present only within a few metres to a few tens of metres from the top of the crystal pile and the final porosity may be <10% (e.g. Shirley, 1986). Hence degassing of the thick stratigraphic section below the J-M Reef was required to form the rather small amount of olivine in OB-I. This process was again repeated to form the small amount of olivine in OB-II after crystallization of N-II and GN-II.

https://doi.org/10.1180/minmag.2016.080.063 Published online by Cambridge University Press

In contrast, compaction would be less effective at reducing interstitial liquid in a thick plagioclase mush owing to the modest density contrast between plagioclase and liquid. The net result is that the anorthosite units, which can be in excess of 500 m thick, had a much larger amount of interstitial liquid available to degas than during the normal growth of a crystal mush. The mush above an anorthosite would thus experience a flux of material out of the anorthosites that is qualitatively and quantitatively different than would occur in the normal situation. The process of vapour migrating out of the anorthosite and reacting with the overlying mush is broadly analogous to the 'gas sparging' that occurs when vapour from degassing mafic magmas that underplate intermediate to silicic crystal mushes migrates into the overlying mush (e.g. Bachmann and Bergantz, 2006).

Discussion

The problematic nature of olivine

As discussed above, the reappearance of olivine in the stratigraphic section has been attributed to a variety of mechanisms that can operate from magmatic to subsolidus conditions. These are summarized as follows. (1) The reintroduction of a more primitive, olivine-saturated magma, as is commonly suggested for the reappearance of olivine in the Ultramafic series. This is complicated by the fact that the sill/dyke suite and Basal series rocks are generally lacking in olivine. (2) Mixing of magmas to produce olivine-saturated hybrid liquids, as has been proposed by the orthomagmatic models to explain OB-I and the J-M Reef. (3) Hydration of the magma column to favour olivine over pyroxene, as suggested here as an alternative to drive a magma to crystallize olivine ± chromite over pyroxene. (4) Hydration melting of a (gabbro) norite + liquid protolith, as suggested for the hydromagmatic model for OB-I and suggested here for the formation of olivine gabbro after gabbronorite of the Middle Banded series. (5) Subsolidus replacement of pyroxene, as proposed for discordant dunite of the Peridotite zone and troctolite-anorthosite bodies of the Banded series.

A dry Stillwater?

The possibility that many of the more interesting features of the Stillwater Complex are due to volatiles gives rise to the question of what would the Stillwater Complex look like if, indeed, it were a perfectly dry magma?

In the following discussion, some interpretations would not be disputed by most Stillwater investigators. An example would be the secondary nature of olivine in OB-II. Other interpretations, such as the possibility that the olivine of the Peridotite zone is the result of magma hydration, would be actively disputed. With this caveat, an interpretation of what the Stillwater Complex would have looked like without the volatile modification is shown in Fig. 37. From the bottom to top, these features of the complex would be as follows:

Basal series

The dry Basal series would still look much the same. Quick cooling of the Basal series rocks would freeze in interstitial liquid, leading to a relatively noritic assemblage at the base. As the pile grew, compaction would become dominant over cooling and would lead to less interstitial liquid with height and the rocks become orthopyroxenite.

Ultramafic series

If the general lack of olivine in the sill/dyke suite or in the Basal series is typical of the Stillwater parent liquid and if indeed olivine saturation requires a hydrated magma, then olivine would not crystallize. However, even if olivine were to crystallize, a drier magma would make for more limited olivine, as suggested by the replacement of granular harzburgite by poikilitic harzburgite (Fig. 7). Furthermore, as Cr is incorporated into pyroxene, there is unlikely to be significant build-up of Cr in the magma as there would be if the magma were olivine saturated. Thus, little or no chromite need precipitate, resulting in no or reduced chromitite layers.

Banded series

The Banded series would have no olivine-bearing zones. Olive-bearing zone I would not have occurred and instead the rock would continue the modal and compositional trends of N-I and GN-I such that massive gabbronorite would be continuous up to the base of the Middle Banded series. Given that the modal layering could be driven by volatile-rich liquids favouring mafic minerals over plagioclase (e.g. McBirney, 1987), the modal layering in the footwall to OB-I and again just below OB-II would not be present.

Influx and mixing of more primitive magma with the increasing volume of evolved magma in the

https://doi.org/10.1180/minmag.2016.080.063 Published online by Cambridge University Press

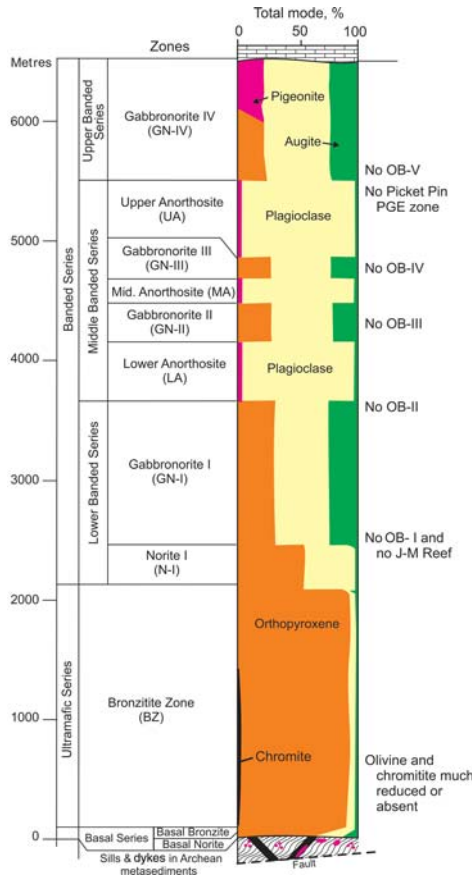

FIG. 37. A 'dry' Stillwater Complex? A proposed simplified Stillwater mineral mode stratigraphy that would result if volatiles either did not alter the original magmatic crystallization sequence or modify the originally precipitated magmatic assemblage as discussed in the text.

chamber leads to increasingly modest compositional offsets, but overall the chamber sees a fractionation trend of more evolved compositions with stratigraphic height. The magma would still become sulfide-saturated at some point, but actual sulfide modes need only be in cotectic proportions. Ore metal tenor at the level of sulfide saturation might be similar to the J-M Reef, but ore grade would be 1–2 orders of magnitude lower owing to the much smaller volume of sulfide. Except perhaps for some S moved by interstitial liquids, sulfide modes would be cotectic and no zones would be present that contain higher than cotectic abundances. Hydrous minerals and evidence of loss of S from sulfides would be absent. Ore metal and S abundances below the level of S saturation would be low, controlled by trapped liquid abundance.

The Middle Banded series would still contain three thick anorthosite units, but sandwiched in between the anorthosites would be gabbronorite rather than troctolite and olivine gabbro. No degassing of the anorthosites means no Picket Pin PGE zone at the top of the Middle Banded series, and no OB-V. Instead, the base of the Upper Banded series would continue with the precipitation of gabbronorite and a continuing Fe-enrichment trend.

Conclusions

This review has highlighted a number of ways in which changes in the Stillwater crystallization sequence need not have been due to magmas with

https://doi.org/10.1180/minmag.2016.080.063 Published online by Cambridge University Press

different liquid lines of descent but instead could have occurred by processes happening within the Stillwater magma chamber. Instead, it is proposed that there is continuous if variable interaction of upwards-migrating vapour with the mush-magma system at the top of the crystal pile. At its extreme, the process can favour the formation of olivine (± chromite) over pyroxene. These mechanisms include volatile phase boundary shifts in the parent liquid induced by added H_2O, incongruent melting of pyroxene by hydration of a partly molten mush, and the subsolidus replacement of pyroxene by olivine and chromite by silica-undersaturated fluids.

This review has highlighted a number of areas of Stillwater research in which more study is warranted. These include the following:

Isotopic disequilibrium studies

Recent work on other intrusions has highlighted the importance of both intra- and inter-granular isotopic disequlibrium. Such focused studies have not been widely applied to the Stillwater Complex. Of particular interest would be the studies of the isotopic systems such as Sm-Nd which apparently are resistant to modification by the mid-Proterozoic heating event (DePaolo and Wasserburg, 1979). The isotopic characteristics of pegmatoidal rocks as compared with host rocks, and that of included fluid inclusions, could be perhaps particularly instructive. That of the high-temperature carbonates found below the J-M Reef and comparison with the host minerals is another potential study.

Compaction in the Ultramafic series

There is increasing recognition of the effects of concurrent compaction and crystallization of the interstitial liquid on modifying mineral and bulk-rock compositions (e.g. Meurer and Boudreau 1998*a*). The degree to which local variations seen in the Ultramafic series may be the result of compaction-driven processes such as these have not been well-studied. Much of the analysis of the Ultramafic series have involved mineral composition (microprobe) or whole-rock ore element studies. Bulk-rock analysis combined with petrographic and mineral composition data can elucidate the role of compaction and interstitial liquid crystallization in modifying the original precipitated assemblage.

Of particular interest would be a more complete study of the Bronzitite zone. Current work has focused on mineral compositions, but as discussed for the thick anorthosite units of the Middle Banded series, crystallization and migration of the interstitial liquid can strongly affect bulk-rock incompatible element abundances. Given that orthopyroxene of the Bronzitite zone would re-equilibrate much easier than plagioclase, it remains an open question as to the degree mineral separate studies of this unit represent initial magmatic compositions or have been modified by evolved interstitial liquids.

The nature of the regional unconformity of OB-I and the J-M Reef

Little is known about the nature of this unconformity. It has already been noted that, in the normal position of OB-I, there is little change in mineral compositional trends from the footwall to hanging wall units, particularly in plagioclase. At the very least it would be interesting to see if this is also true across the unconformity (albeit at slightly less-evolved compositions) or if there is a distinctive offset in mineral trends at the unconformity.

The compositional characteristics of the olivine-bearing units of the Middle and Upper Banded series

Very little has been done on the compositional characteristics of the troctolites above the thick anorthosite units. If they formed by vapour leaching of an initially norite/gabbronorite protolith as suggested here, they may show some characteristic compositional similarities with the discordant troctolites.

Acknowledgements

I came of age as a geologist during a major burst of Stillwater studies in the 1970's, and this review and the ideas presented herein are the result of almost 40 years of working and thinking about these rocks. I would like to thank my mentors in these early years, A.R. McBirney for encouraging unconventional thinking, and I.S. McCallum for keeping me focused on the evidence in the rocks. The thoughtful comments of I.S. McCallum, S.A. Morse and an anonymous reviewer markedly improved this manuscript; I apologize for making you trudge through my too many typos.

References

Abbott, Jr., D.M., Bullock, R.L., Gibbs, B. and Kunter, R. S. (2011) Technical report for the mining operations at Stillwater Mining Company, Stillwater Mine, 45°23′ N, 109°53′W, East Boulder Mine, 45°30′N, 109°05′ W: Denver, Colorado, Behre Dolbear & Company,

https://doi.org/10.1180/minmag.2016.080.063 Published online by Cambridge University Press

Ltd., Project 11-030, 87 pp. URL: http://secfilings.nyse.com/filing.php?ipage=7682024.

Aird, H.M. and Boudreau, A.E. (2013) High-temperature carbonate minerals in the Stillwater Complex, Montana, USA. *Contributions to Mineralogy and Petrology*, **166**, 1143–1160.

Aird, H.M., Ferguson, K.M., Lehrer, M.L. and Boudreau, A.E. (2016) A study of the trace sulfide mineral assemblages in the Stillwater Complex, Montana. *Mineralium Deposita*, doi: 10.1007/s00126-016-0664-x.

Armitage, G.J. (1992) *The petrogenesis of potholes in the UG2 chromitite layer, Crocodile River Mine, Western Bushveld complex*. Unpublished PhD dissertation, University of Natal, Pietermaritzburg, South Africa.

Bachmann, O. and Bergantz, G.W. (2006) Gas percolation in upper-crustal silicic crystal mushes as a mechanism for upward heat advection and rejuvenation of near-solidus magma bodies. *Journal of Volcanology and Geothermal Research*, **149**, 85–102.

Barnes, S.J. and Campbell, I.H. (1988) Role of late magmatic fluids in Merensky-type platinum deposits: a discussion. *Geology*, **16**, 488–491.

Barnes, S.J. and Naldrett, A.J. (1985) Geochemistry of the J-M (Howland) Reef of the Stillwater Complex, Minneapolis Adit Area. I. Sulfide chemistry and sulfide-olivine equilibrium. *Economic Geology*, **80**, 627–645.

Barnes, S.J. and Naldrett, A.J. (1986) Geochemistry of the J-M Reef of the Stillwater Complex, Minneapolis Adit Area II. Silicate mineral chemistry and petrogenesis. *Journal of Petrology*, **27**, 791–825.

Barnes, S.-J., Pagé, P., Prichard, H.M., Zientek, M.L. and Fisher, P.C. (2015) Chalcophile and platinum-group element distribution in the Ultramafic series of the Stillwater Complex, MT, USA – implications for processes enriching chromite layers in Os, Ir, Ru, and Rh. *Mineralium Deposita*, **51**, 25–47.

Boorman, S., Boudreau, A.E. and Kruger, F.J. (2004) The Lower zone – Critical Zone transition of the Bushveld Complex: A quantitative textural study. *Journal of Petrology*, **45**, 1209–1235.

Boudreau, A.E. (1986) *The role of fluids in the petrogenesis of platinum-group element deposits in the Stillwater Complex, Montana*. Unpublished PhD dissertation, University of Washington, Seattle, USA.

Boudreau, A.E. (1987) Pattern formation during crystallization and the formation of fine-scale layering. Pp. 453–471 in: *Origins of Igneous Layering* (I. Parsons, editor). NATO ASI Series, Series C: Mathematical and Physical Sciences, **Vol. 186**. Kluwer Academic, Dordrecht, The Netherlands.

Boudreau, A.E. (1988) Investigations of the Stillwater Complex: Part IV. The role of volatiles in the petrogenesis of the J-M Reef, Minneapolis adit section. *The Canadian Mineralogist*, **26**, 193–208.

Boudreau, A.E. (1992) Volatile fluid overpressure in layered intrusions and the formation of potholes. *Australian Journal of Earth Sciences*, **39**, 277–287.

Boudreau, A.E. (1994) Pattern formation during crystallization in two crystal, two component systems: *South African Journal of Geology*, **97**, 473–485.

Boudreau, A.E. (1995) Crystal aging and the formation of fine-scale layering. *Mineralogy and Petrology*, **54**, 55–69.

Boudreau, A.E. (1999) Fluid fluxing of cumulates: The J-M reef and associated rocks of the Stillwater Complex, Montana. *Journal of Petrology*, **40**, 755–772.

Boudreau, A.E. (2011) The evolution of texture and layering in layered intrusions. *International Geology Review*, **53**, 330–353.

Boudreau, A.E., Mathez, E.A. and McCallum I.S. (1986) Halogen geochemistry of the Stillwater and Bushveld Complexes: Evidence for transport of the platinum-group elements by Cl-rich fluids. *Journal of Petrology*, **27**, 967–986.

Boudreau, A.E. and McBirney, A.R. (1997) The Skaergaard Layered series. Part. III. Non-dynamic Layering. *Journal of Petrology*, **38**, 1003–1020.

Boudreau, A.E. and McCallum, I.S. (1985) Features of the Picket Pin Pt-Pd deposit. Pp. 346–357 in: *Stillwater Complex, Montana: Geology and Guide* (G.K. Czamanske and M.L. Zientek, editors). Montana Bureau of Mines and Geology, Special Publication, **92**. Billings, Montana, USA.

Boudreau, A.E. and McCallum, I.S. (1986) Investigations of the Stillwater Complex. Part III. The Picket Pin Pt-Pd deposit. *Economic Geology*, **81**, 1953–1975.

Boudreau, A.E. and McCallum, I.S. (1989) Investigations of the Stillwater Complex: Part V. Apatite as indicators of evolving fluid composition. *Contributions to Mineralogy and Petrology*, **102**, 138–153.

Boudreau, A.E. and McCallum, I.S. (1992*a*) Concentration of platinum-group elements by magmatic fluids in layered intrusions. *Economic Geology*, **87**, 1830–1848.

Boudreau, A.E. and McCallum, I.S. (1992*b*) Infiltration metasomatism in layered intrusions – An example from the Stillwater Complex, Montana. *Journal of Volcanology and Geothermal Research*, **52**, 171–183.

Boudreau, A.E., Stewart, M.A. and Spivack, A.J. (1997) Stable Cl isotopes and origin of high-Cl magmas of the Stillwater Complex, Montana. *Geology*, **25**, 791–794.

Bow, C., Wolfgram, D., Turner, A., Barnes, S., Evans, J., Zdepski, M. and Boudreau, A.E. (1982) Investigations of the Howland reef of the Stillwater Complex, Minneapolis Adit area: Stratigraphy, structure and mineralization. *Economic Geology*, **77**, 1481–1492.

Braun, K., Meurer, W., Boudreau, A.E. and McCallum, I. S. (1994) Compositions of pegmatoids beneath the J-M Reef of the Stillwater Complex, Montana. *Chemical Geology*, **113**, 245–257.

https://doi.org/10.1180/minmag.2016.080.063 Published online by Cambridge University Press

Brozdowski, R.A. (1985) Cumulate xenoliths in the Lodgepole, Enos Mountain and Susie Peak intrusions: a guide. Pp. 368–372 in: *Stillwater Complex, Montana: Geology and Guide* (G.K. Czamanske and M. L. Zientek, editors). Montana Bureau of Mines and Geology, Special Publication **92**. Billings, Montana, USA.

Campbell, I.H. and Murck, B.W. (1993) Petrology of the G and H Chromitite Zones in the Mountain View Area of the Stillwater Complex, Montana. *Journal of Petrology*, **34**, 291–316.

Campbell, I.H., Naldrett, A.J. and Barnes, S.J. (1983) A model for the origin of the platinum-rich sulfide horizons in the Bushveld and Stillwater Complexes. *Journal of Petrology*, **24**, 133–165.

Cawthorn, R.G. and Walraven, F. (1998) Emplacement and crystallization time for the Bushveld Complex. *Journal of Petrology*, **39**, 1669–1687.

Childs, J.F., Evans, J.R., Wood, K.Y., Koski, M.S. and Evans, J.D. (2002) Some preliminary descriptive aspects of ballroom mineralization at the Stillwater palladium-platinum Mine, Stillwater Mining Company, Nye, Montana. Pp. 91–92 in: *9th International Platinum Symposium, Abstract with Program, 21–25 July 2002*. Billings, Montana, USA.

Chutas, N.I., Prevec, S., Bates, E. Coleman, D. and Boudreau, A.E. (2011) Pb and Sr isotopic disequilibrium between orthopyroxene and plagioclase in the Critical zone, Bushveld Complex, S. *Africa. Contributions to Mineralogy and Petrology*, **163**, 653–668.

Cooper, R.W. (1997) Magmatic unconformities and stratigraphic relations in the peridotite zone, Stillwater Complex, Montana. *Canadian Journal of Earth Sciences*, **34**, 407–425.

Corkery, J.T. (2002) Petrographic implications for the Picket Pin PGE deposit, Stillwater Complex, Montana: Pp. 97–100 in: *9th International Platinum Symposium, Abstract with Program, 21–25 July 2002.* Billings, Montana, USA.

Corkery, J.T. (2003) Petrographic observations and implications for the Picket Pin PGE deposit, Stillwater Complex, Montana. *Geological Society of America Abstracts with Programs*, **35(6)**, 231.

Corson, S.R., Childs, J.F., Dahy, J.P., Keith, D.W., Koski, M.S. and LeRoy, L.W. (2002) The reef package stratigraphy that contains the J-M platinum-palladium Reef of the Stillwater Complex, Montana. Pp. 101–102 in: *9th International Platinum Symposium, Abstract with Program, 21–25 July 2002.* Billings, Montana, USA.

Crawford, A.J., Fallon, T.J. and Green, D.H. (1989) Classification, petrogenesis and tectonic setting of boninites. Pp. 1–49 in: *Boninites (A.J Crawford, editor).* Unwin Hyman, London.

Criscenti. L.J. (1984) *The origin of macrorhythmic units in the Stillwater Complex*. Unpublished MS thesis, University of Washington, Seattle, USA.

Czamanske, G.K. and Bohlen, S.R. (1990) The Stillwater Complex and its anorthosites: an accident of magmatic underplating? *American Mineralogist*, **75**, 37–45.

Czamanske, G.K. and Loferski, P.J. (1996) Cryptic trace-element alteration of anorthosite, Stillwater Complex, Montana. *The Canadian Mineralogist*, **34**, 559–576.

Czamanske, G.K. and Scheidle, D.L. (1985) Characteristics of Banded-series anorthosites. Pp. 334–345 in: *Stillwater Complex, Montana: Geology and Guide* (G.K. Czamanske and M.L. Zientek, editors). Montana Bureau of Mines and Geology, Special Publication, **92**. Billings, Montana, USA.

Czamanske, G.K. and Zientek, M.L. (editors) (1985) *Stillwater Complex, Montana: Geology and Guide.* Montana Bureau of Mines and Geology, Special Publication, **92**. Billings, Montana, USA.

Czamanske, G.K., Zientek, M.L. and Manning, C.E. (1991) Low-K granophyres of the Stillwater Complex, Montana. *American Mineralogist*, **76**, 1646–1661.

Dahy, J.P., Corson, S.R., Geraghty, E.P., Koski, M.S., Langston, R.B. and Leroy, L.W. (1995) Stratigraphic relationships of the J-M Reef package within the troctolite–anorthosite zone I, Stillwater Complex, Stillwater Mine, Montana. *Geological Society of America, Abstracts with Programs*, **27**, 7–8.

DePaolo, D.J. and Wasserburg, G.J. (1979) Sm-Nd age of the Stillwater Complex and the mantle evolution curve for neodymium. *Geochimica et Cosmochimica Acta*, **43**, 999–1008.

Dunn, T. (1986) An investigation of the oxygen isotope geochemistry of the Stillwater Complex. *Journal of Petrology*, **27**, 987–997.

Emeleus, C.H. and Troll, V.R. (2104) The Rum Igneous Centre, Scotland. *Mineralogical Magazine*, **78**, 805–839.

Foose, M.P. and Nicholson, S.W. (1990) Sulfide inclusions within the B Chromitite, Stillwater Complex, Montana. *U.S. Geological Survey Bulletin*, **1674**, D1–D21.

Ford, C.E., Biggar, G.M., Humphries, D.J., Wilson, G., Dixon, D. and O'Hara, M.J. (1972). Role of water in the evolution of the lunar crust; an experimental study of sample 14310; an indication of lunar calc-alkaline volcanism. *Proceedings of the Third Lunar Science Conference, Geochimica et Cosmochimica Acta, Supplement 3*, **1**, 207–229.

Friedman, R.M., Wall, C.J., Scoates, J.S., Weis, D.A. and Meurer, W.P. (2011) Exploring the U-Pb systematics of titanite from the Archean Stillwater Complex. *American Geophysical Union, Fall Meeting 2011.* Abstract V51A-2504.

https://doi.org/10.1180/minmag.2016.080.063 Published online by Cambridge University Press

Gee, J.S., Meurer, W.P., Selkin, P.A. and Cheadle, M.J. (2004) Quantifying three-dimensional silicate fabrics in cumulates using cumulative distribution functions. *Journal of Petrology*, **45**, 1983–2009.

Gitlin, E.C., Salpas, P.A., McCallum, I.S. and Haskin, L. A. (1985) Small scale compositional heterogeneities in Stillwater anorthosite II. *Lunar and Planetary Science XVI.* Lunar and Planetary Institute, Houston, USA. [Extended abstract p. 272].

Godel, B. and Barnes, S.-J. (2004) Image analysis and composition of platinum-group minerals in the J-M Reef, Stillwater Complex (U.S.A.). *Economic Geology*, **103**, 637–651.

Godel, B. and Barnes, S.-J. (2008) Platinum-group elements in sulphide minerals and the whole rocks of the J-M Reef (Stillwater Complex): Implication for the formation of the reef. *Chemical Geology*, **248**, 272–294.

Godel, B., Barnes, S.-J. and Maier, W.D. (2006) 3-D distribution of sulphide minerals in the Merensky Reef (Bushveld Complex, South Africa) and the J-M Reef (Stillwater Complex, USA) and their relationship to microstructures using X-Ray computed tomography. *Journal of Petrology*, **47**, 1853–1872.

Godel, B. Maier, W.D. and Barns, S.-J. (2008) Platinum-group elements in the Merensky and J-M reefs: A review of recent studies. *Journal Geological Society of India*, **72**, 595–609.

Gualda, G.A.R. and Ghiorso, M.S. (2015) MELTS_Excel: A Microsoft Excel-based MELTS interface for research and teaching of magma properties and evolution. *Geochemistry, Geophysics, Geosystems*, **16**, 315–324.

Hamlyn, P.R. and Keays, R.R. (1986) Sulfur saturation and second-stage Melts: Application to the Bushveld platinum metal deposits. *Economic Geology*, **81**, 1431–1445.

Hamlyn, P.R., Keays, R.R., Cameron, W.E., Crawford, A. J. and Waldron, H.M. (1985) Precious metals in magnesian low-Ti lavas: Implications for metallogenesis and sulfur saturation in primary magmas. *Geochimica et Cosmochimica Acta*, **49**, 1797–1811.

Hanley, J.J., Mungall, J.E., Pettke, T., Spooner, E.T.C. and Bray, C.J. (2008) Fluid and halide melt inclusions of magmatic origin in the Ultramafic and Lower Banded series, Stillwater Complex, Montana, USA. *Journal of Petrology*, **49**, 1133–1160.

Harmer, R.E., Auret, J.M. and Eglington, B.M. (1995) Lead isotope variations within the Bushveld complex, Southern Africa: a reconnaissance study. *Journal of African Earth Sciences*, **21**, 595–606.

Harper, M.P. (2004) *Platinum Group Element Mineralization in "Ballrooms" of the J-M Reef of the Stillwater Complex, Montana*. Unpublished MS thesis, Brigham Young University, Provo, USA.

Haskin, L.A. and Salpas P.A. (1985) Petrogenesis of Stillwater anorthosites of the middle banded zone: causes of geochemical trends. *Lunar and Planetary Science XVI.* Lunar and Planetary Institute, Houston, USA. [Extended abstract, p. 325].

Haskin, L.A. and Salpas, P.A. (1992) Genesis of compositional characteristics of Stillwater AN-I and AN-II thick anorthosite units. *Geochimica et Cosmochimica Acta*, **56**, 1187–1212.

Helz, R.T. (1985) Compositions of fine-grained mafic rocks from sills and dikes associated with the Stillwater Complex. Pp. 97–117 in: *Stillwater Complex, Montana: Geology and Guide* (G.K. Czamanske and M.L. Zientek, editors). Montana Bureau of Mines and Geology, Special Publication, **92**. Billings, Montana, USA.

Helz, R.T. (1995) The Stillwater Complex, Montana: A subvolcanic magma chamber. *American Mineralogist*, **80**, 1343–1346.

Hess, H.H. (1960) Stillwater igneous complex, Montana – a quantitative mineralogical study. *Geological Society of America Memoir*, **80**. Geological Society of America, Boulder, Colorado, USA.

Horan, M.F., Morgan, J.W., Walker, R.J. and Cooper, R.W. (2001) Re-Os isotopic constraints on magma mixing in the Peridotite zone of the Stillwater Complex, Montana, USA. *Contributions to Mineralogy and Petrology*, **141**, 446–457.

Irvine, T.N. (1975) Crystallization sequences in the Muskox intrusion and other layered intrusions II. *Origin of chromitite layers and similar deposits of other magmatic ores: Geochimica et Cosmochimica Acta*, **39**, 991–1020.

Irvine, T.N. (1977) Origin of chromite layers in the Muskox intrusion and other stratiform intrusions: A new interpretation. *Geology*, **5**, 273–277.

Irvine, T.N., Keith, D.W. and Todd, S.G. (1983) The J-M platinum-palladium reef of the Stillwater Complex, Montana: II. Origin by double-diffusive convective magma mixing and implications for the Bushveld Complex. *Economic Geology*, **78**, 1287–1334.

Jackson, E.D. (1961) Primary textures and mineral associations in the ultramafic zone of the Stillwater Complex, Montana. *U.S. Geological Survey Professional Paper*, 358. Reston, Virginia, USA, 106 pp.

Jackson, E.D. (1963) Stratigraphic and lateral variation of chromite composition in the Stillwater Complex. *Mineralogical Society of America Special Paper*, **1**, 46–54.

Jones, W.R., Peoples, J.W. and Howland, A.L. (1960) Igneous and tectonic structures of the Stillwater Complex, Montana. *U.S. Geological Survey Bulletin*, **1071-H**, 281–340.

Kahlweit, M., (1975) Ostwald ripening of precipitates. *Advances in Colloidal Interface Science*, **5**, 1–35.

Kanitpanyacharoen, W. and Boudreau, A.E. (2012). Sulfide-associated mineral assemblages in the

https://doi.org/10.1180/minmag.2016.080.063 Published online by Cambridge University Press

Bushveld Complex, South Africa: platinum-group element enrichment by vapor refining by chloride-carbonate fluids. *Mineralium Deposita*, **48**, 193–210.

Keays, R.R., Lightfoot, P.C. and Hamlyn, P.R. (2102) Sulfide saturation history of the Stillwater Complex, Montana: chemostratigraphic variation in platinum group elements. *Mineralium Deposita*, **47**, 151–173.

Kelemen, P.B., Whitehead, J.A., Aharonov, E. and Jordahl, K.A. (1995) Experiments on flow focusing in soluble porous media, with applications to melt extraction from the mantle. *Journal of Geophysical Research*, **100(B1)**, 475–496.

Kleinkopf, M.D., (1985) Regional gravity and magnetic anomalies of the Stillwater Complex area. Pp. 33–38 in: *The Stillwater Complex, Montana: Geology and Guide* (G.K. Czamanske and M.L. Zientek, editors) Montana Bureau of Mines and Geology Special Publication, **92**. Billings, Montana, USA.

Kushiro, I. (1975) On the nature of silicate melt and its significance in magma genesis: regularities in the shift of the liquidus boundaries involving olivine, pyroxene, and silica minerals. *American Journal of Science*, **275**, 411–431.

Kushiro, I., Yoder, H. S. and Nishikawa, M. (1968) Effect of water on the melting of enstatite. *Geological Society of America Bulletin*, **79**, 1685–1692.

Labotka, T.C. (1985) Petrogenesis of metamorphic rocks beneath the Stillwater Complex: Assemblages and conditions of metamorphism. Pp. 70–76 in: *Stillwater Complex, Montana: Geology and Guide* (G.K. Czamanske and M.L. Zientek, editors). Montana Bureau of Mines and Geology, Special Publication, **92**. Billings, Montana, USA.

Labotka, T.C. and Kath, R.L. (2001) Petrogenesis of the contact-metamorphic rocks beneath the Stillwater Complex, Montana. *Geological Society of America Bulletin*, **113**, 1312–1323.

Lambert, D.D. and Simmons, E.C. (1987) Magma evolution in the Stillwater Complex, Montana: I. Rare earth element evidence for the formation of the Ultramafic series. *American Journal of Science*, **287**, 1–32.

Lambert, D.D. and Simmons, E.C. (1988) Magma evolution in the Stillwater Complex, Montana: II. Rare earth element evidence for the formation of the J-M Reef. *Economic Geology*, **83**, 1109–1126.

Lambert, D.D., Walker, R.J., Morgan, J.W., Shirey, S.B., Carlson, R.W., Zientek, M.L., Lipin, B.R., Koski, M. S. and Cooper, R.L. (1994) Re-Os and Sm-Nd isotope geochemistry of the Stillwater Complex, Montana: Implications for the petrogenesis of the J-M Reef. *Journal of Petrology*, **35**, 1717–1753.

Lambert, D.D., Morgan, J.W., Walker, R.J., Shirey, S.B., Carlson, R.W., Zientek, M.L. and Koski, M.S. (1989) Re-Os and Sm-Nd isotope systematics of the Stillwater Complex, Montana. *Science*, **244**, 1169–1174.

Latypov, R (2015) Basal reversals in sills and layered intrusions. Pp. 259–294 in: *Layered Intrusions* (B. Charlier, O. Namur, R. Latypov and C. Tegner, editors). Springer, Berlin.

Lechler, P.J., Arehart, G.B. and Knight, M. (2002) Multielement and isotopic geochemistry of the J-M Reef, Stillwater intrusion. Pp. 245–248 in: *Montana: 9th International Platinum Symposium, Abstract with Program, 21–25 July 2002.* Billings, Montana, USA.

Lenaz, D., Garuti, G., Zaccarini, F., Cooper, R.W. and Princivalle, F. (2012) The Stillwater Complex chromitites: The response of chromite crystal chemistry to magma injection. *Geologica Acta*, **10**, 33–41.

LeRoy, L.W. (1985) Troctolite-Anorthosite zone I and the J-M Reef: Frog Pond adit to the Graham Creek area. Pp. 325–333 in: *Stillwater Complex, Montana: Geology and Guide* (G.K. Czamanske and M. L. Zientek, editors.). Montana Bureau of Mines and Geology, Special Publication, **92**. Billings, Montana, USA.

Li, C. and Ripley, E.M. (2006) Formation of Pt-Fe alloy by desulphurization of Pt-Pd sulphide in the J-M Reef of the Stillwater Complex, Montana. *The Canadian Mineralogist*, **44**, 895–903.

Li, C. and Ripley, E.M. (2009) Sulfur contents at sulfide-liquid or anhydrite saturation in silicate melts: empirical equations and example applications. *Economic Geology*, **104**, 405–412.

Lipin, B.R. (1993) Pressure increases, the formation of chromite seams, and the development of the Ultramafic series in the Stillwater Complex, Montana. *Journal of Petrology*, **34**, 955–976.

Lipin, B.R. and Zientek, M.L. (2002) The Stillwater Complex, Montana: The root of a flood basalt province? Pp. 265–268 in: *9th International Platinum Symposium, Abstract with Program, 21–25 July 2002.* Billings, Montana, USA.

Lipman, P.W., Banks, N.G. and Rhodes, M.J. (1985) Degassing-induced crystallization of basaltic magma and effects on lava rheology. *Nature*, **317**, 604–607.

Loferski, P.J. and Arculus, R.J. (1993) Multiphase inclusions in plagioclase from anorthosites in the Stillwater Complex, Montana: implications for the origin of the anorthosites. *Contributions to Mineralogy and Petrology*, **114**, 63–78.

Loferski, P.J., Lipin, B.R. and Cooper, R.W. (1990) Petrology of chromite-bearing rocks from the lowermost cyclic units in the Stillwater Complex, Montana. *U.S. Geological Survey Bulletin*, **1674E**, E1–E28.

Loferski, P.J., Arculus, R.J. and Czamanske, G.K. (1994) Rare earth element evidence for the Petrogenesis of the Banded Series of the Stillwater Complex, Montana, and its anorthosites. *Journal of Petrology*, **35**, 1623–1649.

Maier, W.D. and Barnes, S.-J. (1999) Platinum-group elements in silicate rocks of the Lower, Critical, and

https://doi.org/10.1180/minmag.2016.080.063 Published online by Cambridge University Press

Main zones at Union Section, western Bushveld complex. *Journal of Petrology*, **40**, 1647–1671.

Manning, C.E. and Aranovich, L.Y. (2014) Brines at high pressure and temperature: Thermodynamic, petrologic and geochemical effects. *Precambrian Research*, **253**, 6–16.

Marsh, B.D. (2004) A magmatic mush column Rosetta Stone: the McMurdo Dry Valleys of Antarctica. *EOS Transactions, American Geophysical Union*, **85**, 497–502.

Mathez, E.A. and Waight, T.E. (2003) Lead isotopic disequilibrium between sulfide and plagioclase in the Bushveld Complex and the chemical evolution of large layered intrusions. *Geochimica et Cosmochimica Acta*, **67**, 1875–1888.

McBirney, A.R. (1987) Constitutional zone refining of layered mafic intrusions. Pp. 437–452 in: *Origins of Igneous Layering* (I. Parsons, editor). NATO ASI Series, Series C: Mathematical and Physical Sciences, vol. **186**. Kluwer Academic, Dordrecht, The Netherlands.

McBirney, A.R. (2008) Factors governing the textural development of Skaergaard gabbros: A review. *Lithos*, **111**, 1–5.

McBirney, A.R. and Creaser, R.A. (2003) The Skaergaard layered series, part VII: Sr and Nd Isotopes. *Journal of Petrology*, **44**, 757–771.

McBirney, A.R. and Noyes, R.M. (1979) Crystallization and layering of the Skaergaard Intrusion. *Journal of Petrology*, **20**, 487–564.

McCallum, I.S. (1996) The Stillwater Complex. Pp. 441–483 in: *Layered Intrusions* (R.G. Cawthorn, editor). Elsevier Science, Amsterdam.

McCallum, I.S., Raedeke, L.D. and Mathez, E.A., (1977) Stratigraphy and petrology of the Banded zone of the Stillwater Complex, Montana. *EOS*, **58**, 1245.

McCallum, I.S., Raedeke, L.D. and Mathez, E.A. (1980) Investigations in the Stillwater Complex: Part I. Stratigraphy and structure of the Banded zone. Pp. 59–87 in: *The Jackson Volume.* Vol. 280-A, American Journal of Science (A. Irving and M. Dungan, editors). Kline Geology Laboratory, Yale University, New Haven, Connecticut.

McCallum, I.S., Thurber, D.W., O'Brien, H.E. and Nelson, B.K. (1999) Lead isotopes in sulfides from the Stillwater Complex, Montana: Evidence for subsolidus remobilization. *Contributions to Mineralogy and Petrology*, **137**, 206–219.

Meurer, W.P. and Boudreau, A.E. (1996*a*) The petrology and mineral compositions of the Middle Banded series of the Stillwater Complex, Montana. *Journal of Petrology*, **37**, 583–607.

Meurer, W.P. and Boudreau, A.E. (1996*b*) Evaluation of models for halogen variations in apatite from layered intrusions using a detailed study of apatite from OB-III and OB-IV of the Middle Banded series, Stillwater Complex, Montana. *Contributions to Mineralogy and Petrology*, **123**, 225–236.

Meurer, W.P. and Boudreau, A.E. (1996*c*) Compaction of density-stratified cumulates: effect on trapped-liquid distribution. *Journal of Geology*, **104**, 115–120.

Meurer, W.P. and Boudreau, A.E. (1998*a*) Compaction of igneous cumulates. Part I – Geochemical consequences for cumulates and liquid fractionation trends. *Journal of Geology*, **106**, 281–292.

Meurer, W.P. and Boudreau, A.E. (1998*b*) Compaction of igneous cumulates. Part II – Compaction and the development of igneous foliation. *Journal of Geology*, **106**, 293–304.

Meurer, W.P., Klaber, S.A. and Boudreau, A.E. (1997) Discordant bodies from Olivine-Bearing zones III and IV of the Stillwater Complex, Montana – Evidence for post-cumulus fluid migration in layered intrusions. *Contributions to Mineralogy and Petrology*, **130**, 81–92.

Meurer, W.P., Willmore, C.C. and Boudreau, A.E. (1998) Metal redistribution during fluid exsolution and migration in the Middle Banded series of the Stillwater Complex, Montana. *Lithos*, **47**, 143–156.

Mogk, D.W. and Mueller, P.A. (1990) Evidence for Archean accretionary tectonics in the northern Wyoming Province, SW Montana. *Geological Society of America Abstracts with Programs*, **22**, 262.

Newton, R.C. and Manning, C.E. (2000) Quartz solubility in H_2O-NaCl and H_2O-CO_2 solutions at deep crust-upper mantle pressures and temperatures: 2–15 kbar and 500–900°C. *Geochimica et Cosmochimica Acta*, **64**, 2993–3005.

Nicholson, D.M. and Mathez, E.A. (1991) Petrogenesis of the Merensky Reef in the Rustenburg section of the Bushveld Complex. *Contributions to Mineralogy and Petrology*, **107**, 293–309.

Nunes, P.D. (1981) The age of the Stillwater Complex: a comparison of U-Pb zircon and Sm-Nd isochron systematics. *Geochimica et Cosmochimica Acta*, **45**, 1961–1963.

Nunes, P.D. and Tilton, G.R. (1971) Uranium-lead ages of minerals from the Stillwater Complex and associated rocks, Montana. *Geological Society of America Bulletin*, **82**, 2231–2250.

Page, N.J (1971) Sulfide minerals in the G and H chromitite zones of the Stillwater Complex, Montana. *U.S. Geological Survey Professional Paper*, **694**. Reston, Virginia, USA.

Page, N.J. (1977) *Stillwater Complex, Montana: rock succession, metamorphism and structure of the Complex and adjacent rocks.* U.S. Geological Survey Professional Paper, **999**. Reston, Virginia, USA.

Page, N.J. (1979) *Stillwater Complex, Montana - Structure, mineralogy and petrology of the basal zone with emphasis on the occurrence of sulfides*. U.S.

https://doi.org/10.1180/minmag.2016.080.063 Published online by Cambridge University Press

Geological Survey Professional Paper, **1038**. Reston, Virginia, USA.

Page, N.J. and Moring, B.C. (1990) *Petrology of the noritic and gabbronoritic rocks below the J-M reef in the Mountain View area, Stillwater Complex, Montana.* U.S. Geological Survey Bulletin **1674-C**. Reston, Virginia, USA.

Page, N.J. and Zientek, M.L. (1987) *Composition of primary postcumulus amphibole and phlogopite within an olivine cumulate in the Stillwater Complex, Montana.* U.S. Geological Survey Bulletin, **1674-A**. Reston, Virginia, USA.

Page, N.J, Zientek, M.L., Czamanske, G.K. and Foose, M. P. (1985) Sulfide mineralization in the Stillwater Complex and underlying rocks. Pp. 93–96 in: *Stillwater Complex, Montana: Geology and Guide* (G.K. Czamanske and M.L. Zientek, editors), Montana Bureau of Mines and Geology Special Publication, **92**. Billings, Montana, USA.

Pagé, P., Barnes, S.J. and Zientek, M.L. (2011) Formation and evolution of the chromitites of the Stillwater Complex: a trace element study. Pp. 678–680 in: *Let's Talk Ore Deposits: Proceedings of the 11th SGA Biennial Meeting, Antofagasta, Chile* (Barra, F., editors). Society for Geology Applied to Mineral Deposits.

Papike, J.J., Spilde, M.N., Fowler, G.W. and McCallum, I. S. (1995) SIMS studies of planetary cumulates: Orthopyroxene from the Stillwater Complex, Montana. *American Mineralogist*, **80**, 1208–1221.

Pass, K.D. and Salpas, P.A. (1990) Toward an understanding of the bulk composition of thick Stillwater anorthosite unit An II. *Lunar and Planetary Science XXI*. Lunar and Planetary Institute, Houston, USA. [Extended abstract, p. 938].

Pass, K.D. and Salpas, P.A. (1991) Progress toward understanding the petrogenesis of anorthosite in the Stillwater Complex, Montana: The bulk composition of AN II. *Journal of the Alabama Academy of Science*, **62**, 938.

Peoples, J.W. and Howland, A.L. (1941) Chromite deposits of the eastern part of the Stillwater complex, Stillwater County, Montana. *U.S. Geological Survey Bulletin*, **922-N**, 371–416.

Premo, W.R., Helz, R.T., Zientek, M.L. and Langston, R. B. (1990) U-Pb and Sm-Nd ages for the Stillwater Complex and its associated sills and dikes, Beartooth Mountains, Montana: Identification of a parent magma? *Geology*, **18**, 1065–1068.

Prevec, S.A., Ashwal, L.D. and Mkaza, M.S. (2005) Mineral disequilibrium from the Merensky pegmatoid, western Bushveld Complex, South Africa: new Sm–Nd isotopic evidence. *Contributions to Mineralogy and Petrology*, **149**, 306–315.

Raedeke, L.D. (1982) *Petrogenesis of the Stillwater Complex*. Unpublished PhD dissertation, University of Washington, Seattle, USA.

Raedeke, L.D. and McCallum, I.S. (1980) A comparison of fractionation trends in the lunar crust and the Stillwater Complex. Pp. 133–153 in: *Proceedings of the conference on the lunar highlands crust* (R.B. Merrill and J.J. Papike, editors). *Geochimica et Cosmochimica Acta*, sup. 12, 133–153.

Raedeke, L.D. and McCallum, I.S. (1984) Investigations in the Stillwater Complex: Part II. Petrology and petrogenesis of the ultramafic series. *Journal of Petrology*, **25**, 395–420.

Raedeke, L.D. and Vian, R.W. (1986) A three dimensional view of mineralization in the Stillwater J-M Reef. *Economic Geology*, **81**, 1187–1195.

Ryder, G. and Spettel, B (1985) The Parental Magma for Some Rocks from the Norite 1 Subzone of the Stillwater Complex: A Lunar Analog Study. *Proceedings of the 15th Lunar and Planetary Science Conference, Part 2, Journal of Geophysical Research*, **89**(Supplement), C545–C559.

Salpas, P.A. and Moss, B. (1989) A preliminary compositional study of anorthosite and related rocks from the Lower Banded series of the Stillwater Complex. *Lunar and Planetary Science XX*. Lunar and Planetary Institute, Houston, USA. [Extended abstract, p. 972].

Salpas, P.A. and Pass, K.D. (1990) Geochemistry of the base of the main anorthosite bearing series, Stillwater Complex. *Lunar and Planetary Science XXI*. Lunar and Planetary Science Institute, Houston, USA. [Extended abstract, Pp. 1065–1066].

Salpas, P.A., Haskin, L.A. and McCallum, I.S. (1983) Stillwater anorthosites: A lunar analog? *Proceedings of the 14th Lunar and Planetary Science Conference, Journal of Geophysical Research*, **88**(Supplement), B27–B39.

Salpas, P.A., Haskin, L.A. and McCallum, I.S. (1984) The scale of compositional heterogeneities in Stillwater anorthosites AN I and AN II. *Lunar and Planetary Sciences XV.* Lunar and Planetary Institute, Houston, USA. [Extended abstract, p. 713].

Salpas, P.A., Haskin, L.A. and McCallum, I.S. (1987) Trace element distributions among subunits of a Stillwater anorthosite boulder. *Lunar and Planetary Science XVIII*, Lunar and Planetary Institute, Houston, USA. [Extended abstract, p. 872].

Scheidle, D.L. (1983) *Plagioclase zoning and compositional variation in Anorthosites I and II along the Contact Mountain Traverse, Stillwater Complex, Montana*. Unpublished MS thesis, Stanford University, Stanford, USA.

Segerstrom, K. and Carlson, R.R. (1982) *Geologic map of the banded upper zone of the Stillwater Complex and adjacent rocks, Stillwater, Sweet Grass, and Park Counties, Montana.* U.S. Geological Survey Miscellaneous Investigations series Map 1-1383, 2 sheets, scale 1 : 24,000.

https://doi.org/10.1180/minmag.2016.080.063 Published online by Cambridge University Press

Selkin, P.A., J.S. Gee, J.S., Tauxe, L., Meurer, W.P. and Newell, A.J. (2000) The effect of remanence anisotropy on paleointensity estimates: a case study from the Archean Stillwater Complex. *Earth and Planetary Science Letters*, **183**, 403–416

Selkin, P.A., Gee. J.S., Meurer, W.P. and Hemming, S.R. (2008) Paleointensity record from the 2.7 Ga Stillwater Complex, Montana. *Geochemistry, Geophysics, Geosystems*, **9**, DOI: 10.1029/2008GC001950

Shirley, D.N. (1986) Compaction of igneous cumulates. *Journal of Geology*, **94**, 795–809.

Spandler, C., Mavrogenes, J. and Arculus, R. (2005) Origin of chromitites in layered intrusions: Evidence from chromite-hosted melt inclusions from the Stillwater Complex. *Geology*, **33**, 893–896.

Sun, S.-S., Nesbitt, R.W. and McCulloch, M.T. (1989). Geochemistry and petrogenesis of Archean and early Proterozoic siliceous high-magnesian basalts. Pp. 149–173 in: *Boninites* (A.J Crawford, editor), Unwin Hyman, London.

Talkington, R.W. and Lipin, B.R. (1986) Platinum-group minerals in chromite seams of the Stillwater Complex, Montana. *Economic Geology*, **81**, 1179–1186.

Thurber, M.W. and McCallum, I.S. (1990) The ultramafic series-Banded series contact in the Stillwater Complex: Evidence for thermal erosion. *Lunar and Planetary Science XXI*. Lunar and Planetary Institute, Houston, USA. [Extended abstract, pp. 1254–1255].

Todd, S.G., Keith, D.W., LeRoy, L.W., Shissel, D.J., Mann, E.L. and Irvine, T.N. (1982) The J-M platinum-palladium reef of the Stillwater Complex, Montana: I. *Stratigraphy and petrology. Economic Geology*, **77**, 1454–1480.

Turner, A.R., Wolfgram, D. and Barnes, S.J. (1985) Geology of the Stillwater county sector of the J-M Reef, including the Minneapolis adit. Pp. 210–231 in: *Stillwater Complex, Montana: Geology and Guide* (G. K. Czamanske and M.L. Zientek, editors). Montana Bureau of Mines and Geology, Special Publication **92**. Billings, Montana, USA.

Vaniman, D.T., Papike, J.J. and Labotka, T. (1980) Contact-metamorphic effects of the Stillwater Complex, Montana: the concordant iron formation. *American Mineralogist*, **65**, 1087–1102.

Wall, C.J., Scoates, J.S., Friedman, R.M. and Meurer, W.P. (2009) Revisiting the age of the Stillwater Complex. *American Geophysical Union, Fall Meeting 2009*, Abstract V21A-1959.

Wall, C.J., Scoates, J.S., Friedman, R.M. and Meurer, W.P. (2010) Refining the precise age and duration of magmatism related to the Stillwater Complex. *11th International Platinum Symposium, Sudbury, Ontario, June 20–24, 2010.* [Extended abstract].

Wall, C.J., Scoates, J.S., Friedman, R.M. and Meurer, W.P. (2012) Age of the Stillwater Complex. *Mineralogical Magazine*, **76**, 2506 [Goldschmidt Montreal Abstract #20565].

Waters, C. and Boudreau, A.E. (1996) A reevaluation of crystal size distributions in chromite cumulates. *American Mineralogist*, **81**, 1452–1459.

Willmore, C.C., Boudreau, A.E. and Kruger, F.J. (2000) The halogen geochemistry of the Bushveld Complex, Republic of South Africa: Implications for chalcophide element distribution in the Lower and Critical Zones. *Journal of Petrology*, **41**, 1517–1539.

Wooden, J.L., Czamanske, G.K. and Zientek, M.L. (1991) A lead isotopic study of the Stillwater Complex, Montana: constraints on crustal contamination and source regions. *Contributions to Mineralogy and Petrology*, **107**, 80–93.

Zientek, M.L. (1983) *Petrogenesis of the Basal zone of the Stillwater Complex, Montana*. Unpublished PhD dissertation, Stanford University, Stanford, USA.

Zientek, M.L., Czamanske, G.K. and Irvine, T.N. (1985) Stratigraphy and nomenclature for the Stillwater Complex. Pp. 21–32 in: *Stillwater Complex, Montana: Geology and Guide* (G.K. Czamanske and M.L. Zientek, editors). Montana Bureau of Mines and Geology, Special Publication **92**. Billings, Montana, USA.

Zientek, M.L., Fries, T.L. and Vian, R.W. (1990) As, Bi, Hg, S, Sb, Sn, and Te geochemistry of the J-M Reef, Stillwater Complex, Montana: constraints on the origin of PGE-enriched sulfides in layered intrusions. *Journal of Geochemical Exploration*, **37**, 51–73.

Zientek, M.L., Cooper, R.W., Corson, S.R. and Geraghty, E.P. (2002) Platinum-group element mineralization in the Stillwater Complex, Montana. Pp. 459–481 in: *Geology, Geochemistry, Mineralogy and Mineral Benefication of Platinum-Group Elements* (L.J Cabri, editor). Special Volume **54**. Canadian Institute of Mining, Metallurgy and Petroleum.

Zientek, M.L., Foose, M.P. and Mei, L. (2008) Palladium, platinum, and rhodium contents of rocks near the lower margin of the Stillwater Complex, Montana. *Economic Geology*, **81**, 1169–1178.

Zientek, M.L. and Ripley, E.M. (1990) Sulfur isotopic studies of the Stillwater Complex and associated rocks, Montana. *Economic Geology*, **85**, 376–391.

https://doi.org/10.1180/minmag.2016.080.063 Published online by Cambridge University Press